The 50th Fluid Dynamics Conference/ The 36th Aerospace Numerical Simulation Symposium
4 July 2018, Miyazaki Citizen's Plaza, Miyazaki, Japan

Summary of Fourth Aerodynamics Prediction Challenge (APC-IV)

Takashi Ishida （JAXA）
APC committee

Contents

- Participants
- Test case 1
- Test case 2
- Test case 3
- Summary

Statistics of submitted data

- Organizations and number of submitted data(total 26 data)
  - National research institutes : JAXA(4)
  - Universities: TAT(1), Tohoku Univ./KIT(1) , Tohoku Univ.(1), Univ. of Tokyo(1)
  - Aerospace industries: KHI(4), MHI(1)
  - Vendors: Ryoyu systems(9), Siemens(2) , Cradle(2)

- Grids
  - JAXA : 17
  - Customs : 10

- Codes
  - Structured solver(8), Unstructured solver(13)
  - Cartesian(LBM(2), BCM(1), UTCart(2))

- Turbulence models
  - Steady: SA(16)
  - Unsteady: DDES(SA)(16), IDDES(SA)(1), IDDES(SST)(1), ILES(2)

3

Participants of case 1-1

ID	Name	Organization	Code	Grid	Turbulence Model	Note
A1	田中 健太郎	菱友システムズ	UPACS (structured solver)	JAXA	SA-noft2	3rd SLAU
A2					SA-noft2(strain rate)	3rd SLAU
A4					SA-noft2	5th SLAU
A5					SA-noft2-R	5th SLAU
A6					SA-noft2(strain rate)	5th SLAU
C1	山本 貴弘	菱友システムズ	FaSTAR (unstructured solver)	JAXA	SA-noft2-R	
D1	石田 崇	JAXA	BCMLBM2D/3D	Custom (直交格子)	ILES	
E1	安田 英将	KHI	Cflow (unstructured solver)	JAXA	SA-noft2	
H1	Peter Burns	Siemens PLM Software	Simcenter STAR-CCM+ (unstructured solver)	JAXA	SA	
H2				Custom (polyhedral)	SA	
I1	中島 吉隆	クレイドル	scFLOW (unstructured solver)	JAXA	SA	
I2				Custom (polyhedral)	SA	
K1	佐々木 大輔	金沢工業大学	BCM	Custom (直交格子)	SA-noft2-R	
M1	周 健文	東京大学	UTCart	Custom (直交格子)	SA-noft2 + Wall function	

4

Participants of case 1-2

ID	Name	Organization	Code	Grid	Turbulence Model	Note
A4	田中 健太郎	菱友システムズ	UPACS (structured solver)	JAXA	SA-noft2	5th SLAU
A5					SA-noft2-R	5th SLAU
A6					SA-noft2 (strain rate)	5th SLAU
A7					SA-noft2 (strain rate)	5th SLAU wiggle-sensor
A8					SA-noft2 (strain rate)	5th SLAU wiggle-sensor-skewsym
C1	山本 貴弘	菱友システムズ	FaSTAR (unstructured solver)	JAXA	SA-noft2-R	
E1	安田 英将	KHI	Cflow (unstructured solver)	JAXA	SA-noft2	
E2				Custom(直交八分木＋物体適合層状格子)	SA-noft2	
H1	Peter Burns	Siemens PLM Software	Simcenter STAR-CCM+ (unstructured solver)	Custom (trimmed)	SA	

5

Participants of case 1-3

ID	Name	Organization	Code	Grid	Turbulence Model	Note
A2	田中 健太郎	菱友システムズ	UPACS (structured solver)	JAXA	SA-noft2 DDES (strain rate)	3rd SLAU
A3					SA-noft2 DDES (strain rate)	5th Roe
A4					SA-noft2 DDES	5th SLAU
A5					SA-noft2-R DDES	5th SLAU
A6					SA-noft2 DDES (strain rate)	5th SLAU
A7					SA-noft2 DDES (strain rate)	5th SLAU wiggle-sensor
A8					SA-noft2 DDES (strain rate)	5th SLAU wiggle-sensor-skewsym
B1	坂井 玲太郎	JAXA	FaSTAR (unstructured solver)	JAXA	SA-noft2-R DDES	dmax
B2					SA-noft2-R DDES	dSLA
B3					SA-noft2-R DDES	dvol
C1	山本 貴弘	菱友システムズ	FaSTAR (unstructured solver)	JAXA	SA-noft2-R DDES	
D1	石田 崇	JAXA	BCMLBM2D/3D	Custom (直交格子)	ILES	

6

Participants of case 1-3

ID	Name	Organization	Code	Grid	Turbulence Model	Note
E1	安田 英将	KHI	Cflow (unstructured solver)	JAXA	SA-noft2 DDES	
E2				Custom(直交八分木＋物体適合層状格子)	SA-noft2 DDES	
G1	西村 信祐	MHI	MHI-LBM	Custom (直交格子)	ILES	
H1	Peter Burns	Siemens PLM Software	Simcenter STAR-CCM+ (unstructured solver)	Custom (trimmed)	SA IDDES	
J1	小島 良実	東京農工大学	FaSTAR (unstructured solver)	JAXA	SST-2003sust IDDES	

7

Participants of case 2-1

ID	Name	Organization	Code	Grid	Turbulence Model	Note
A1	田中 健太郎	菱友システムズ	UPACS (structured solver)	JAXA	SA-noft2	3rd SLAU
C1	山本 貴弘	菱友システムズ	FaSTAR (unstructured solver)	JAXA	SA-noft2-R	
E1	安田 英将	KHI	Cflow (unstructured solver)	JAXA	SA-noft2	
H1	Peter Burns	Siemens PLM Software	Simcenter STAR-CCM+ (unstructured solver)	JAXA	SA	
H2				Custom (polyhedral)	SA	
I1	中島 吉隆	クレイドル	scFLOW (unstructured solver)	JAXA	SA	
I2				Custom (polyhedral)	SA	
K1	佐々木 大輔	金沢工業大学	BCM	Custom (直交格子)	SA-noft2-R	

8

Participants of case 2-2

ID	Name	Organization	Code	Grid	Turbulence Model	Note
C1	山本 貴弘	菱友システムズ	FaSTAR (unstructured solver)	JAXA	SA-noft2-R	
E1	安田 英将	KHI	Cflow (unstructured solver)	JAXA	SA-noft2	
E2				Custom(直交八分木＋物体適合層状格子)	SA-noft2	
H1	Peter Burns	Siemens PLM Software	Simcenter STAR-CCM+ (unstructured solver)	Custom (trimmed)	SA	

9

Participants of case 2-3

ID	Name	Organization	Code	Grid	Turbulence Model	Note
A3	田中 健太郎	菱友システムズ	UPACS (structured solver)	JAXA	SA-noft2 DDES (strain rate)	5th Roe
A6					SA-noft2 DDES (strain rate)	5th SLAU
C1	山本 貴弘	菱友システムズ	FaSTAR (unstructured solver)	JAXA	SA-noft2-R DDES	
E1	安田 英将	KHI	Cflow (unstructured solver)	JAXA	SA-noft2 DDES	
E2				Custom(直交八分木＋物体適合層状格子)	SA-noft2 DDES	
H1	Peter Burns	Siemens PLM Software	Simcenter STAR-CCM+ (unstructured solver)	Custom (trimmed)	SA IDDES	

10

Participants of case 3-1

ID	Name	Organization	Code	Grid	Turbulence Model	Note
A2	田中 健太郎	菱友システムズ	UPACS (structured solver)	JAXA	SA-noft2 DDES (strain rate)	3rd SLAU
A3					SA-noft2 DDES (strain rate)	5th Roe
A6					SA-noft2 DDES (strain rate)	5th SLAU
A7					SA-noft2 DDES (strain rate)	5th SLAU wiggle-sensor
A8					SA-noft2 DDES (strain rate)	5th SLAU wiggle-sensor-skewsym
B1	坂井 玲太郎	JAXA	FaSTAR (unstructured solver)	JAXA	SA-noft2-R DDES	dmax
B2					SA-noft2-R DDES	dSLA
B3					SA-noft2-R DDES	dvol
C1	山本 貴弘	菱友システムズ	FaSTAR (unstructured solver)	JAXA	SA-noft2-R DDES	
D1	石田 崇	JAXA	BCMLBM2D/3D	Custom (直交格子)	ILES	

11

Participants of case 3-1

ID	Name	Organization	Code	Grid	Turbulence Model	Note
F1	上野 陽亮	KHI	Cflow (unstructured solver)	JAXA	SA-noft2 DDES	
F2				Custom(直交八分木＋物体適合層状格子)	SA-noft2 DDES	
G1	西村 信祐	MHI	MHI-LBM	Custom (直交格子)	ILES	
H1	Peter Burns	Siemens PLM Software	Simcenter STAR-CCM+ (unstructured solver)	Custom (trimmed)	SA IDDES	
J1	小島 良実	東京農工大学	FaSTAR (unstructured solver)	JAXA	SST-2003sust IDDES	
L1	玉置 義治	東北大学	UTCart	Custom (直交格子)	SA-DDES-p	

12

Participants of case 3-2

ID	Name	Organization	Code	Grid	Turbulence Model	Note
A2	田中 健太郎	菱友システムズ	UPACS (structured solver)	JAXA	SA-noft2 DDES (strain rate)	3rd SLAU
A3					SA-noft2 DDES (strain rate)	5th Roe
A6					SA-noft2 DDES (strain rate)	5th SLAU
A7					SA-noft2 DDES (strain rate)	5th SLAU wiggle-sensor
A8					SA-noft2 DDES (strain rate)	5th SLAU wiggle-sensor-skewsym
B1	坂井 玲太郎	JAXA	FaSTAR (unstructured solver)	JAXA	SA-noft2-R DDES	dmax
B2					SA-noft2-R DDES	dSLA
B3					SA-noft2-R DDES	dvol
F1	上野 陽亮	KHI	Cflow (unstructured solver)	JAXA	SA-noft2 DDES	
F2				Custom(直交八分木＋物体適合層状格子)	SA-noft2 DDES	
H1	Peter Burns	Siemens PLM Software	Simcenter STAR-CCM+ (unstructured solver)	Custom (trimmed)	SA IDDES	

13

Case 1 : Prediction of aerodynamics

– Case1-1 : 2D steady flow simulation
- Geom. : 30P30N（modified_slat_configF ）
- Grid : provided（required : L2, optional : L1,L3~L5）or custom
- Cond. : M = 0.17, Re = 1.71 x 10^6
- AoA : 0/4/5.5/8/9.5/12/14/16/20/22/24/26 [deg]
  (red : required, black : optional)
- List of data :
  – Aerodynamic coefficients (C_D,C_L,C_m),C_p,C_f
  – Contours of $\tilde{\nu}/\nu$
  – Spatial streamlines
  – Velocity profiles

Legend(paticipant ID / grid type [J:provided by JAXA, C:custom] - grid resolution [L1~L5])

EXP	A1/J-L2	A1/J-L3	A2/J-L2	A4/J-L2	A4/J-L3	A5/J-L3
A6/J-L3	C1/J-L1	C1/J-L2	C1/J-L3	C1/J-L4	C1/J-L5	D1/C-L2
E1/J-L2	E1/J-L3	H1/J-L2	H2/C-L1	H2/C-L2	I1/J-L1	I1/J-L2
I1/J-L3	I1/J-L4	I1/J-L5	I2/C-L2	K1/C-L1	K1/C-L2	M1/C-L4

14

Case 1-1 : α - sweep

CL - Alpha

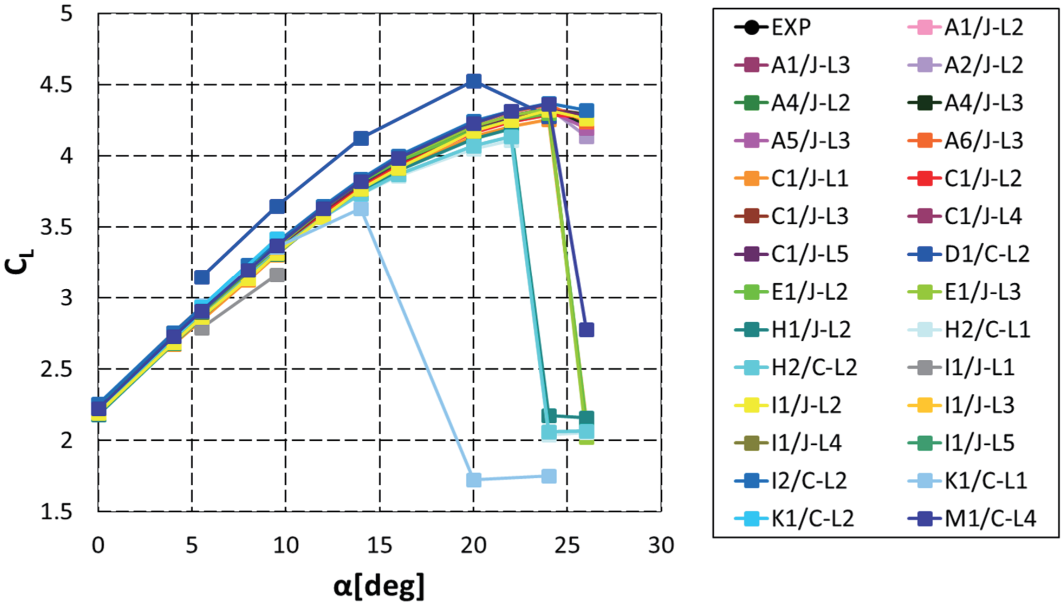

The variation was larger than past APC series even though SA turbulence model was mainly used.

15

Case 1-1 : α - sweep

CL - CD

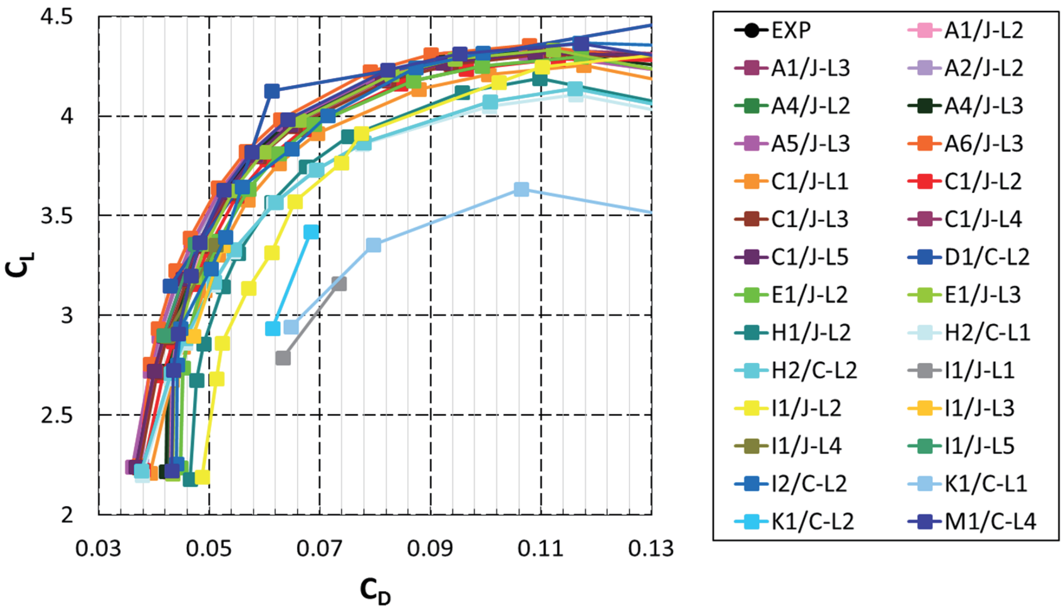

The variation was larger than past APC series even though SA turbulence model was mainly used.

16

α –sweep of APC-III

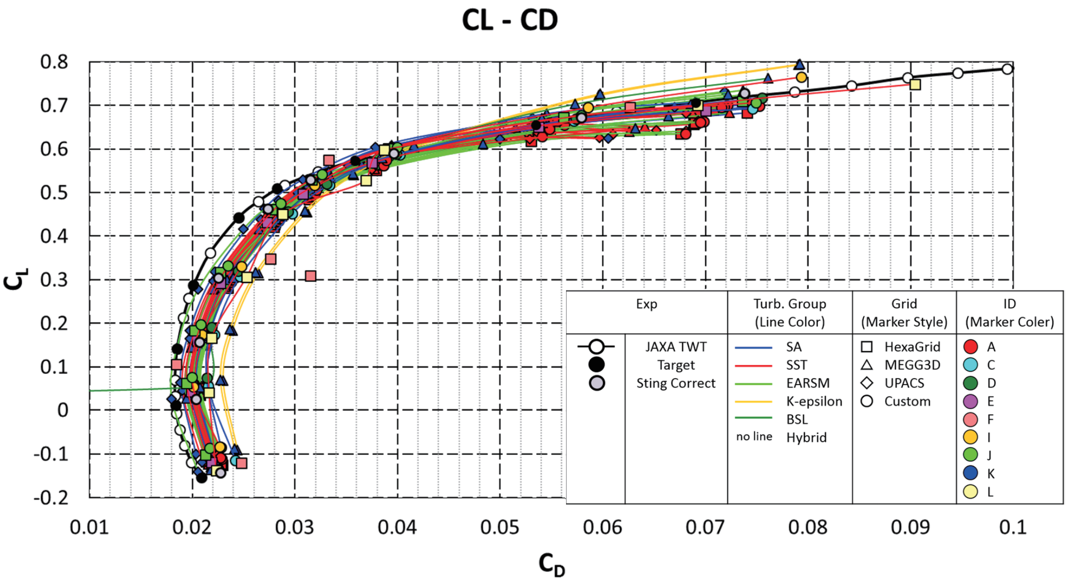

17

α –sweep of APC-II

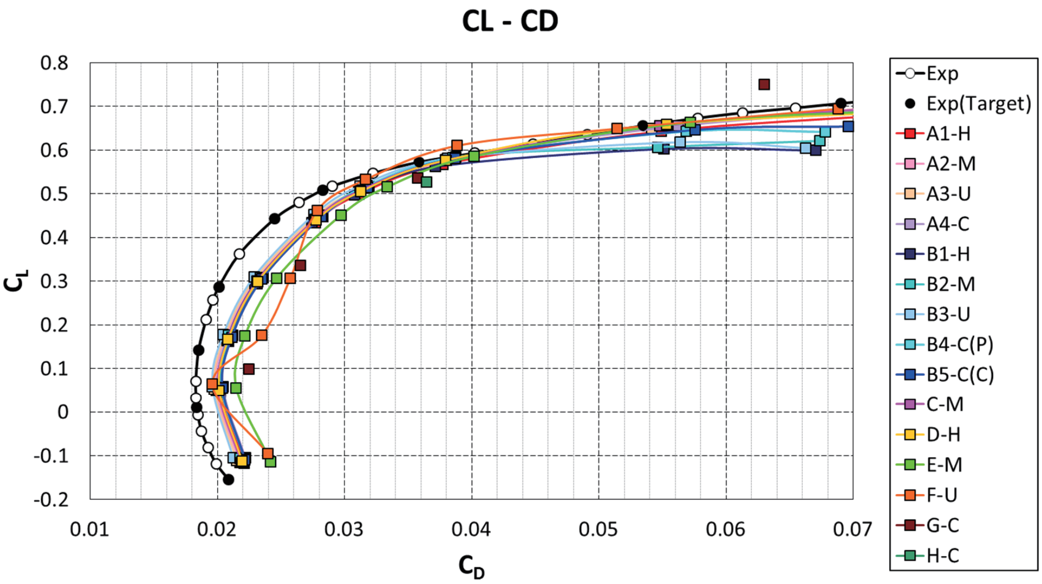

18

Case 1-1 : α - sweep

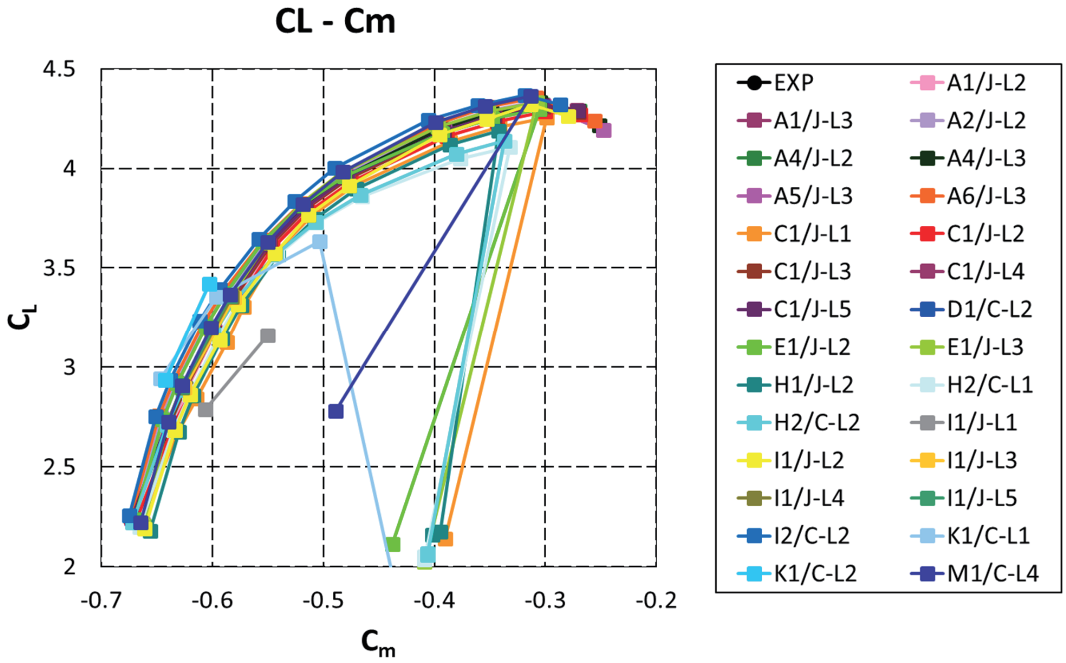

The variation was larger than past APC series even though SA turbulence model was mainly used.

19

Case 1-1 : α - sweep

Comparison of pressure/friction force

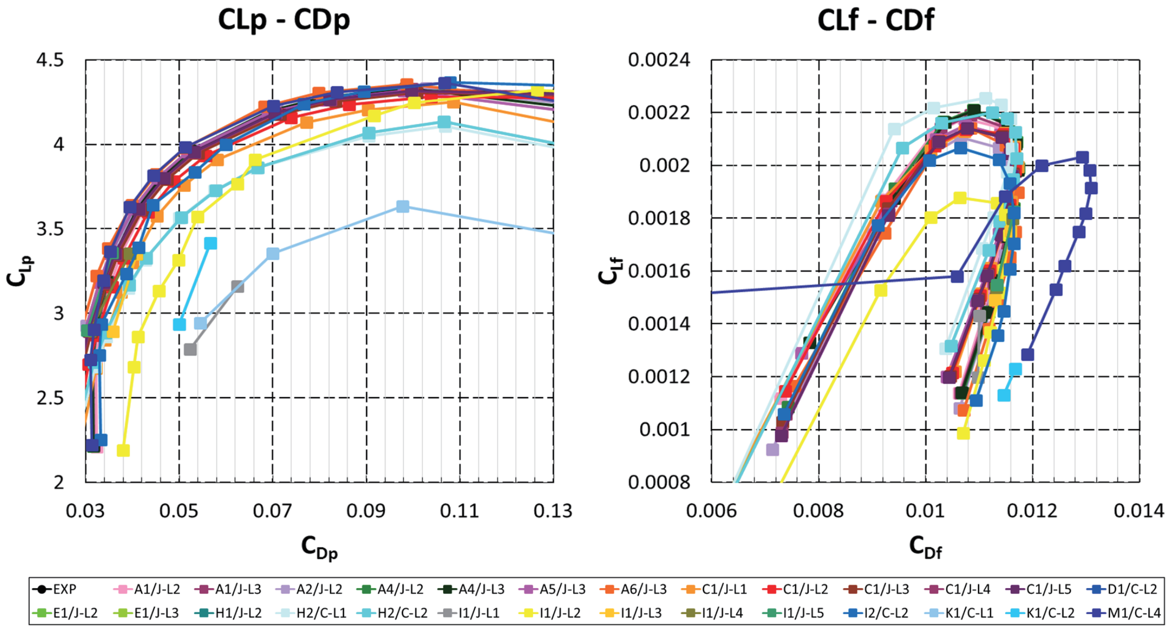

Although pressure force was dominant, friction force had some variation due to grid type.

20

Case 1-1 : α - sweep

Comparison by grid type

Provided grid **CL - Alpha**

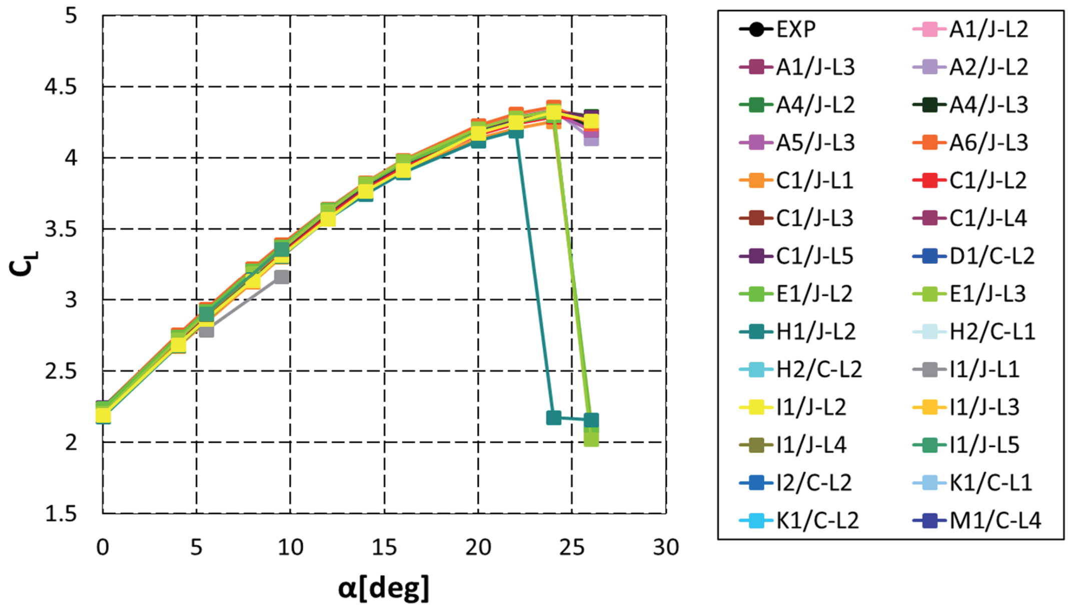

There was large influence on grid type.

21

Case 1-1 : α - sweep

Comparison by grid type

Custom grid **CL - Alpha**

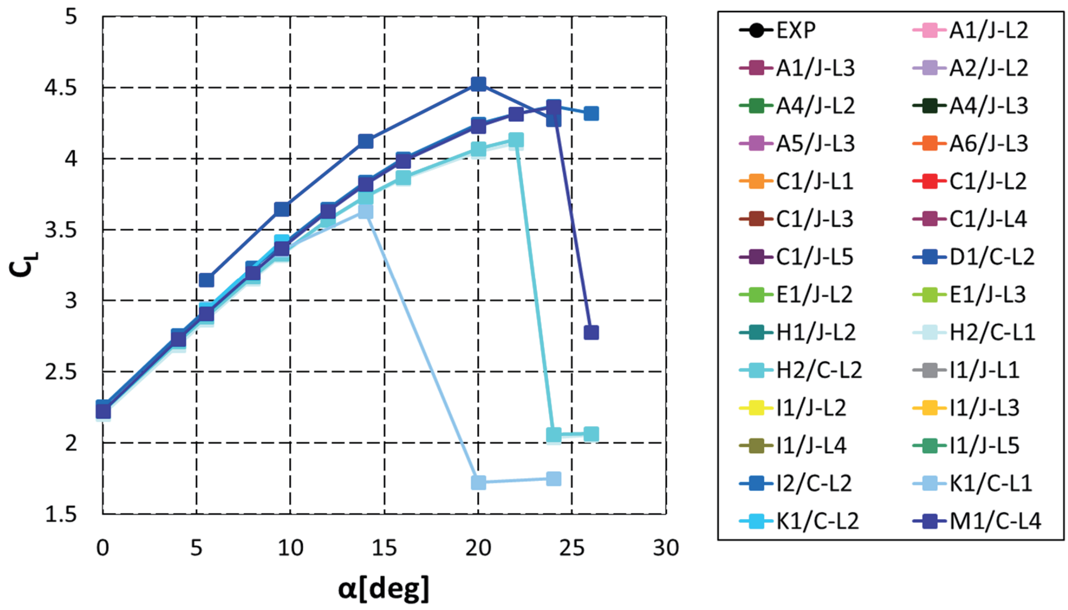

There was large influence on grid type.

22

Case 1-1 : α - sweep

Comparison by grid resolution : provided grid

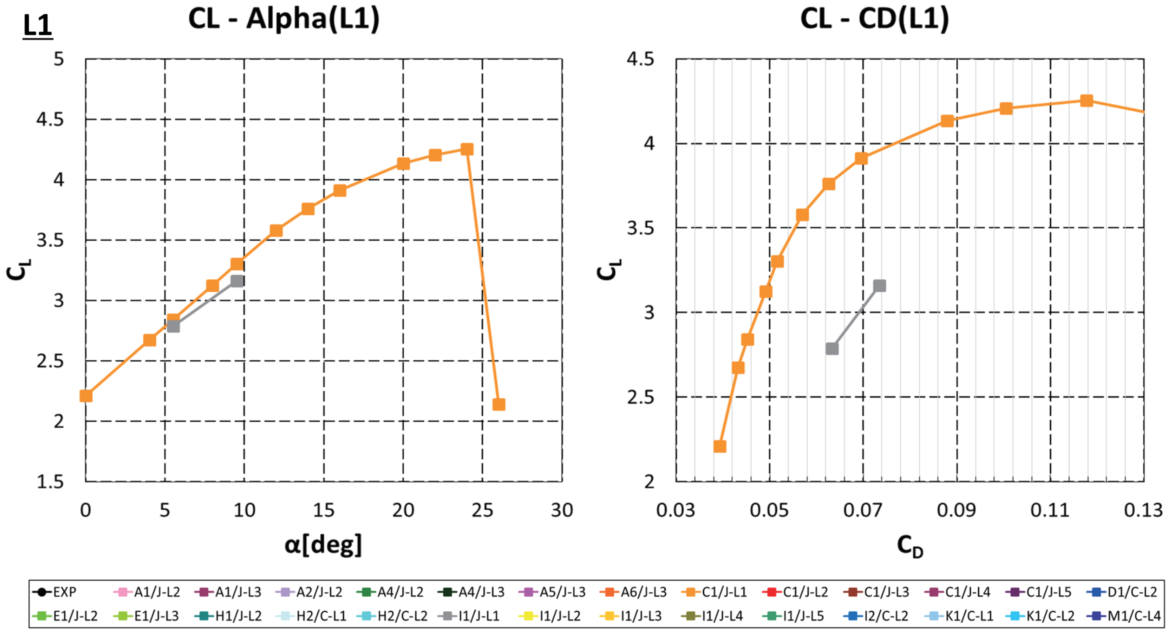

23

Case 1-1 : α - sweep

Comparison by grid resolution : provided grid

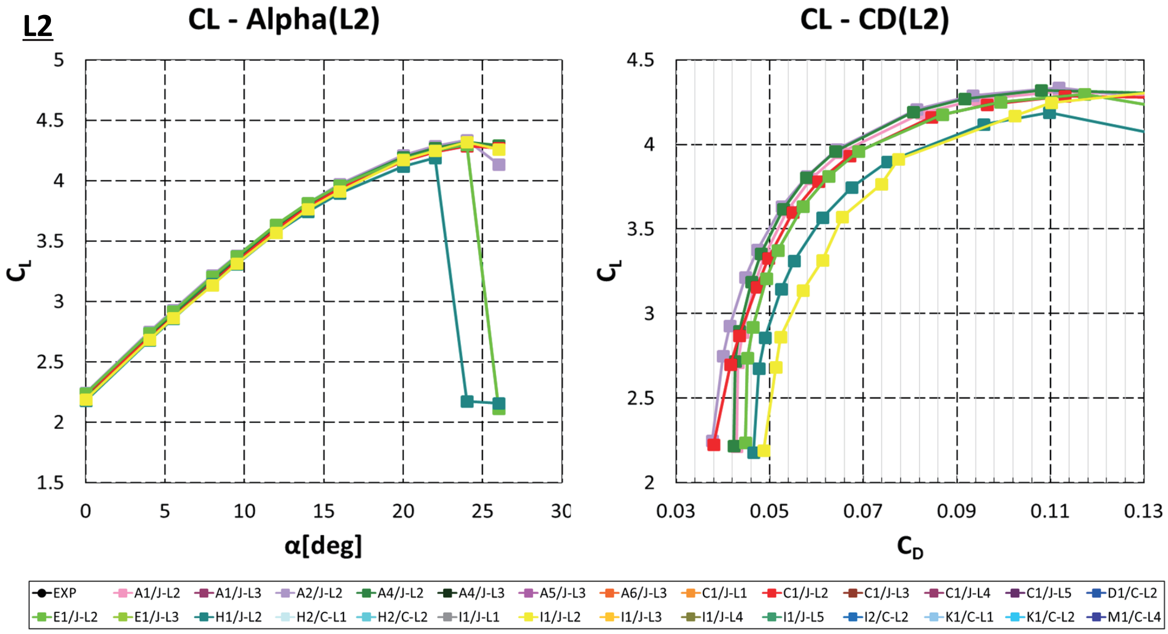

24

Case 1-1 : α - sweep

Comparison by grid resolution : provided grid

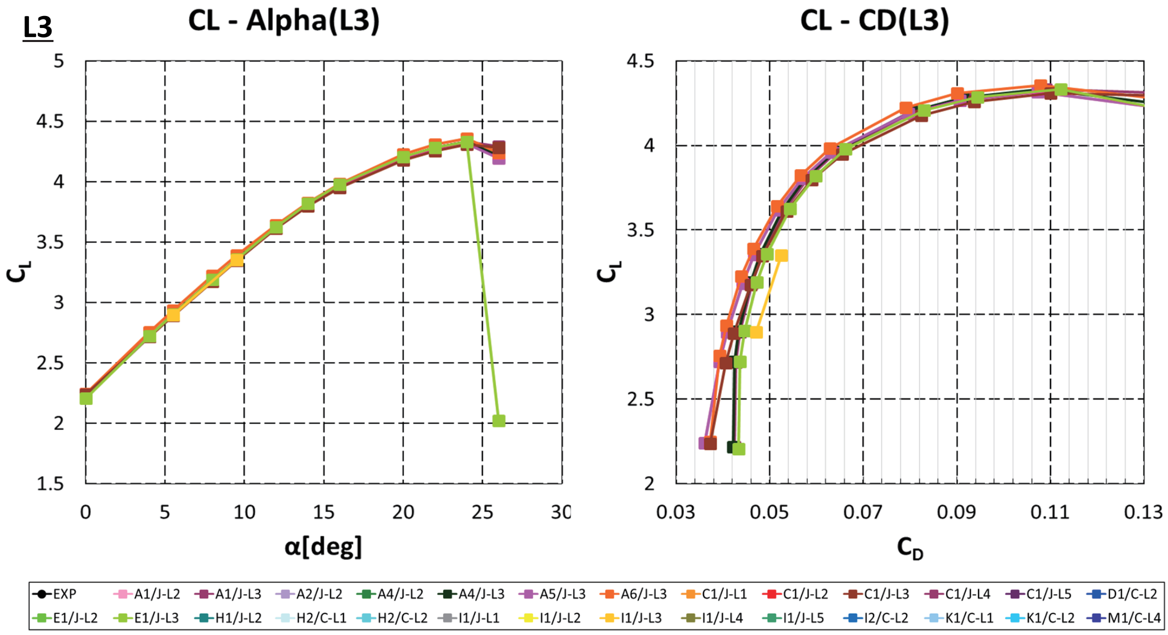

25

Case 1-1 : α - sweep

Comparison by grid resolution : provided grid

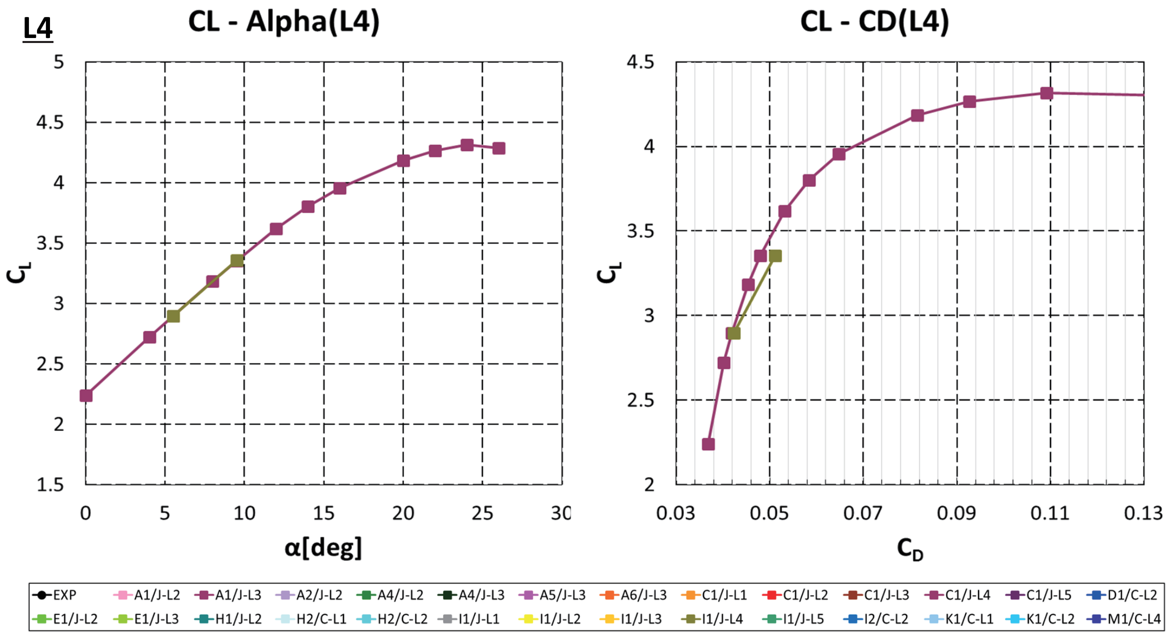

26

Case 1-1 : α - sweep

Comparison by grid resolution : provided grid

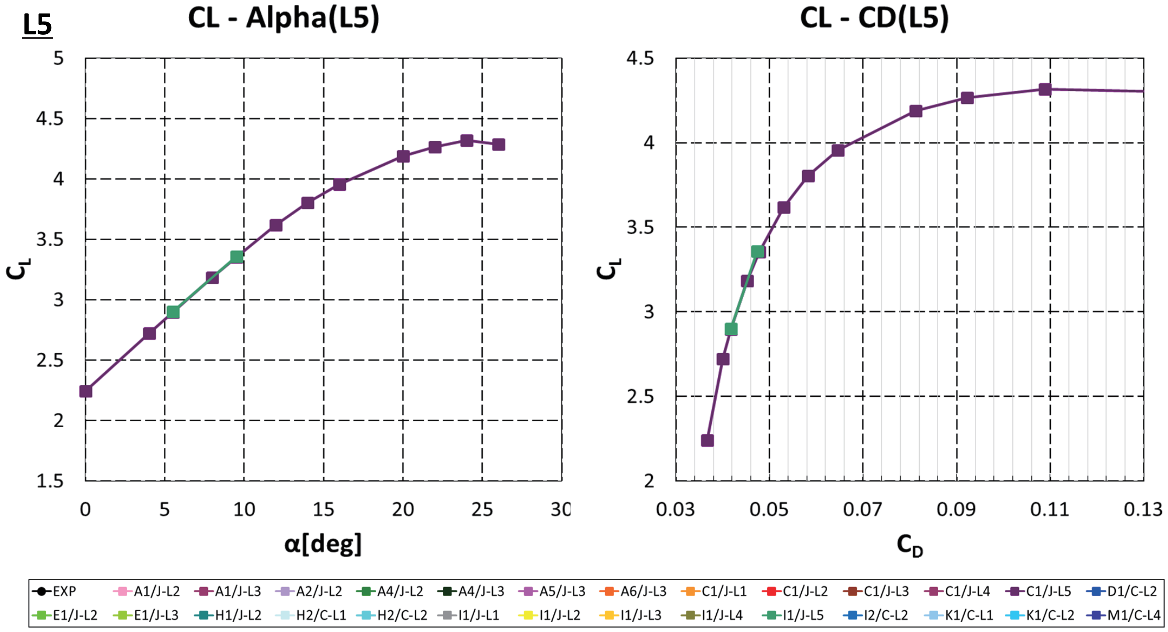

27

Case 1-1 : Cp分布

AoA=5.5deg, Comparison with exp.

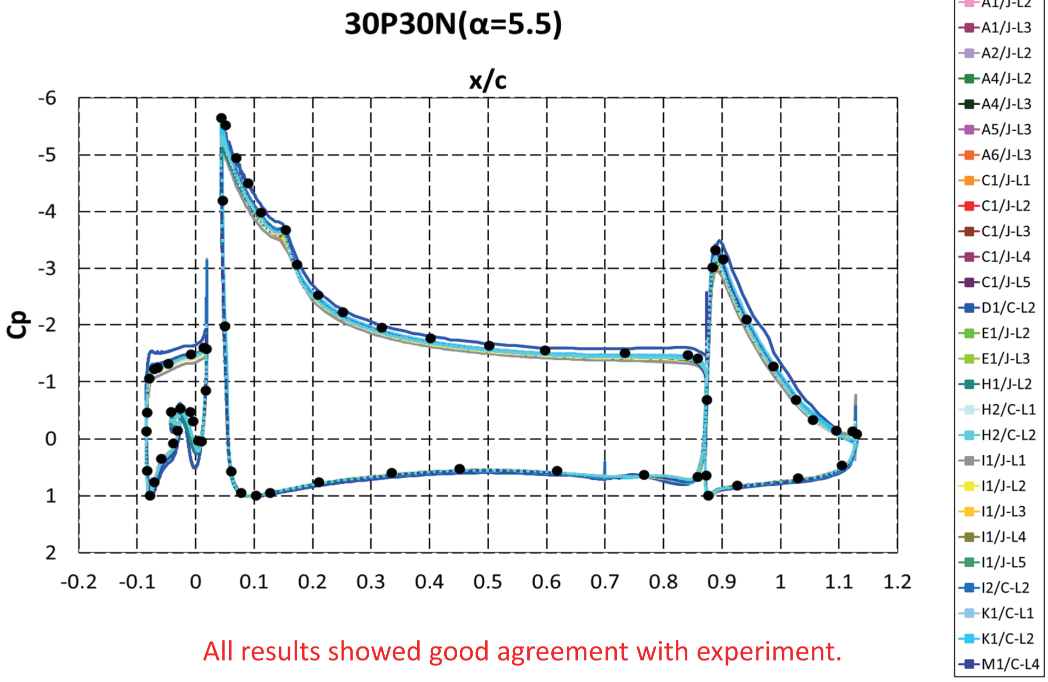

All results showed good agreement with experiment.

28

Case 1-1 : Cp

AoA=5.5deg, Comparison with exp. : provided grid

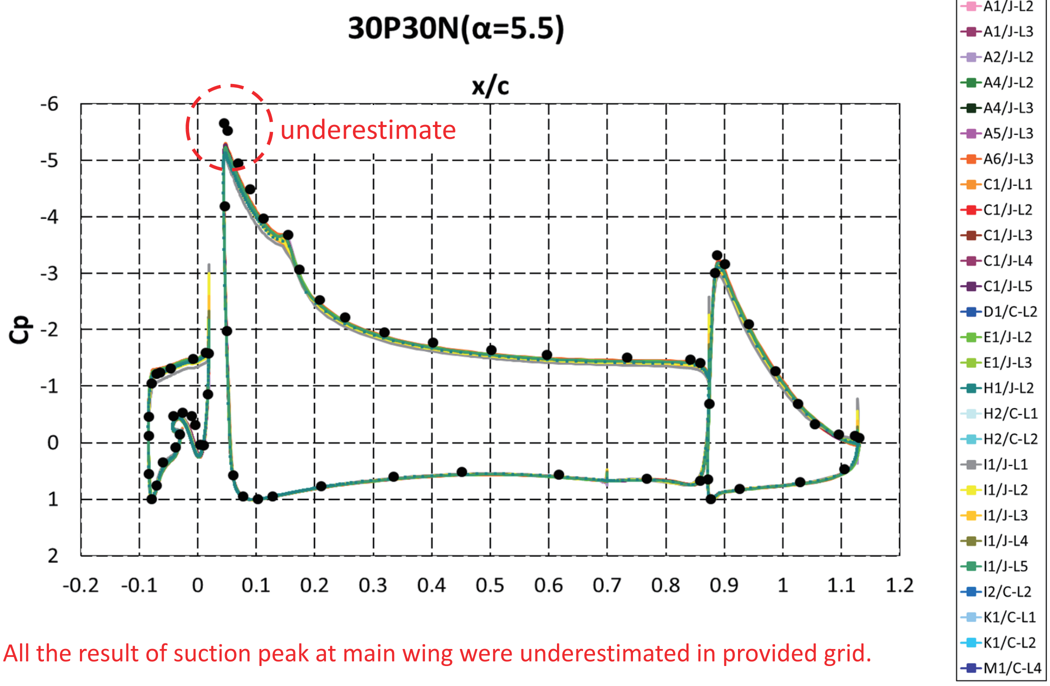

All the result of suction peak at main wing were underestimated in provided grid.

29

Case 1-1 : Cp

AoA=9.5deg, Comparison with exp.

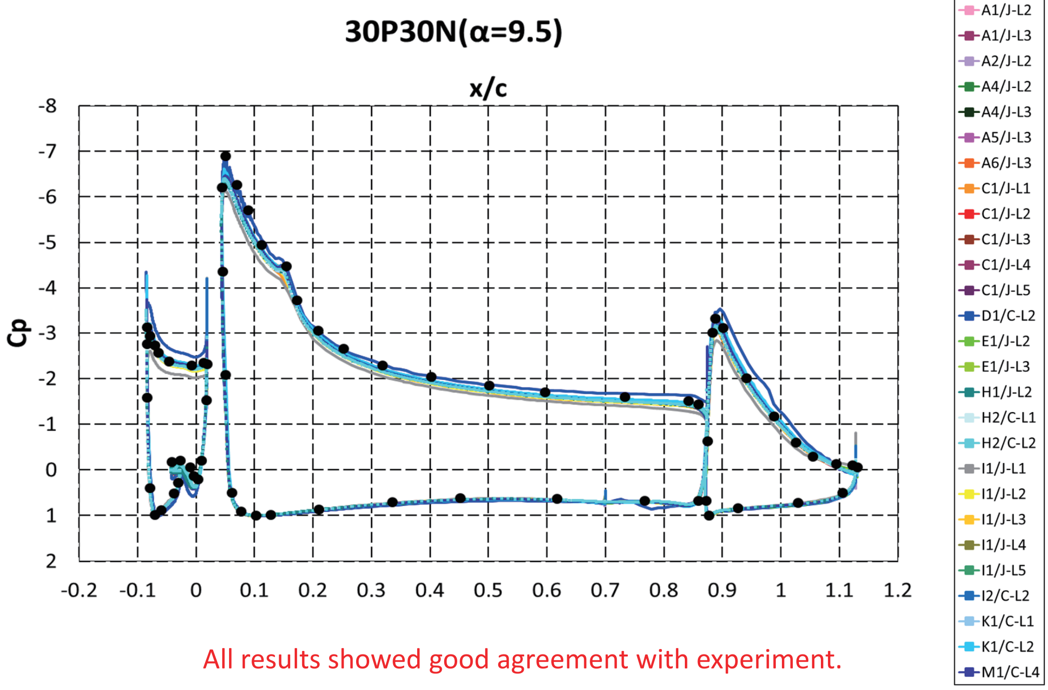

All results showed good agreement with experiment.

30

Case 1-1 : Cp

AoA=14deg, Comparison with exp.

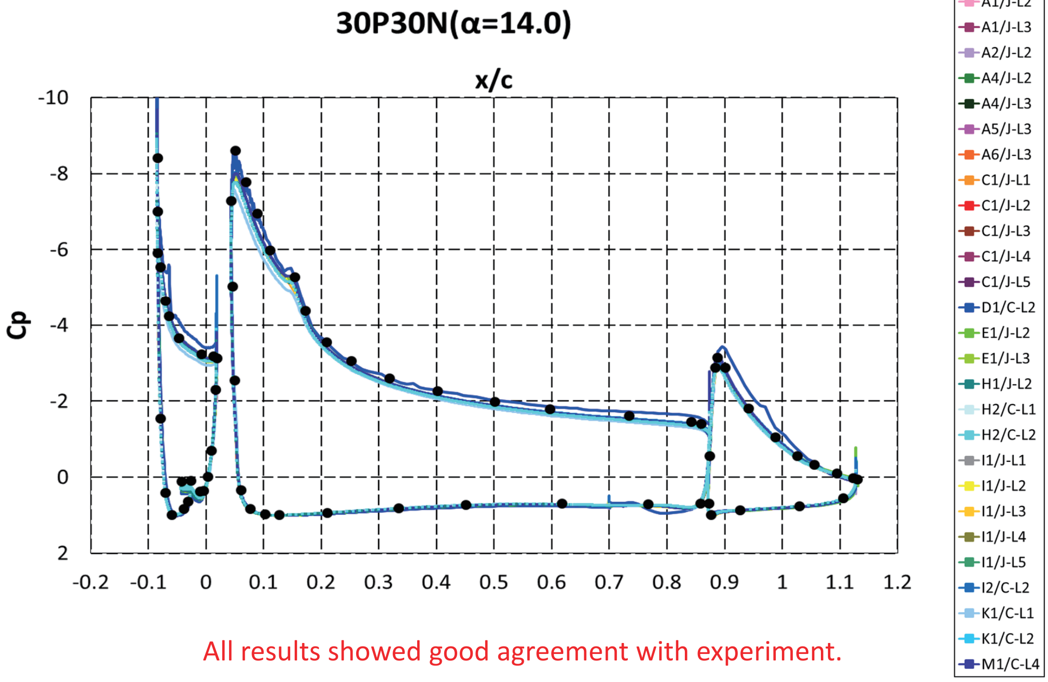

All results showed good agreement with experiment.

31

Case 1-1 : Cp

AoA=24deg, Comparison of high-AoA Cp

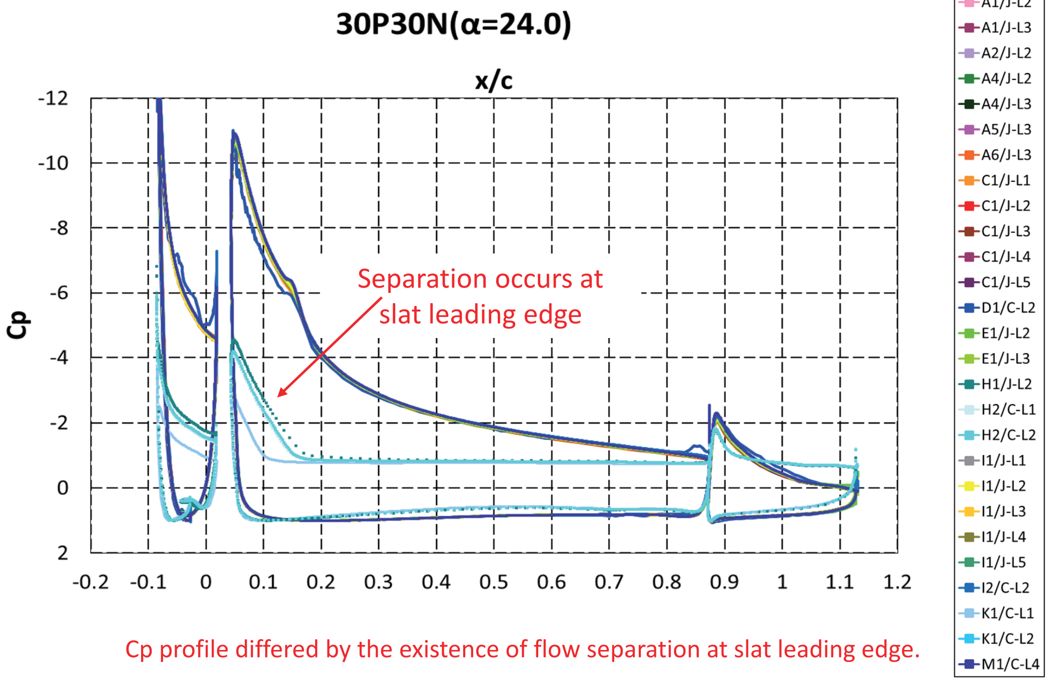

Cp profile differed by the existence of flow separation at slat leading edge.

32

Case 1-1 : $\tilde{\nu}/\nu$

AoA=5.5deg, Comparison of grid type

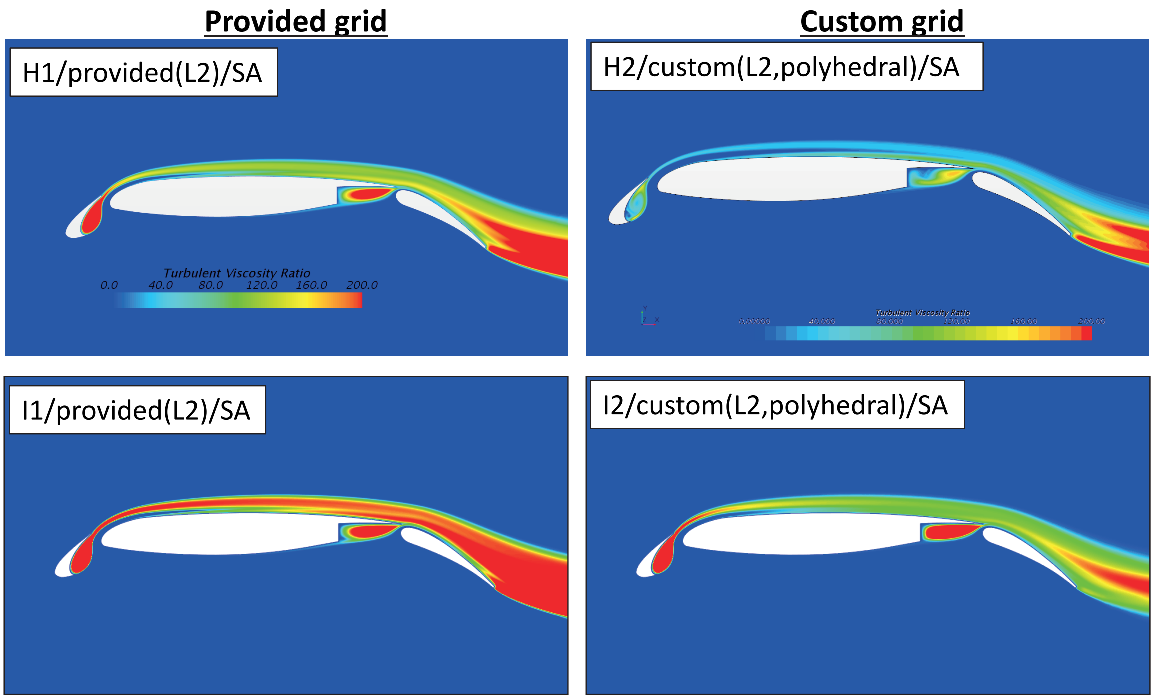

The influence of grid topology was large.

33

Case 1-1 : $\tilde{\nu}/\nu$

AoA=5.5deg, Comparison of SA and SA-R

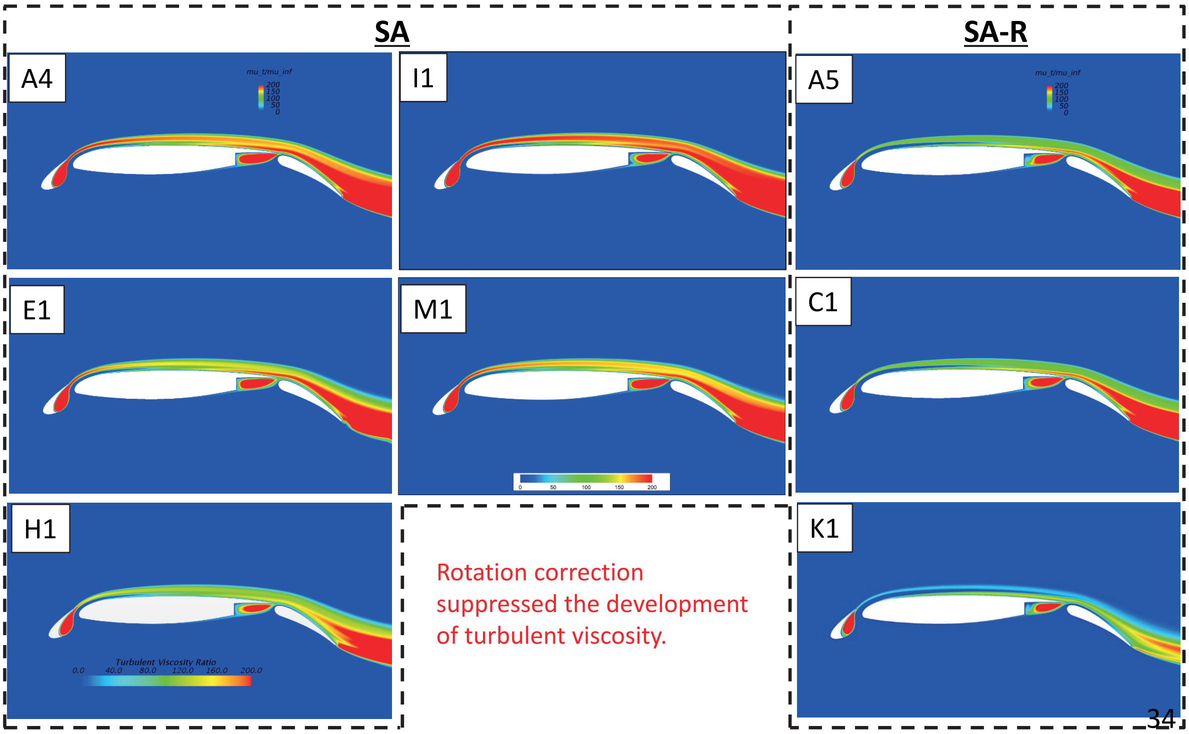

Rotation correction suppressed the development of turbulent viscosity.

34

Case 1-1 : $\tilde{\nu}/\nu$

AoA=5.5deg, Comparison of SA and SA-R

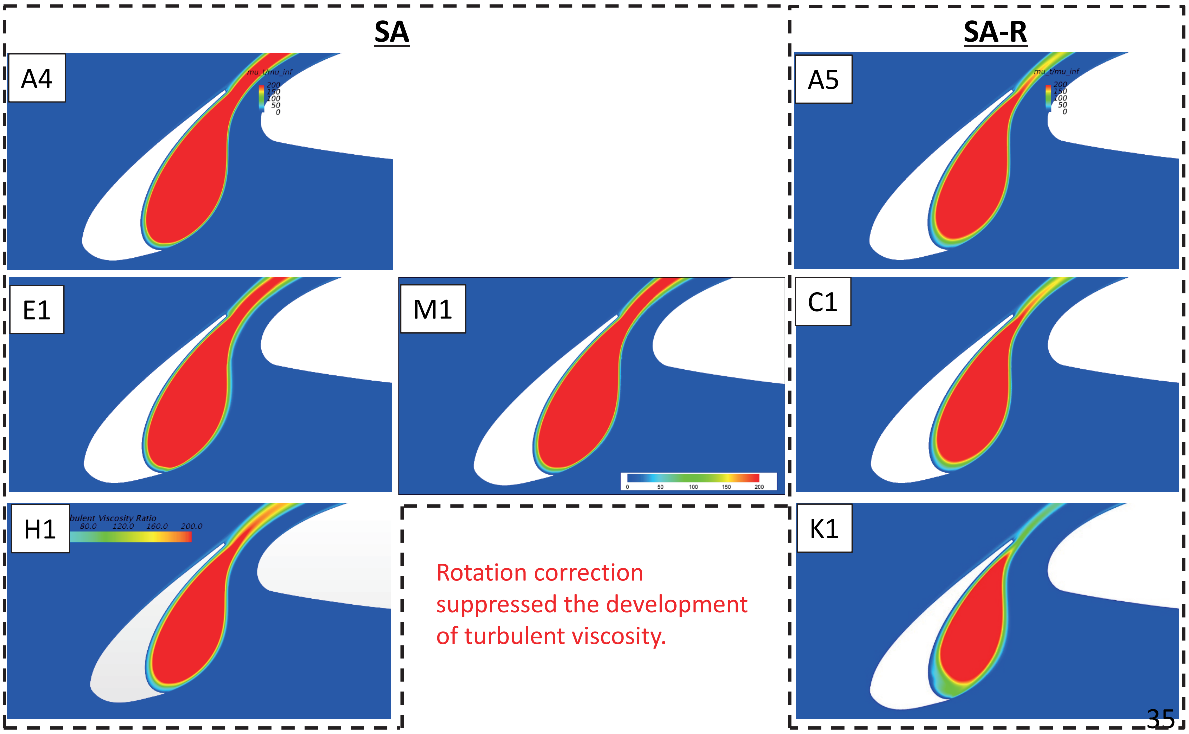

35

Case 1 : Prediction of aerodynamics

– Case1-2 : 2.5D steady flow simulation
- Geom. : 30P30N（modified_slat_configF）
- Grid : provided（required : L2, optional : L1,L3~L5）or custom
- Cond. : M = 0.17, Re = 1.71 x 10^6
- AoA : 0/4/5.5/8/9.5/12/14/16/20/22/24/26 [deg]
  (red : required、black : optional)
- List of data :
  – Aerodynamic coefficients(C_D,C_L,C_m),C_p,C_f
  – Surface contours of C_p,C_f
  – Surface streamline
  – Contours of $\tilde{\nu}/\nu$
  – Spatial streamlines
  – Velocity profiles

36

Case 1-2 : Aerodynamic coefficients

Comparison with 2D simulation

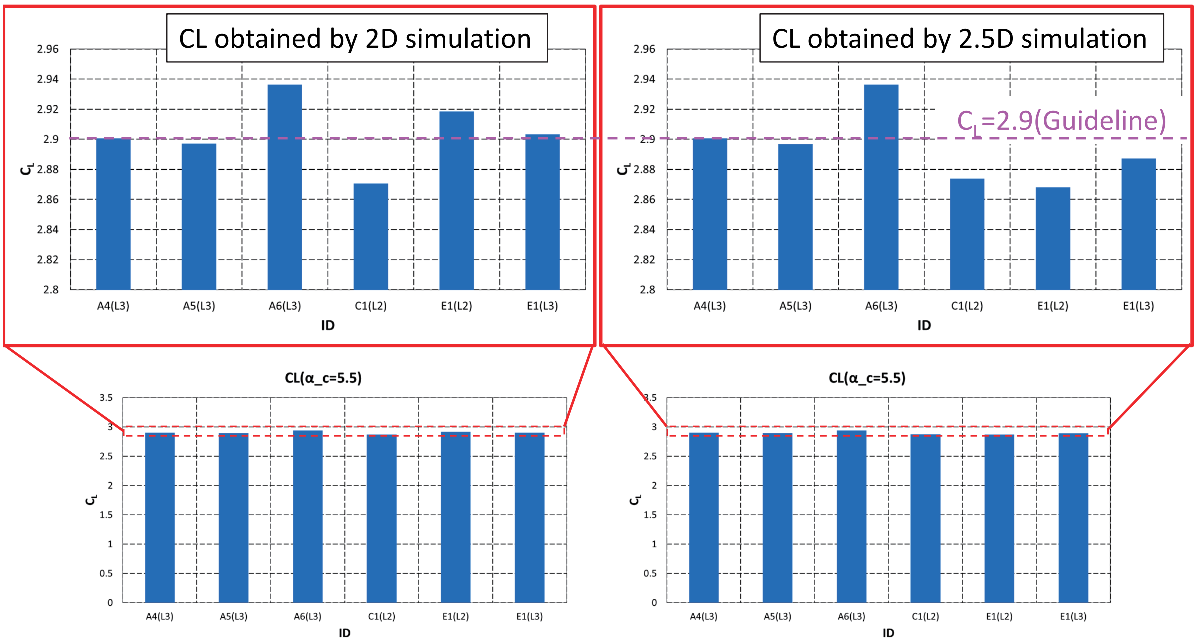

There was little difference between 2D and 2.5D simulations.

Case 1-2 : Cf

AoA=5.5deg

C1/provided(L2)/SA-noft2-R

E1/provided(L2)/SA-noft2

STAR-CCM+

H1/custom(L2,trimmed)/SA

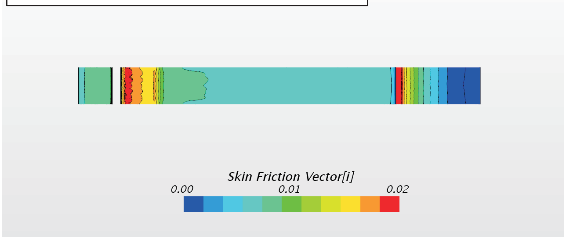

E2/custom(L2,Octree+layer grid)/SA-noft2

The fluctuation of Cf distribution along the spanwise direction disappeared by use of periodic boundary condition.

Case 1-2 : Streamlines on flap

AoA=5.5deg

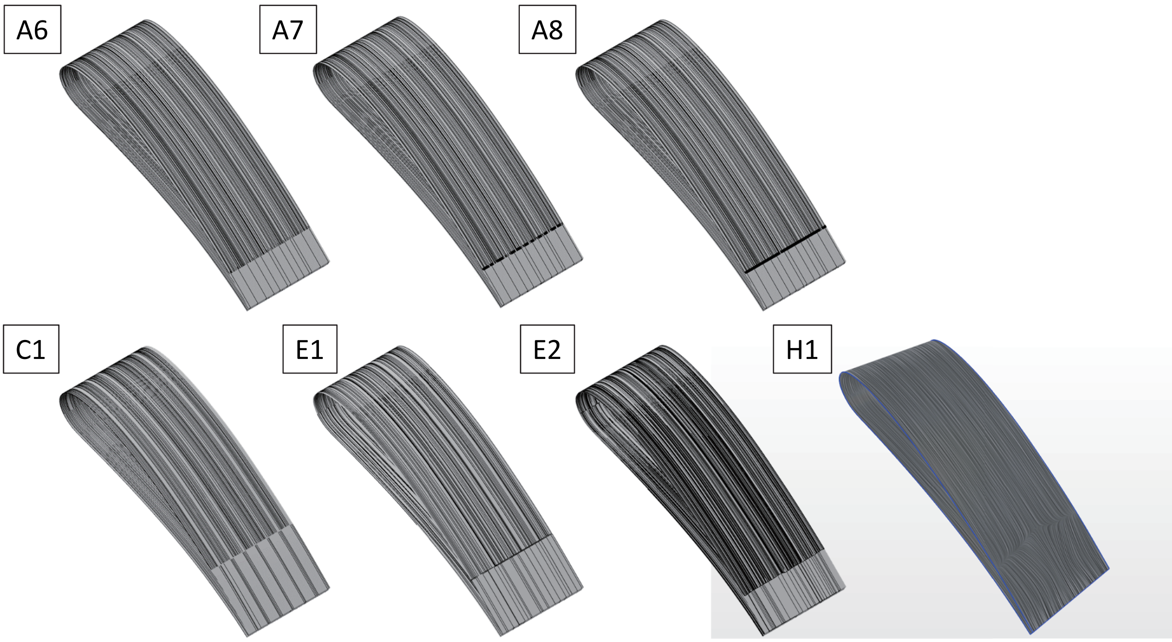

The fluctuation of streamlines along the spanwise direction disappeared by use of periodic boundary condition.

39

Case 1 : Prediction of aerodynamics

– Case1-3 : 2.5D unsteady flow simulation

- Geom. : 30P30N（modified_slat_configF ）
- Grid : provided（required : L2, optional : L1,L3~L5）or custom
- Cond. : M = 0.17, Re = 1.71 x 10^6
- AoA : 5.5/9.5 [deg]
- List of data(time averaged) :
  - Aerodynamic coefficients(C_D,C_L,C_m),C_p,C_f
  - Surface contours of C_p,C_f
  - Surface streamline
  - Contours of
  - Spatial streamline
  - Velocity profiles

Legend(paticipant ID / grid type [J:provided by JAXA, C:custom] - grid resolution [L1~L5])

EXP	A2/J-L2
A2/J-L3	A3/J-L2
A3/J-L3	A4/J-L3
A5/J-L3	A6/J-L2
A6/J-L3	A7/J-L2
A7/J-L3	A8/J-L2
B1/J-L3	B2/J-L3
B3/J-L3	C1/J-L2
D1/C-L2	E1/J-L1
E1/J-L2	E1/J-L3
E2/C-L2	E2/C-L3
G1/C-L2	H1/C-L2
J1/J-L3	

40

Case 1-3 : Cp (unsteady)

AoA=5.5deg, Comparison with steady solution

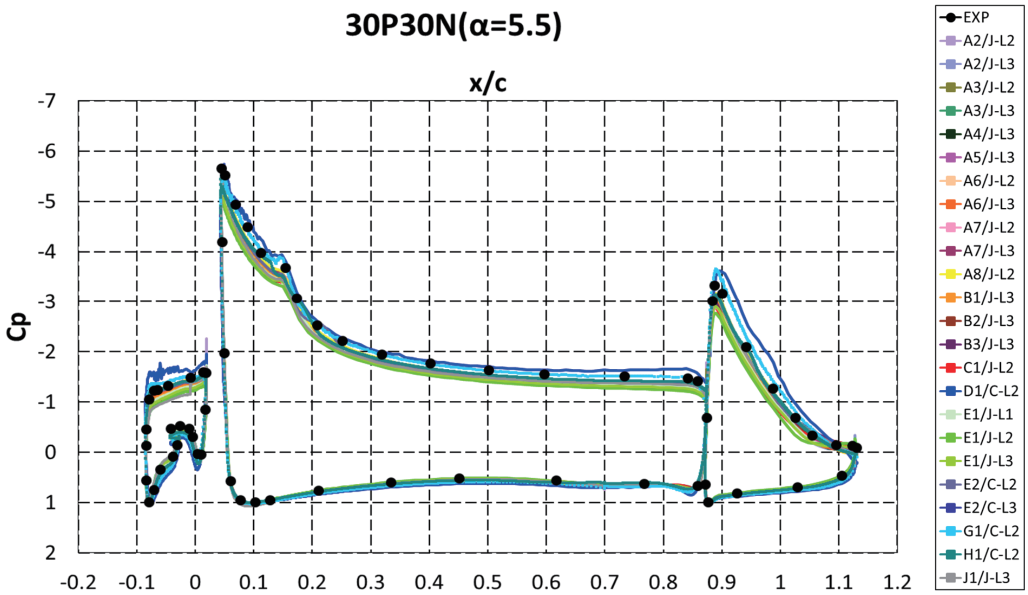

Unsteady results underestimated Cp profile compared to steady solutions.

Case 1-3 : Cp (steady)

AoA=5.5deg

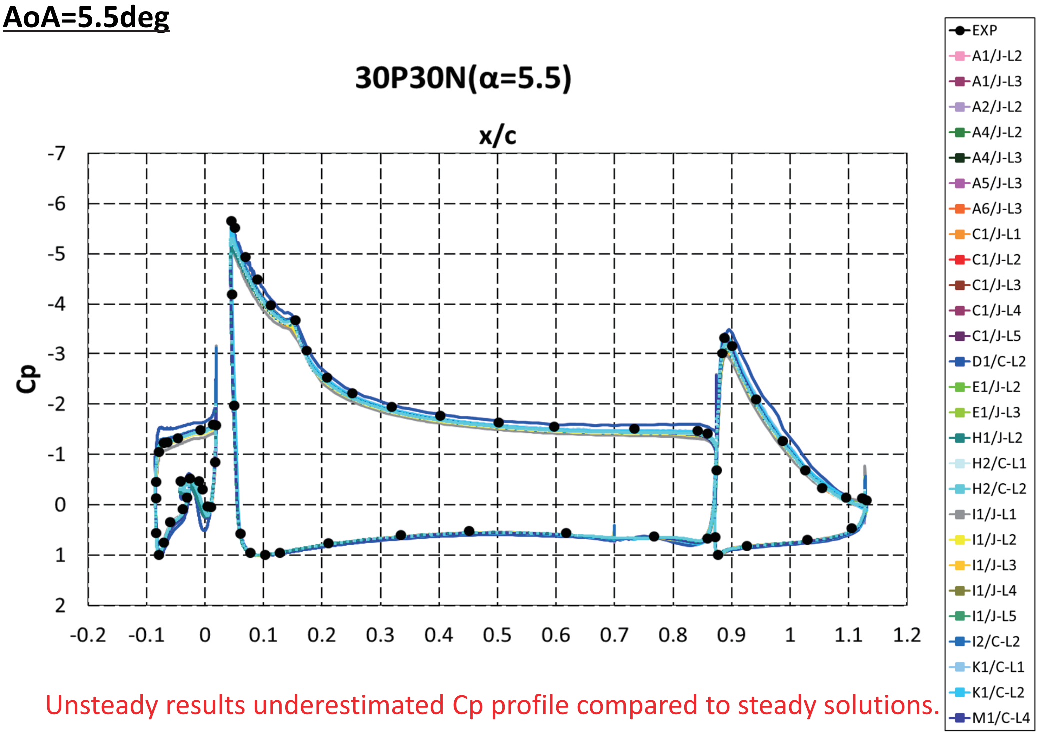

Unsteady results underestimated Cp profile compared to steady solutions.

Case 1-3 : Cp(Slat)

AoA=5.5deg, Comparison of each parts

Slat

Unsteady(averaged)

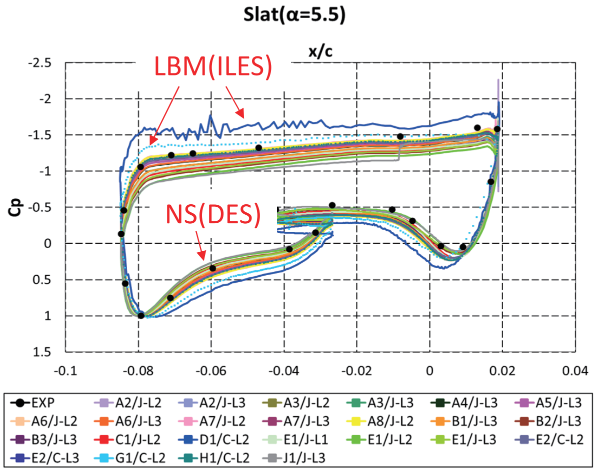

Steady

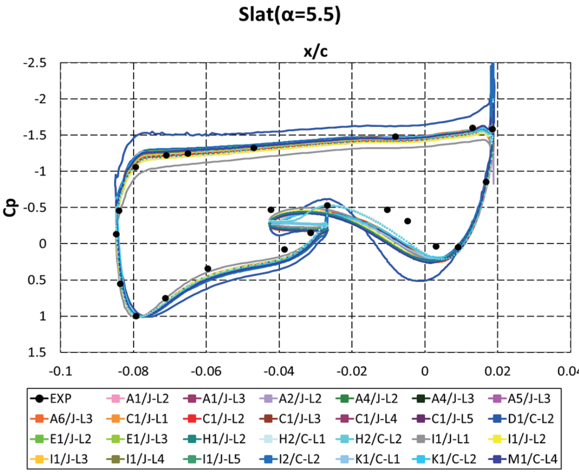

Steady simulations showed good agreement with experiment at upper surface.
Unsteady simulations underestimated Cp at upper surface but show better agreement with experiment at lower surface.
LBM overestimated Cp.

43

Case 1-3 : Cp(Main)

AoA=5.5deg, Comparison of each parts

Main

Unsteady(averaged)

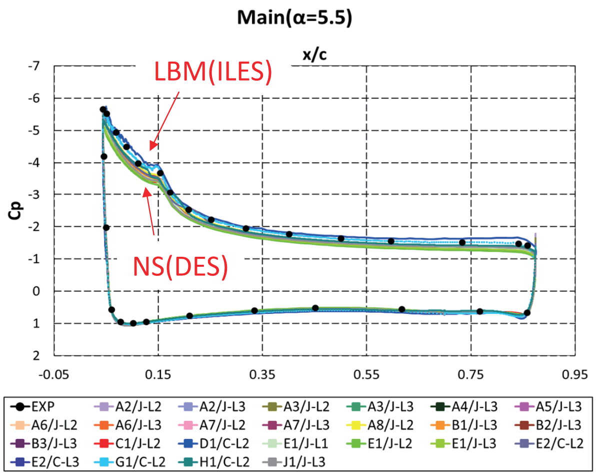

Steady

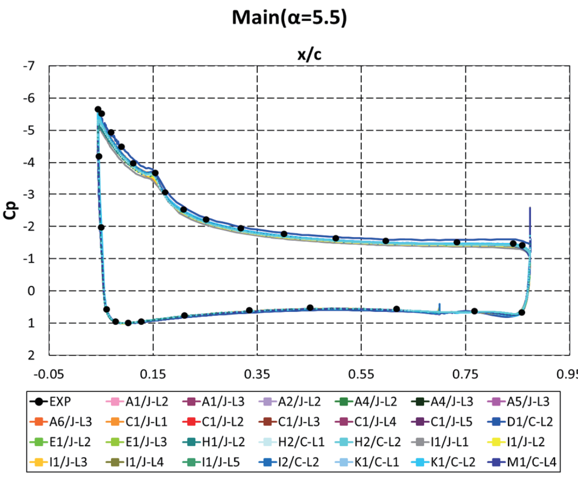

NS results underestimated the suction peak.
Some steady flow simulation results captured the suction peak by use of custom grid.
LBM results showed better agreement with experiment.

44

Case 1-3 : Cp(Flap)

AoA=5.5deg, Comparison of each parts

Flap

Unsteady(averaged)

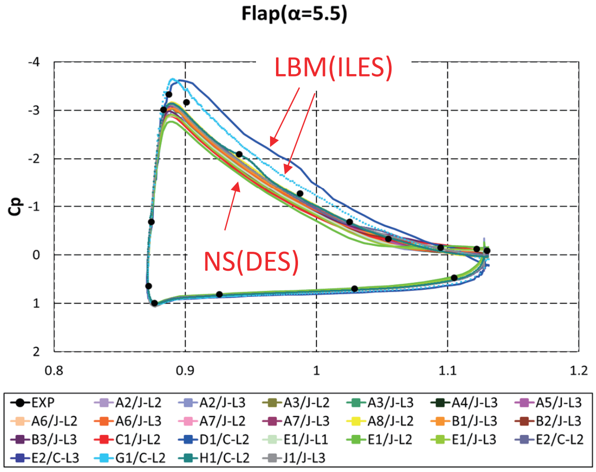

Steady

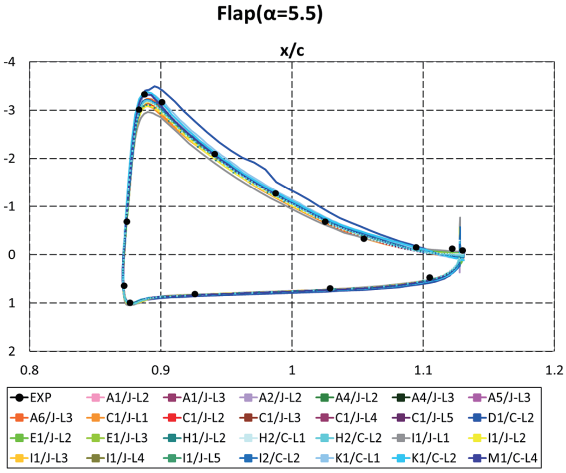

Steady flow simulation by NS showed good agreement with experiment, but unsteady flow simulation by NS underestimated Cp.
LBM results overestimated Cp at upper surface, but the suction peak was better than NS.

Case 1-3 : Cp(unsteady)

AoA=9.5deg, Comparison with steady solution

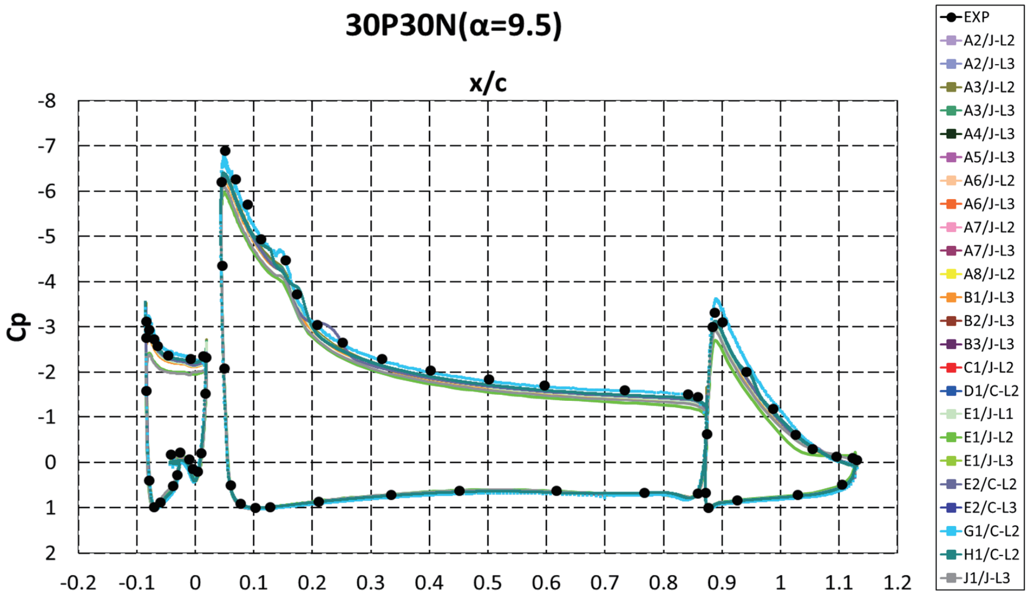

Same trend with AoA=5.5degree was observed.

Case 1-3 : Cp(steady)

AoA=9.5deg, Comparison with steady solution

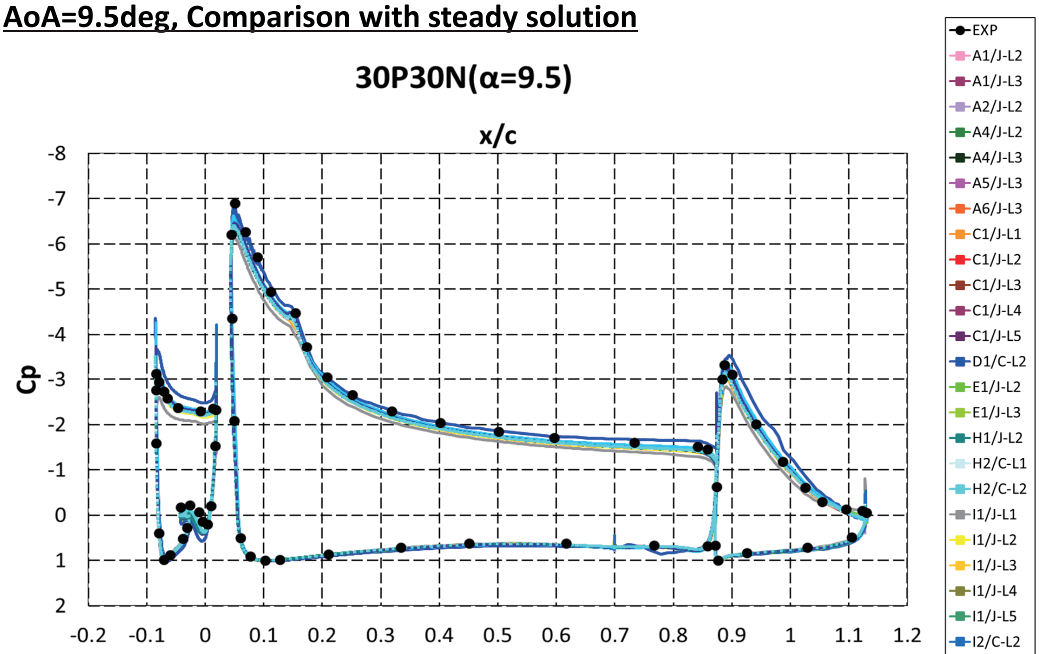

Same trend with AoA=5.5degree was observed.

47

Case 1-3 : Cf分布

AoA=5.5deg, Comparison by solver type

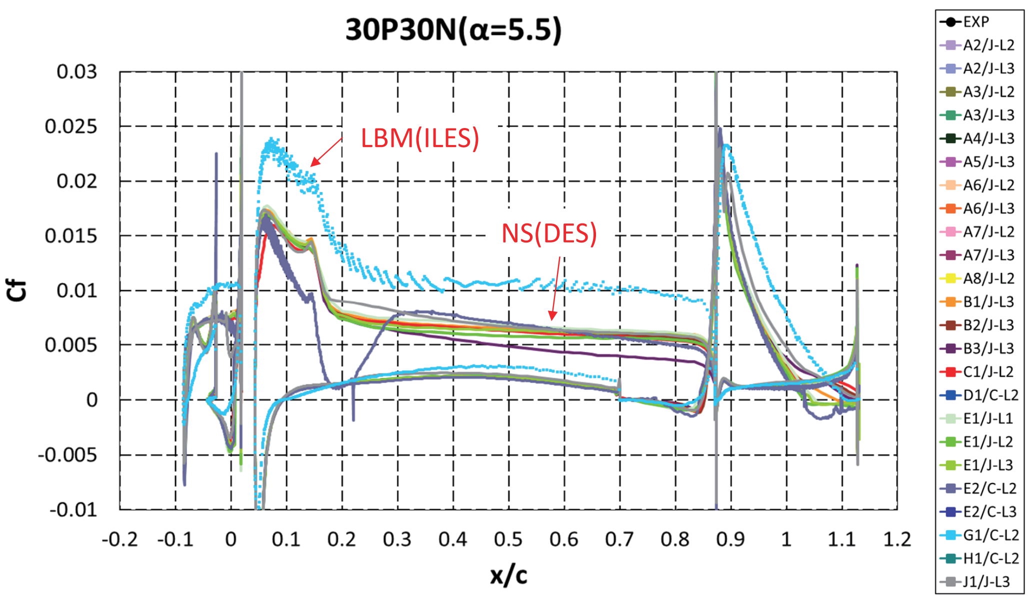

The variation was large and LBM overestimated Cf.

48

Case 1-3 : The position of velocity profile comparison

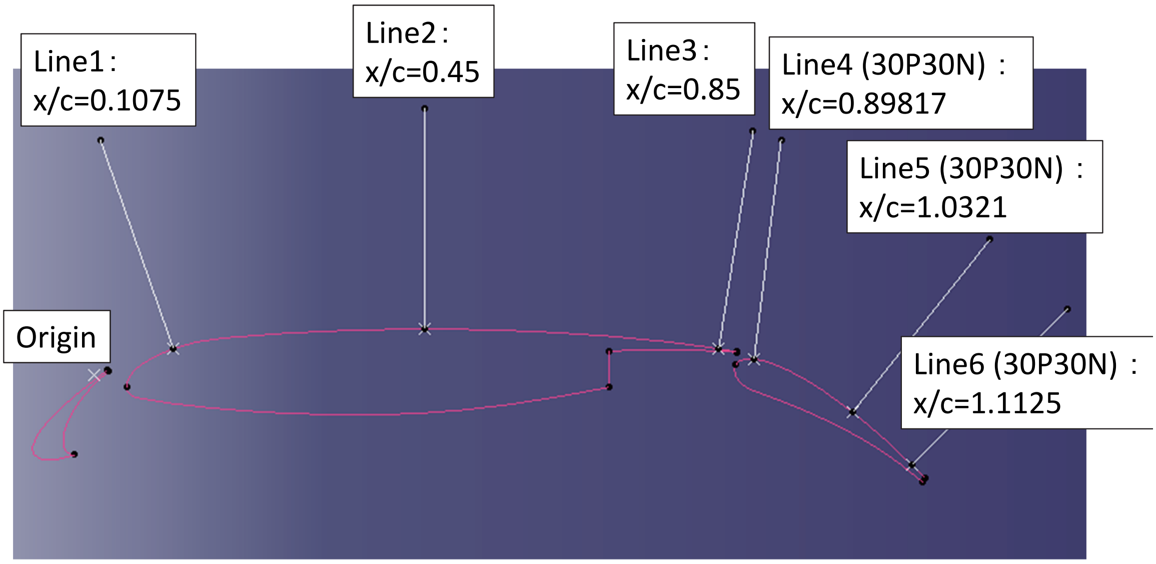

49

Case 1-3 : Velocity profiles(unsteady)

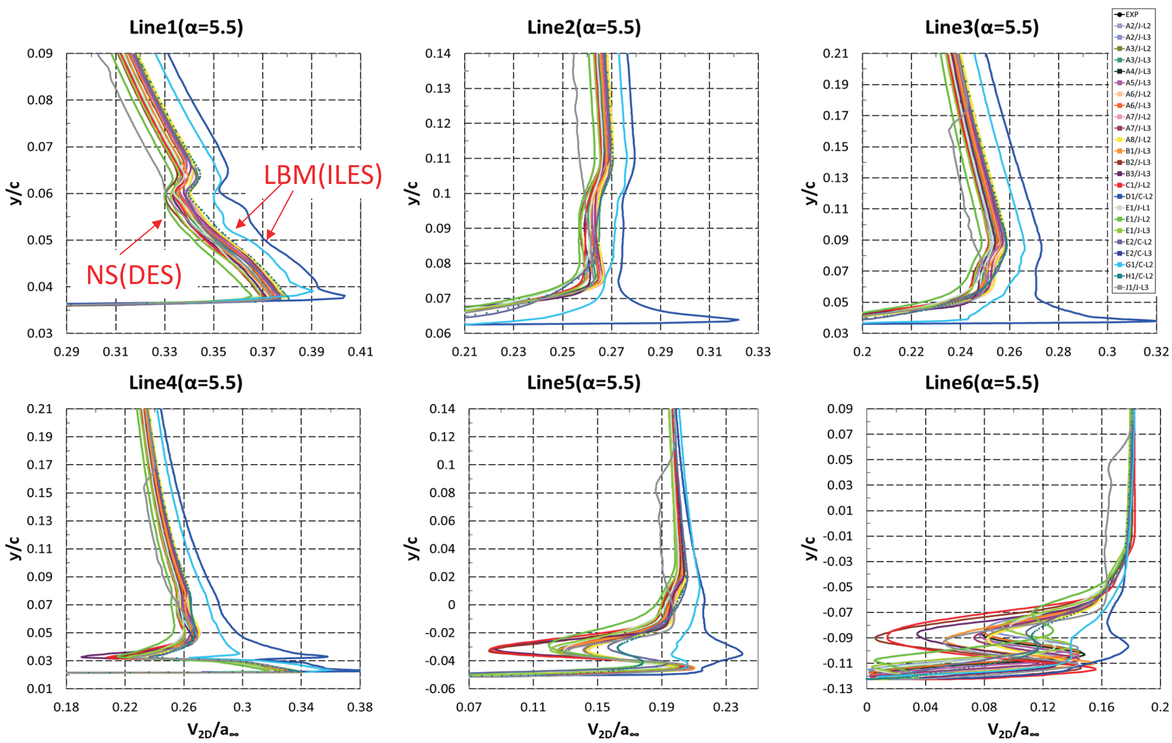

Velocity profiles differed between steady and unsteady flow simulations, and also between NS and LBM. 50

Case 1-3 : Velocity profiles(steady)

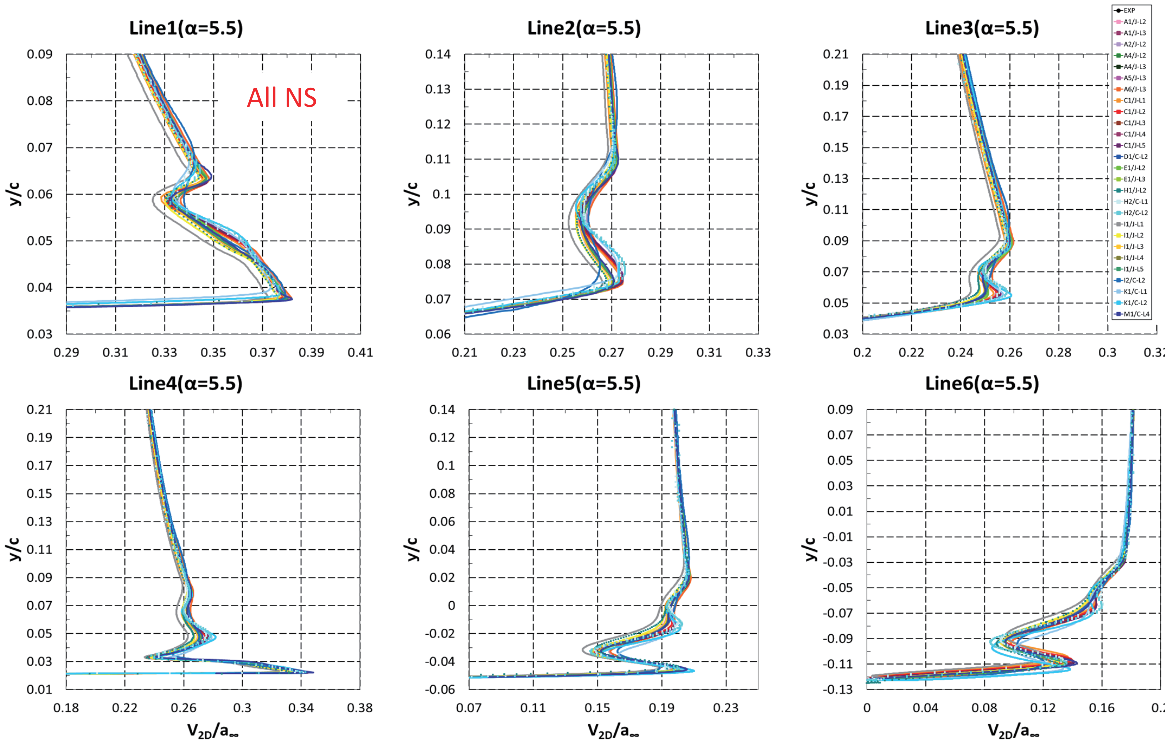

Velocity profiles differed between steady and unsteady flow simulations, and also between NS and LBM. 51

Case 1-3 : Streamlines on flap(L1)

AoA=5.5deg, provided grid, comparison of L1

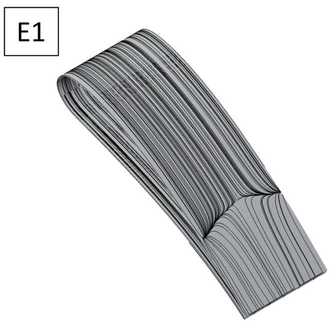

The position of flow separation moved forward by increasing grid resolution.

52

Case 1-3 : Streamlines on flap(L2)

AoA=5.5deg, provided grid, comparison of L2

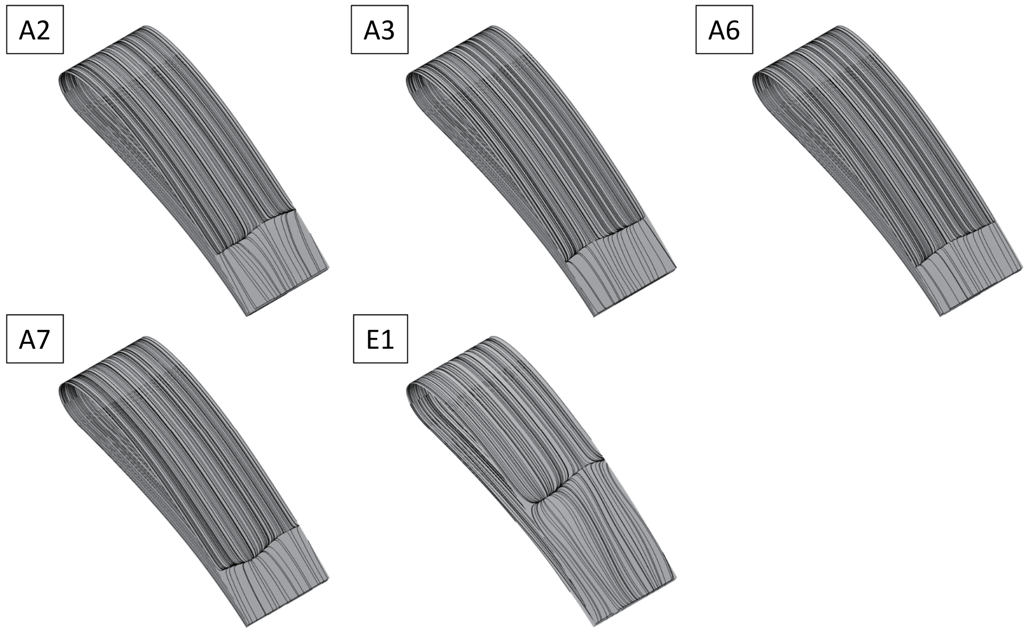

The position of flow separation moved forward by increasing grid resolution.

53

Case 1-3 : Streamlines on flap(L3)

AoA=5.5deg, provided grid, comparison of L3

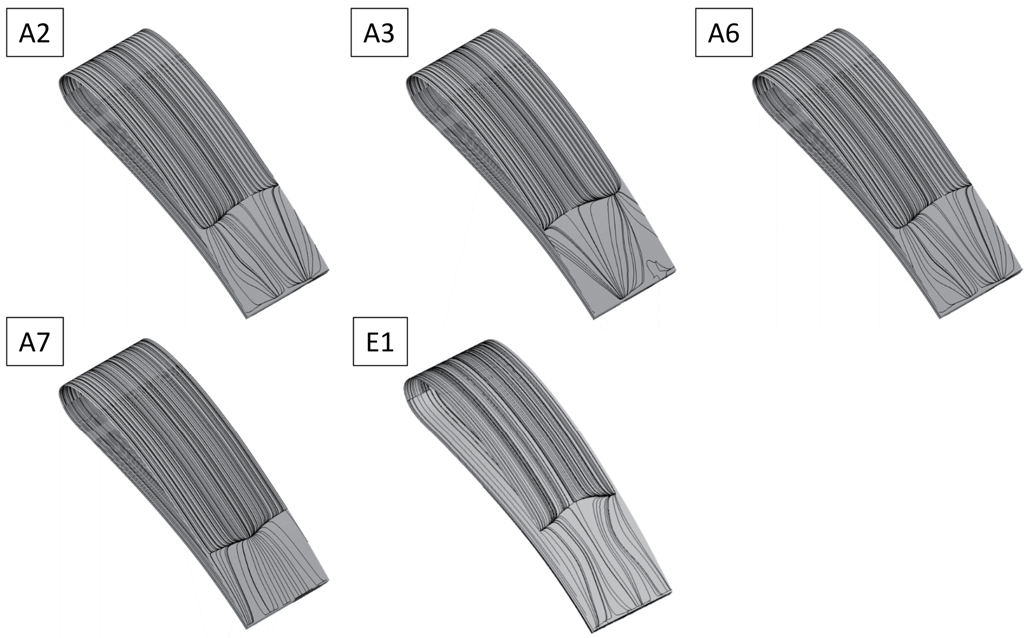

The position of flow separation moved forward by increasing grid resolution.

54

Case 1-3 : $\tilde{\nu}/\nu$ (L1)

AoA=5.5deg, provided grid, comparison of L1

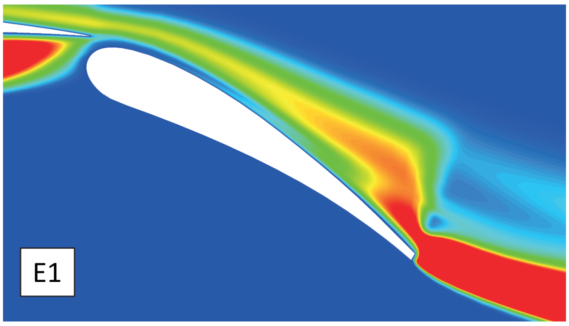

Turbulent viscosity decreased in L3 grid.

Case 1-3 : $\tilde{\nu}/\nu$ (L2)

AoA=5.5deg, provided grid, comparison of L2

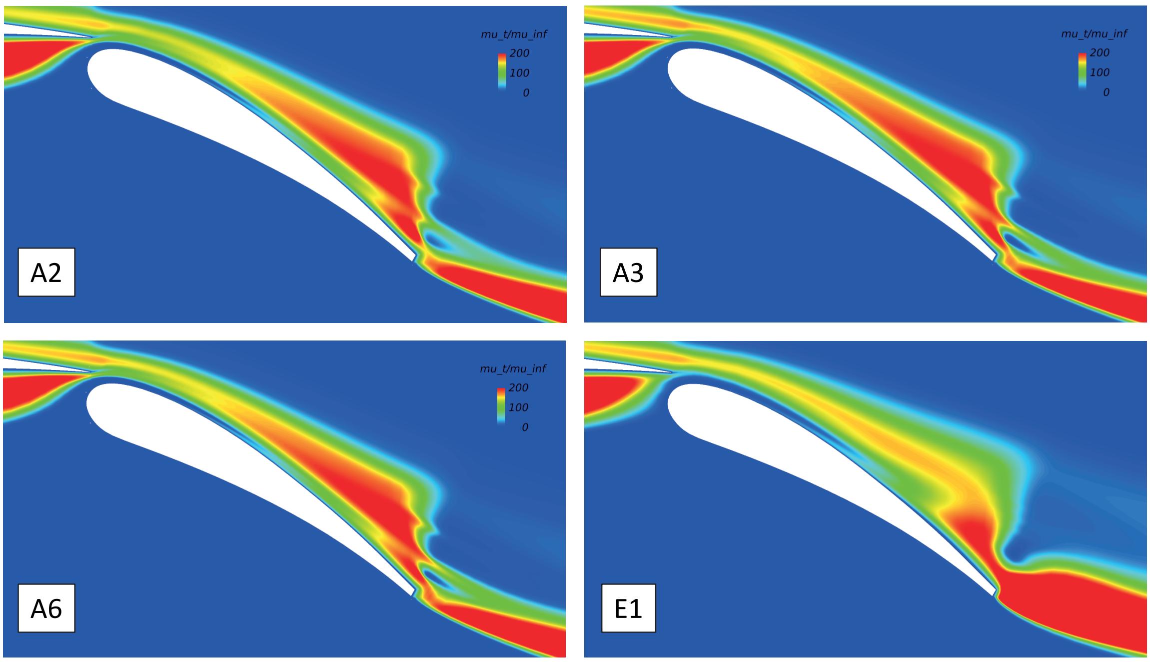

Turbulent viscosity decreased in L3 grid.

Case 1-3 : $\tilde{\nu}/\nu$ (L3)

AoA=5.5deg, provided grid, comparison of L3

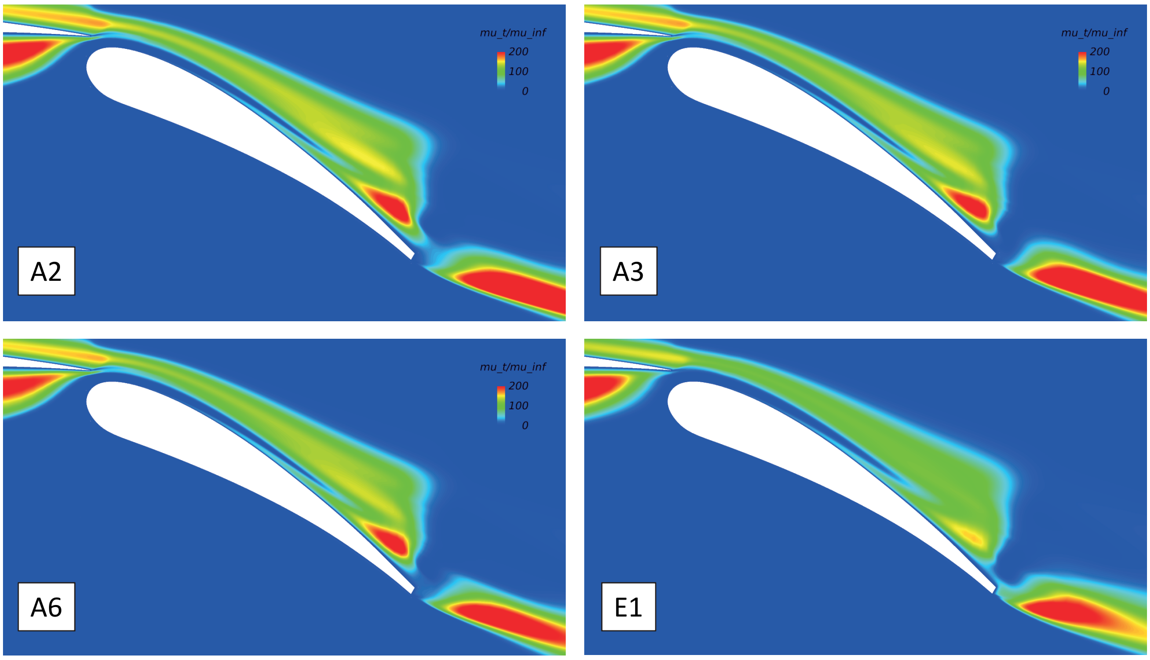

Turbulent viscosity decreased in L3 grid.

57

Case 1 Summary

- Case 1-1 : 2D RANS
  - The variation in results was significant compared with past APC series.
  - There was large influence on type of grid (Cartesian or Unstructured) and flow solver(NS or LBM).
  - Good agreement with experiment was obtained.
  - Cp (especially around the suction peak) was underestimated by the provided grid.
  - The variation was large at high-AoA results with the existence of large separation at slat.
  - Turbulent viscosity was suppressed by rotation correction for SA.
- Case 1-2 : 2.5D RANS
  - Spanwise distribution was disappeared by use of periodic boundary condition.
  - The position of flow separation at flap was almost same in each group due to the use of same turbulence model.
- Case 1-3 : 2.5D unsteady flow simulation
  - Time-averaged Cp by unsteady flow simulation was relatively smaller than RANS.
  - Slat Cp computed by unsteady flow simulation showed good agreement with experiment.
  - Cp by NS < Cp by LBM
  - Velocity profiles showed different trend between NS and LBM.
  - The position of flow separation at flap moved forward by increasing grid resolution.
  - L3 grid produced smaller turbulent viscosity than L2 grid.

58

Case 2 : Prediction of flow separation at flap

– Case2-1 : 2D steady flow simulation
  - Geom. : 30P35N （modified_slat_configF）
  - Grid : provided（required : L2, optional : L1,L3~L5）or custom
  - Cond. : M = 0.17, Re = 1.71 x 10^6
  - AoA : 5.5 [deg]
  - List of data :
    - Aerodynamic coefficients(C_D,C_L,C_m),C_p,C_f
    - Contours of $\tilde{\nu}$ / ν
    - Spatial streamlines
    - Velocity profiles

Legend(paticipant ID / grid type [J:provided by JAXA, C:custom] - grid resolution [L1~L5])

EXP(30P30N)	A1/J-L2
A1/J-L3	C1/J-L2
E1/J-L2	E1/J-L3
H1/J-L2	H2/C-L1
H2/C-L2	I1/J-L2
I2/C-L2	K1/C-L1

Case 2-1 : C_D

Comparison with 30P30N

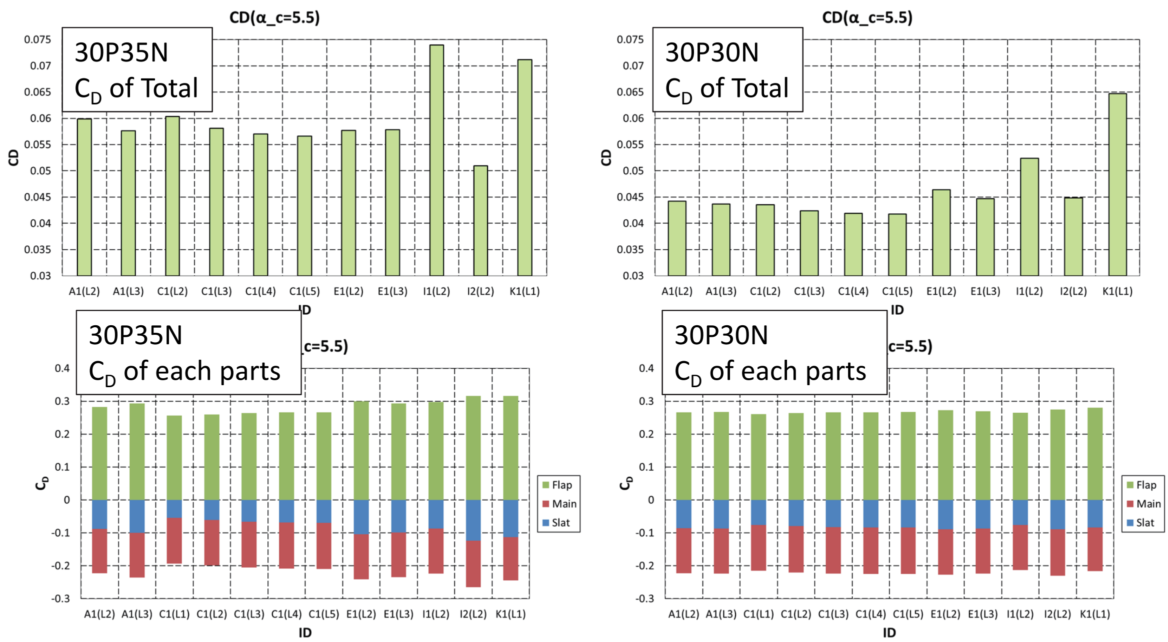

CD of 30P35N increased compared to result of 30P30N.
The variation increased due to flow separation at flap.

Case 2-1 : C_L

Comparison with 30P30N

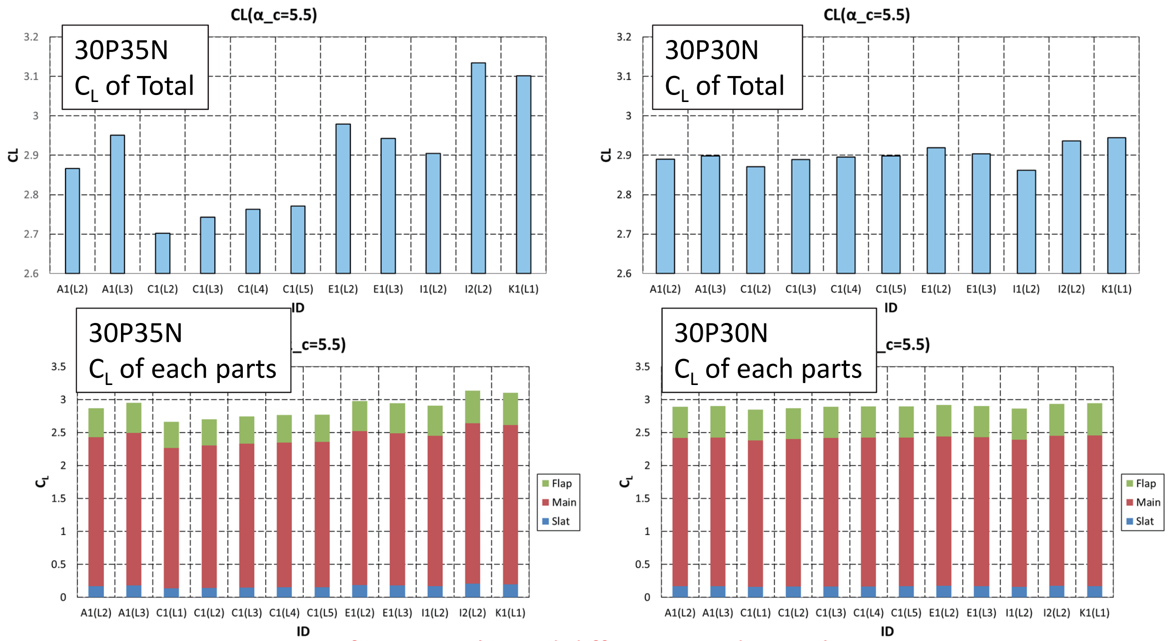

CL of 30P35N showed different trend in each ID.
The variation increased due to flow separation at flap.

61

Case 2-1 : C_m

Comparison with 30P30N

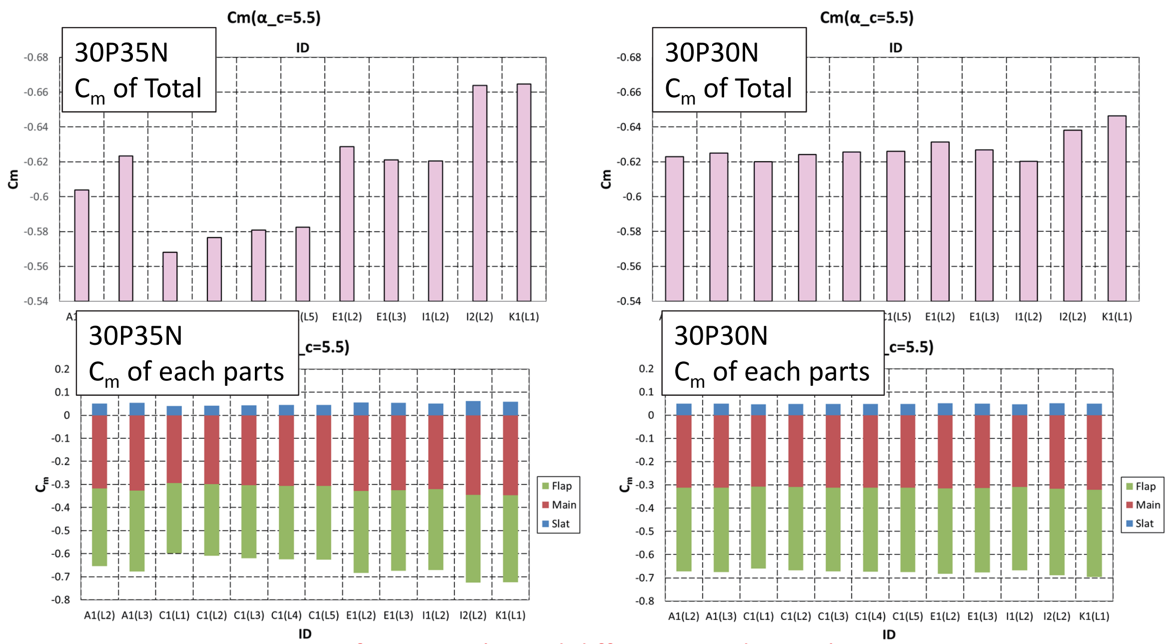

Cm of 30P35N showed different trend in each ID.
The variation increased due to flow separation at flap.

62

Case 2-1 : Cp (Slat)

AoA=5.5deg, Comparison of each parts

※All the submitted data is shown

Slat

30P35N

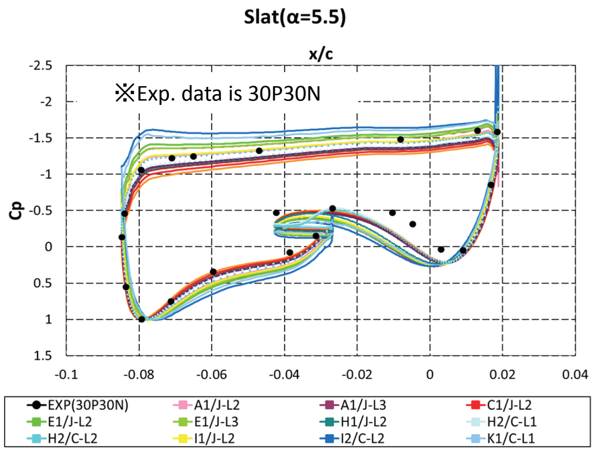

30P30N

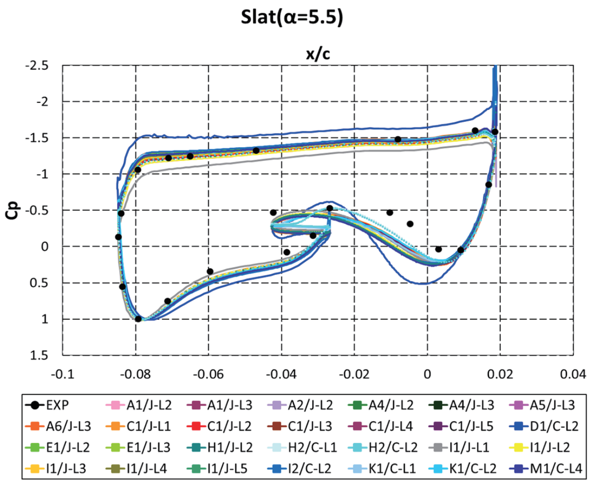

The variation of 30P35N was larger than 30P30N.

63

Case 2-1 : Cp(Main)

AoA=5.5deg, Comparison of each parts

※All the submitted data is shown

Main

30P35N

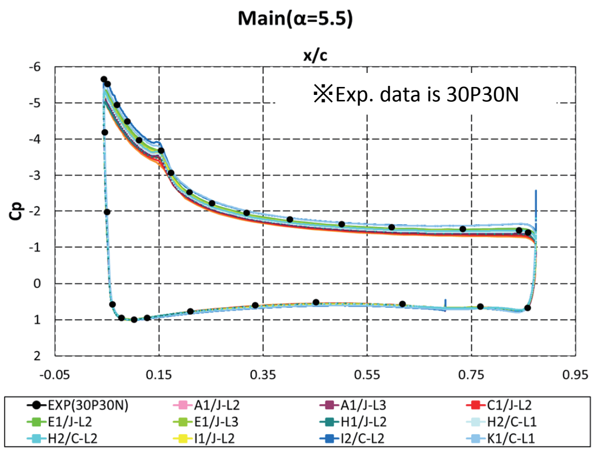

30P30N

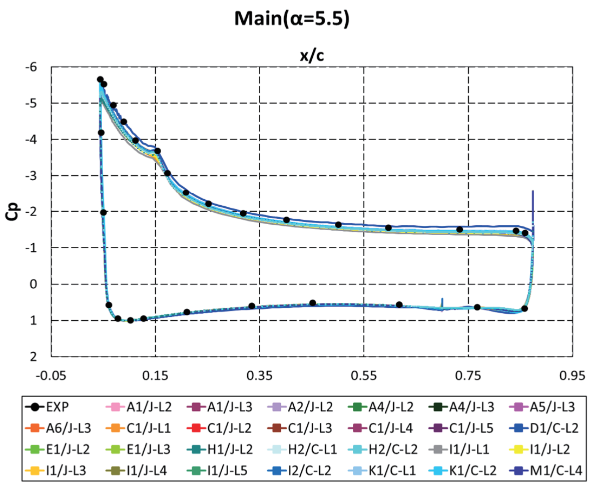

The variation of 30P35N was larger than 30P30N.

64

Case 2-1 : Cp(Flap)

AoA=5.5deg, Comparison of each parts

※All the submitted data is shown

Flap

30P35N

Flap(α=5.5)

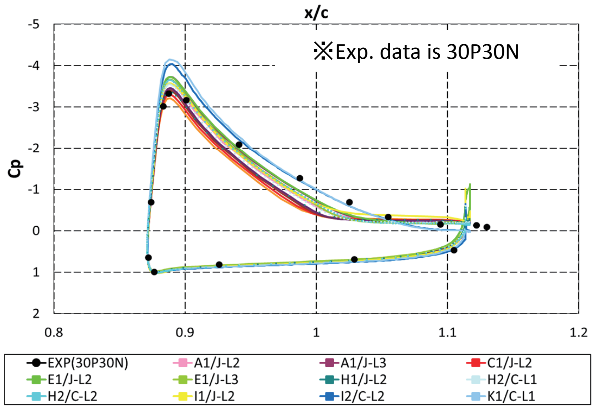

30P30N

Flap(α=5.5)

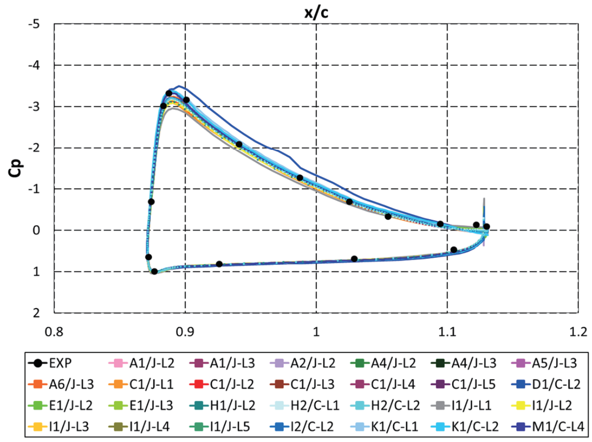

The variation of 30P35N was larger than 30P30N.

Case 2-1 : Cf (Slat)

AoA=5.5deg, Comparison of each parts

※All the submitted data is shown

Slat

30P35N

Slat(α=5.5)

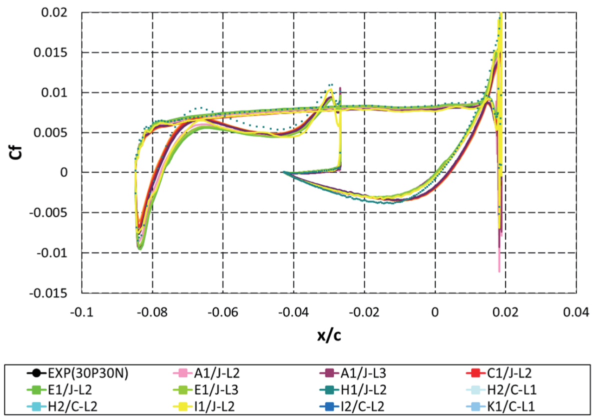

30P30N

Slat(α=5.5)

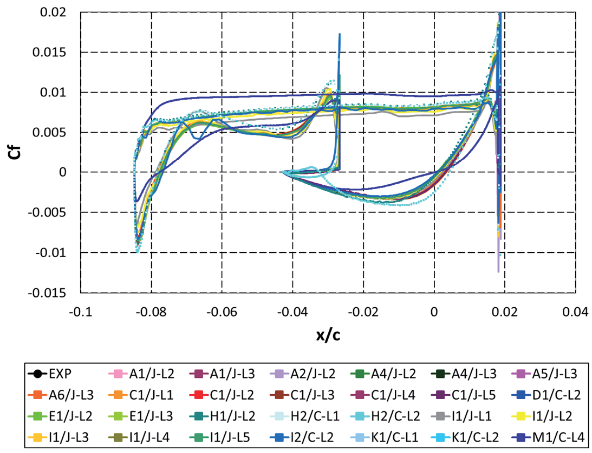

The variation of Cf was large between the type of solver.

Case 2-1 : Cf(Main)

AoA=5.5deg, Comparison of each parts

※All the submitted data is shown

Main

30P35N

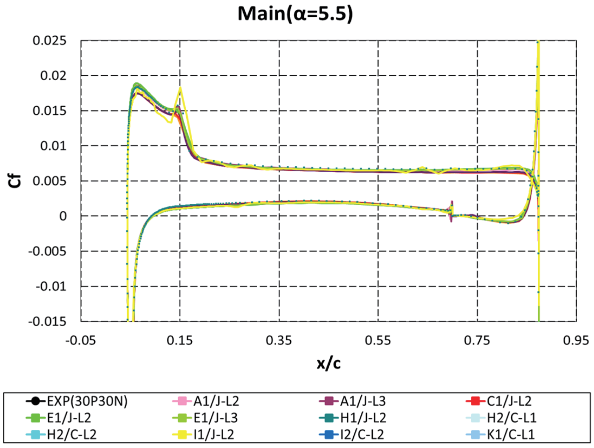

30P30N

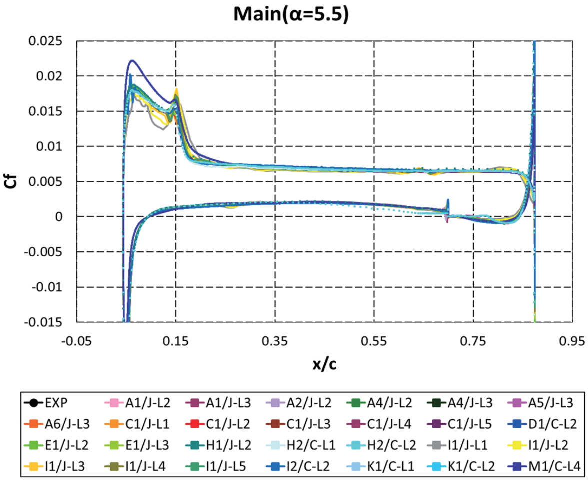

The variation of Cf was large between the type of solver.

Case 2-1 : Cf(Flap)

AoA=5.5deg, Comparison of each parts

※All the submitted data is shown

Flap

30P35N

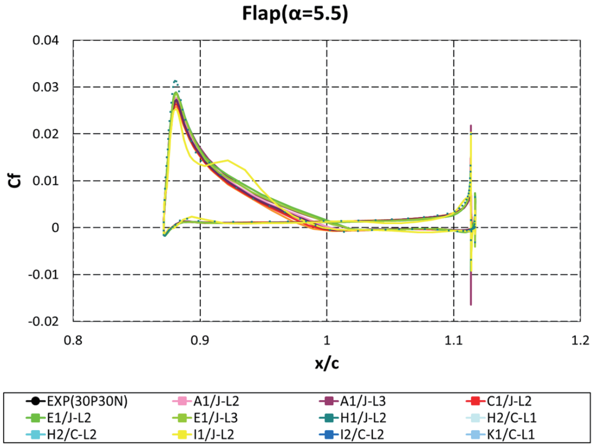

30P30N

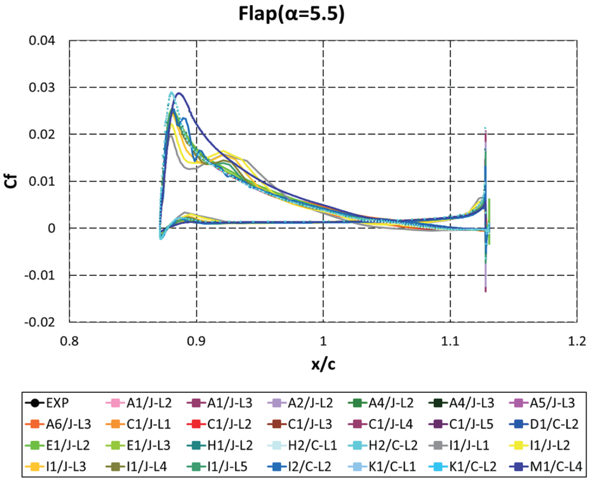

The variation of Cf was large between the type of solver.

Case 2-1 : Cf(Slat)

AoA=5.5deg, Comparison of each parts

※IDs which submit both Case1-1 and Case2-1 are shown

Slat

30P35N

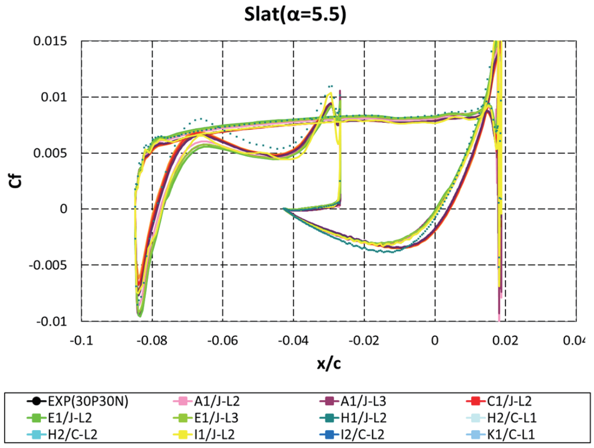

30P30N

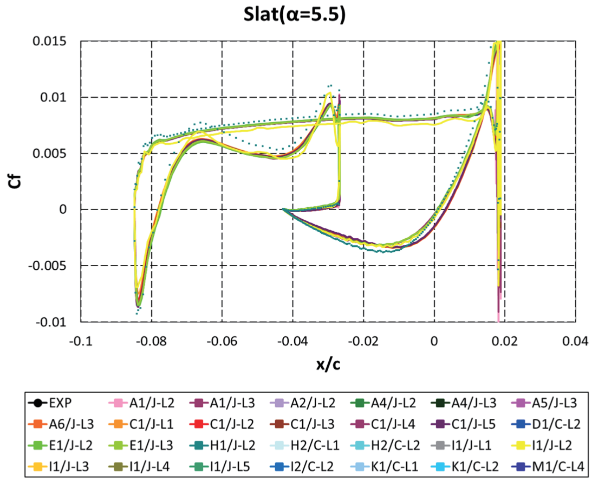

The Cf variation of 30P35N was larger than that of 30P30N.

69

Case 2-1 : Cf(Main)

AoA=5.5deg, Comparison of each parts

※IDs which submit both Case1-1 and Case2-1 are shown

Main

30P35N

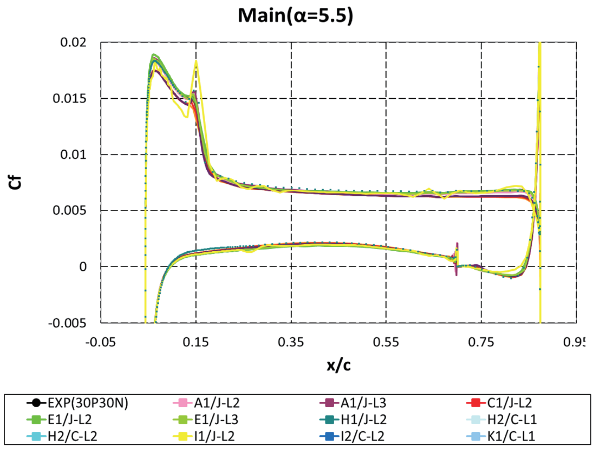

30P30N

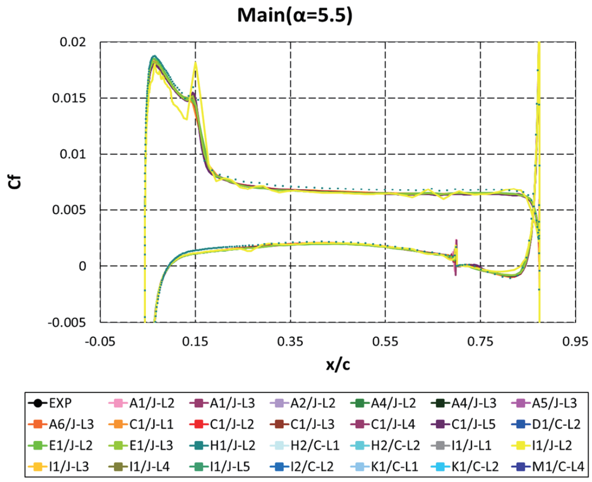

The Cf variation of 30P35N was larger than that of 30P30N.

70

Case 2-1 : Cf(Flap)

AoA=5.5deg, Comparison of each parts

※IDs which submit both Case1-1 and Case2-1 are shown

Flap

30P35N

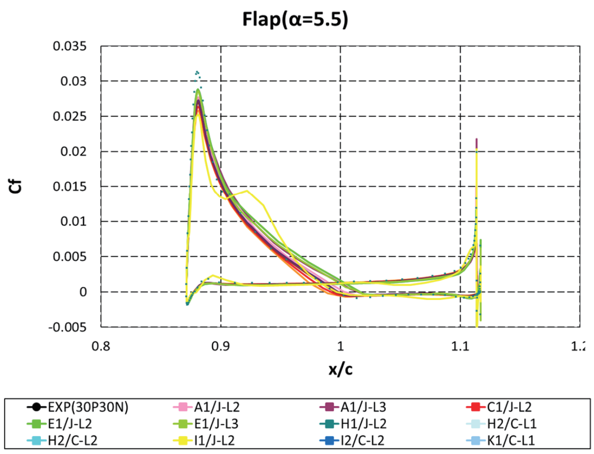

30P30N

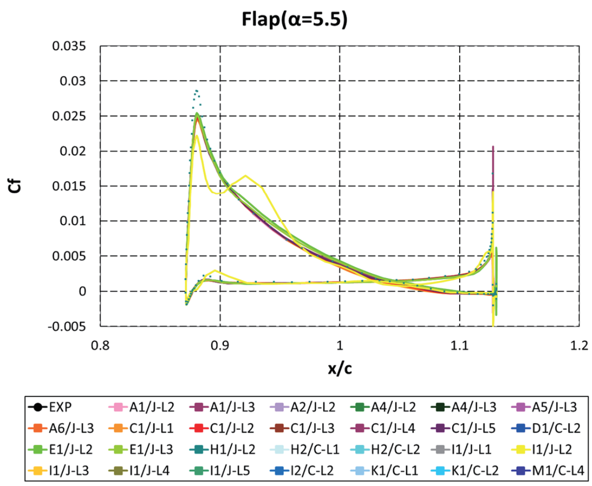

The Cf variation of 30P35N was larger than that of 30P30N.

Case 2-1 : Contours of $\tilde{\nu}$ / ν(30P35N)

AoA=5.5deg, Comparison with 30P30N

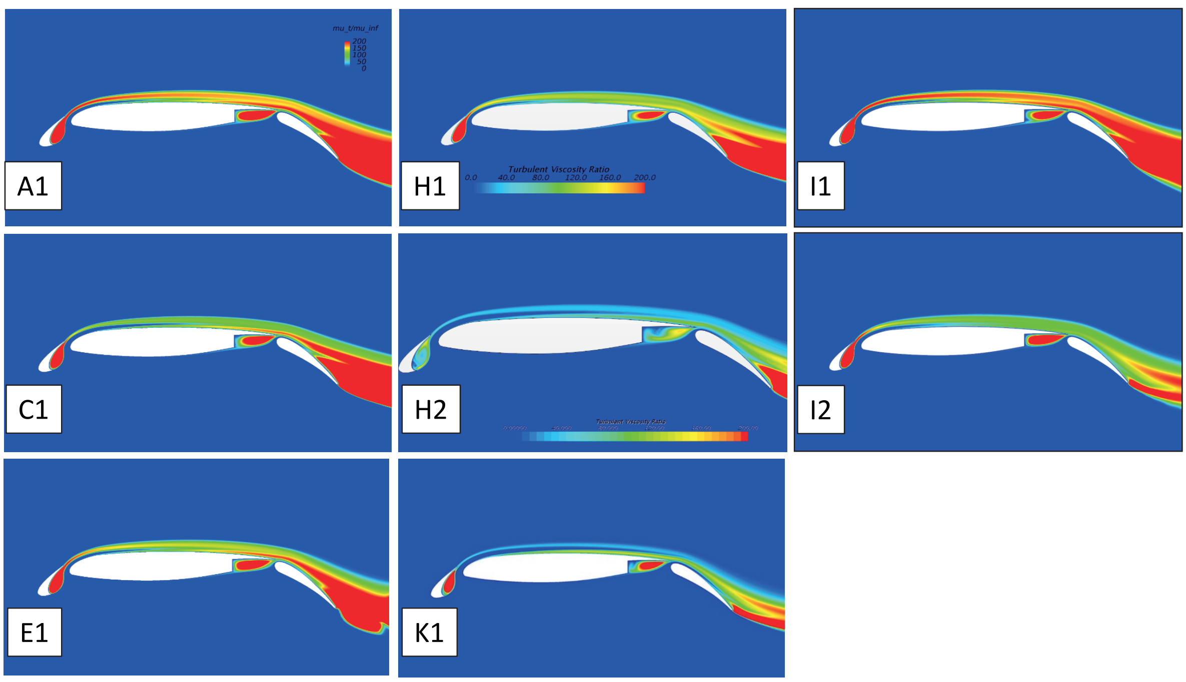

Case 2-1 : Contours of $\tilde{\nu} / \nu$(30P30N)

AoA=5.5deg, Comparison with 30P30N

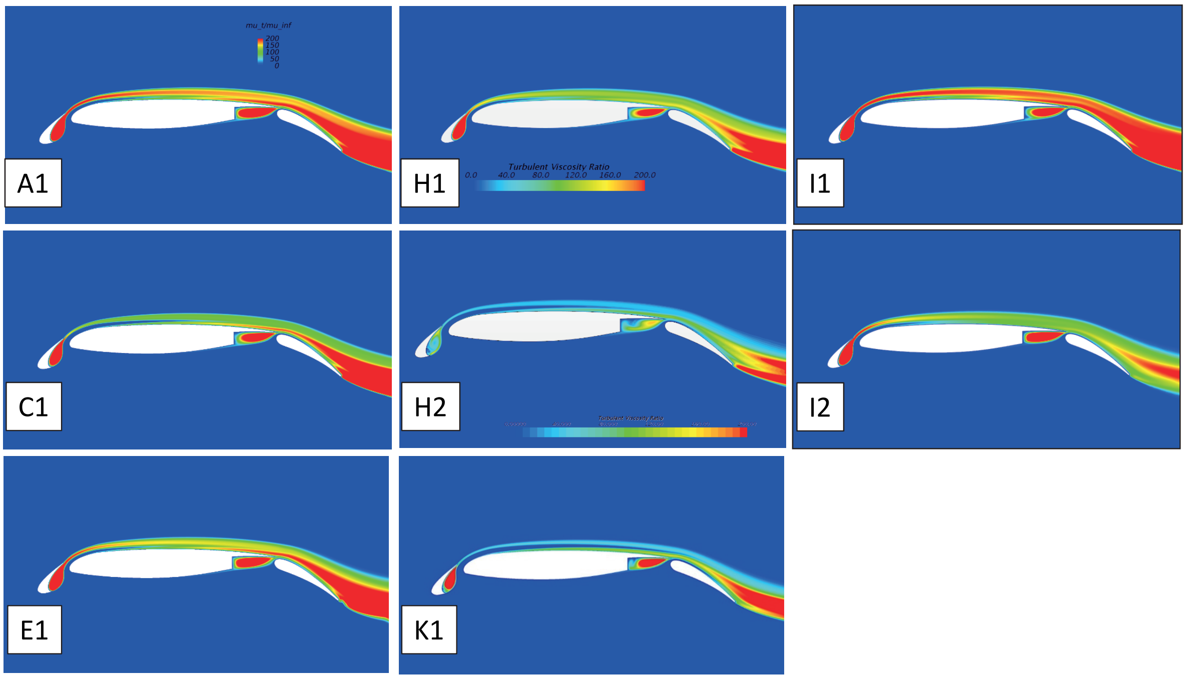

73

Case 2-1 : Contours of $\tilde{\nu} / \nu$(30P35N)

AoA=5.5deg, Comparison with 30P30N

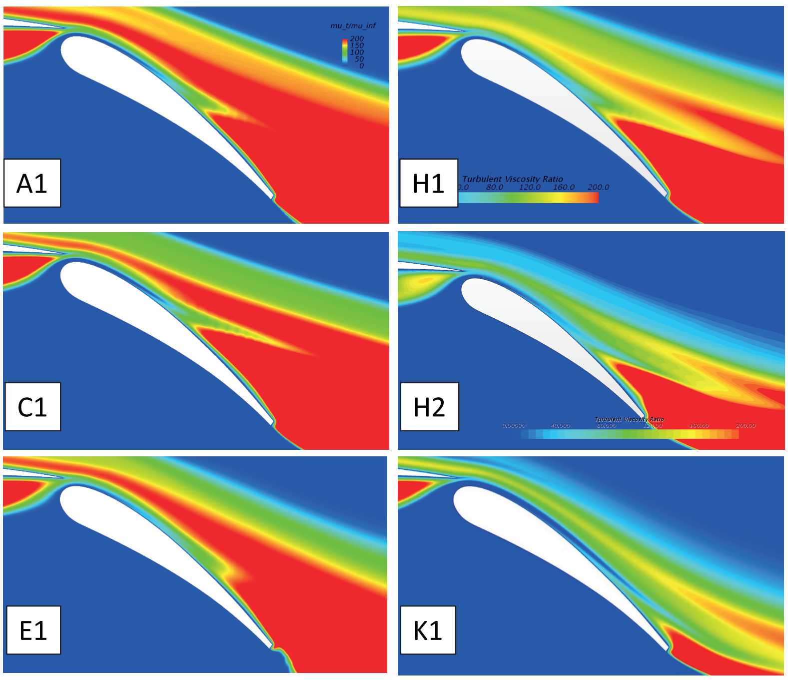

74

Case 2-1: Contours of $\tilde{\nu}$ / ν(30P30N)

AoA=5.5deg, Comparison with 30P30N

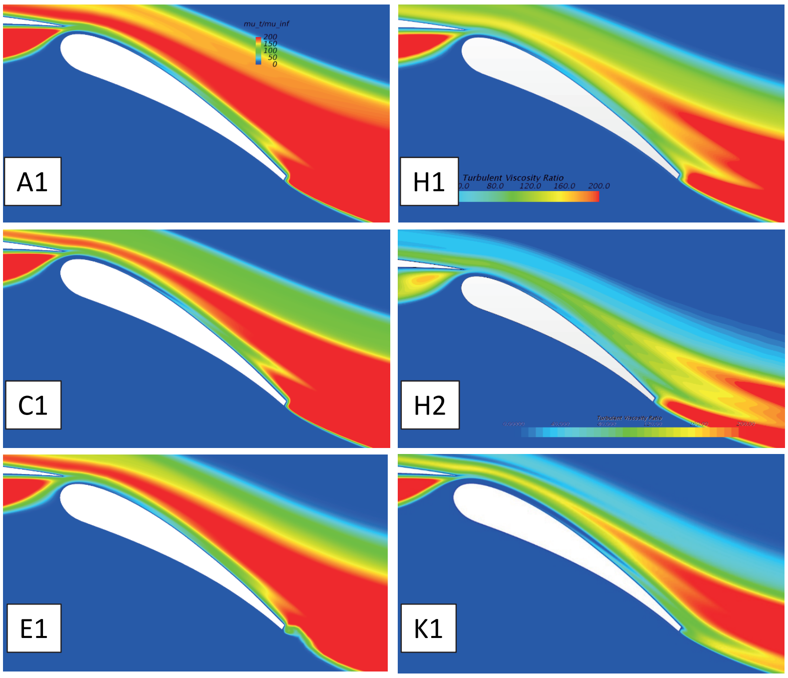

75

Case 2-1 : Spatial streamlines(30P35N)

AoA=5.5deg, Comparison with 30P30N

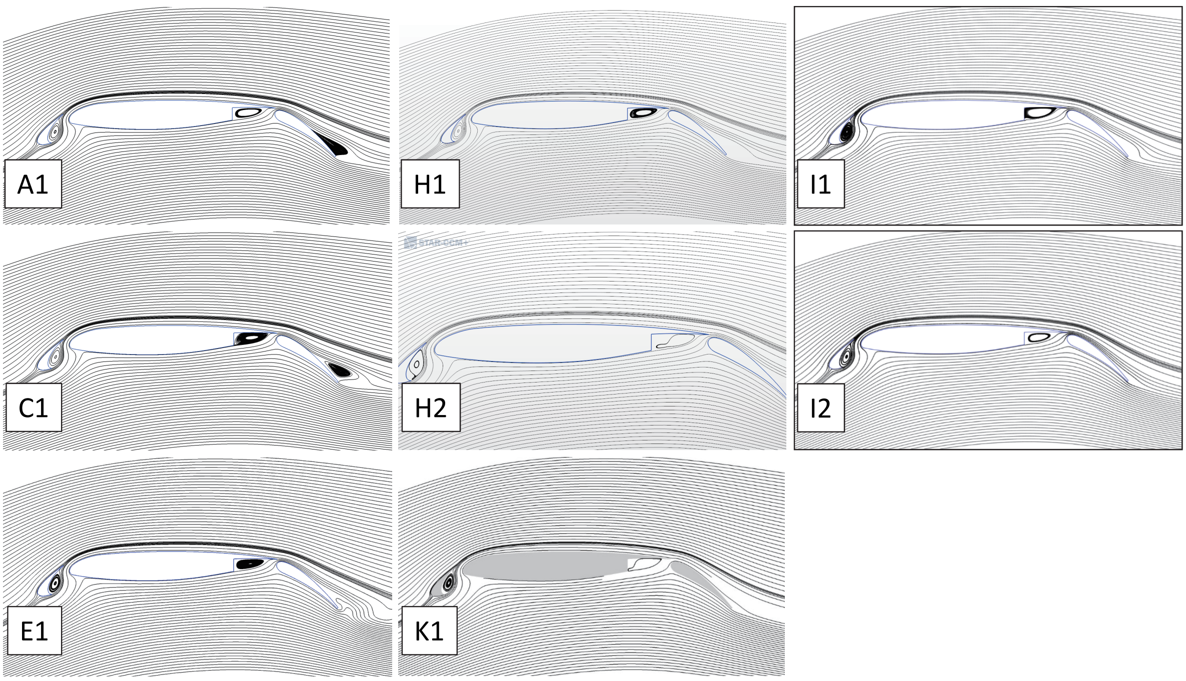

76

Case 2-1 : Spatial streamlines(30P30N)

AoA=5.5deg, Comparison with 30P30N

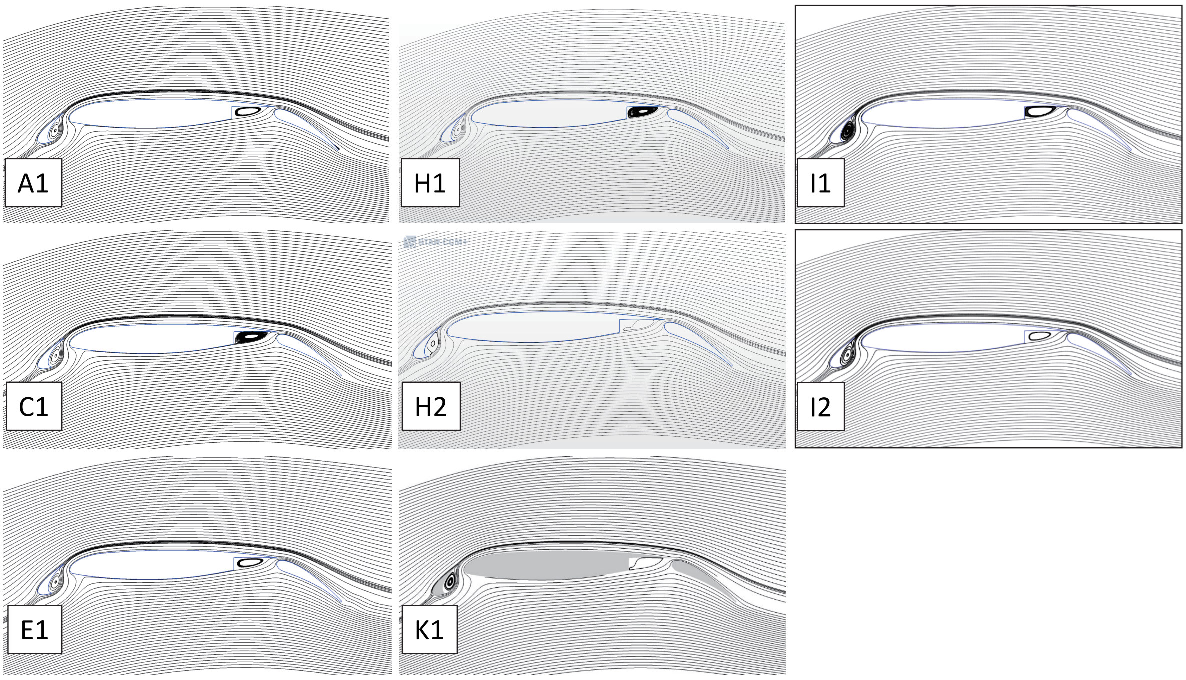

77

Case 2-1 : Spatial streamlines(30P35N)

AoA=5.5deg, Comparison with 30P30N

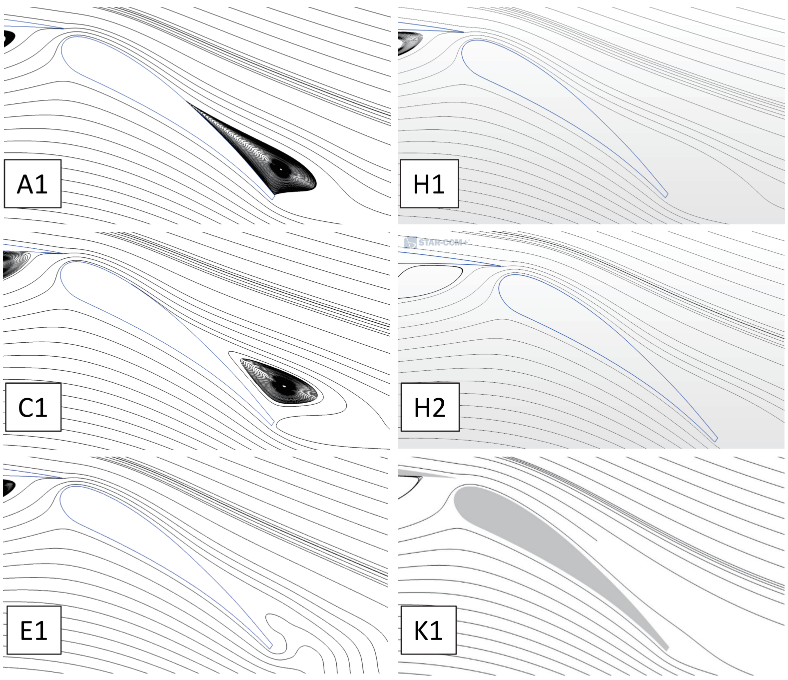

78

Case 2-1 : Spatial streamlines(30P30N)

AoA=5.5deg, Comparison with 30P30N

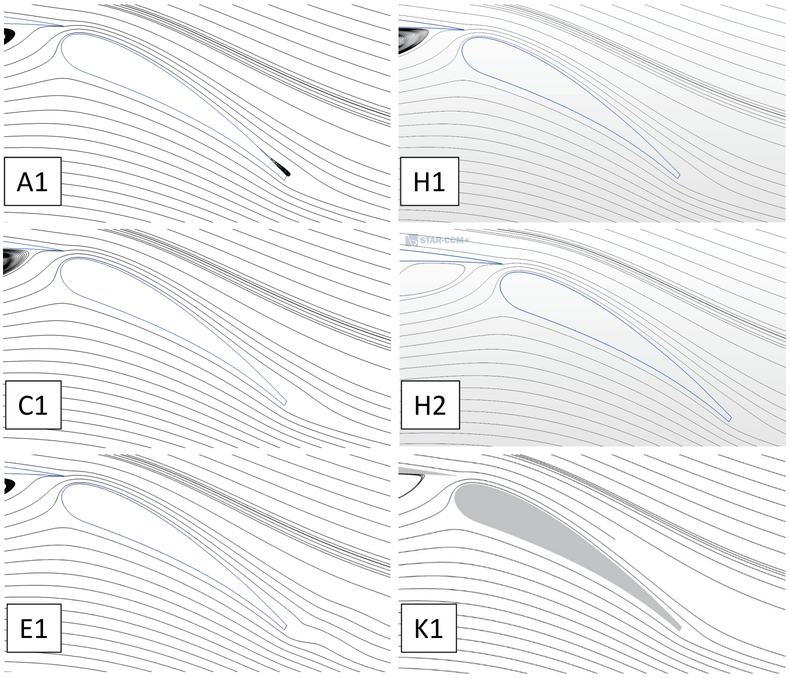

79

Case 2 : Prediction of flow separation at flap

- Case2-2 : 2.5D steady flow simulation
  - Geom. : 30P35N（modified_slat_configF）
  - Grid : provided（required : L2, optional : L1,L3~L5）or custom
  - Cond. : M = 0.17, Re = 1.71 x 10^6
  - AoA : 5.5 [deg]
  - List of data :
    - Aerodynamic coefficients(C_D,C_L,C_m),C_p,C_f
    - Surface contours of C_p,C_f
    - Surface streamlines
    - Contours of $\tilde{\nu} / \nu$
    - Spatial streamlines
    - Velocity profiles

80

Case 2-2：Surface streamlines on flap(30P35N)

AoA=5.5deg, Comparison with 30P30N

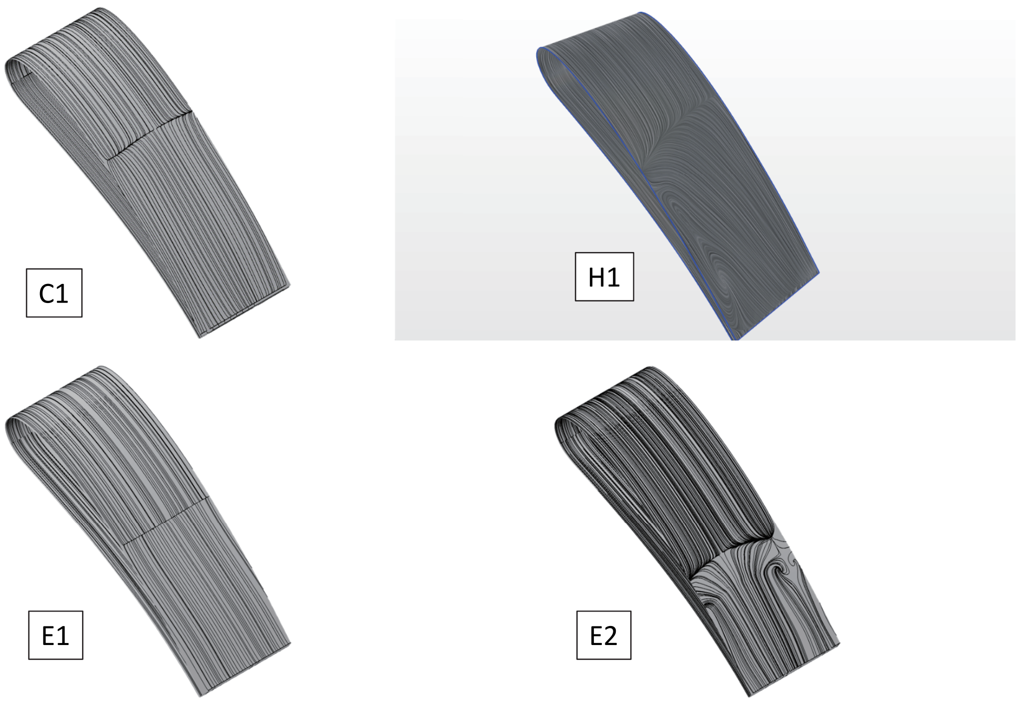

81

Case 2-2：Surface streamlines on flap(30P30N)

AoA=5.5deg, Comparison with 30P30N

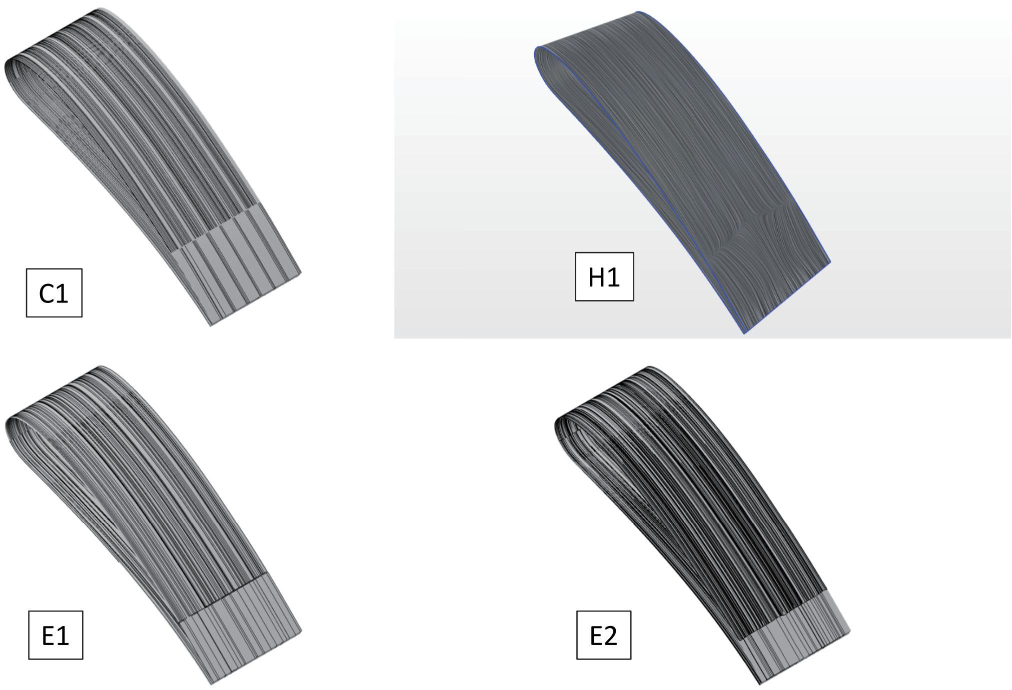

82

Case 2 : Prediction of flow separation at flap

– Case2-3 : 2.5D unsteady flow simulation

- Geom. : 30P35N（modified_slat_configF）
- Grid : provided（required : L2, optional : L1,L3~L5）or custom
- Cond. : M = 0.17, Re = 1.71 x 10^6
- AoA : 5.5 [deg]
- List of data(time averaged) :
  - Aerodynamic coefficients(C_D,C_L,C_m),C_p,C_f
  - Surface contours of C_p,C_f
  - Surface streamlines
  - Contours of $\tilde{\nu}$ / ν
  - Spatial streamlines
  - Velocity profiles

Legend(paticipant ID / grid type [J:provided by JAXA, C:custom] – grid resolution [L1~L5])

- EXP(30P30N)
- A3/J-L2
- A6/J-L2
- C1/J-L2
- E1/J-L1
- E1/J-L2
- E2/C-L2
- H1/C-L2

83

Case 2-3 : Contours of $\tilde{\nu}$ / ν(30P35N)

AoA=5.5deg, Comparison with 30P30N

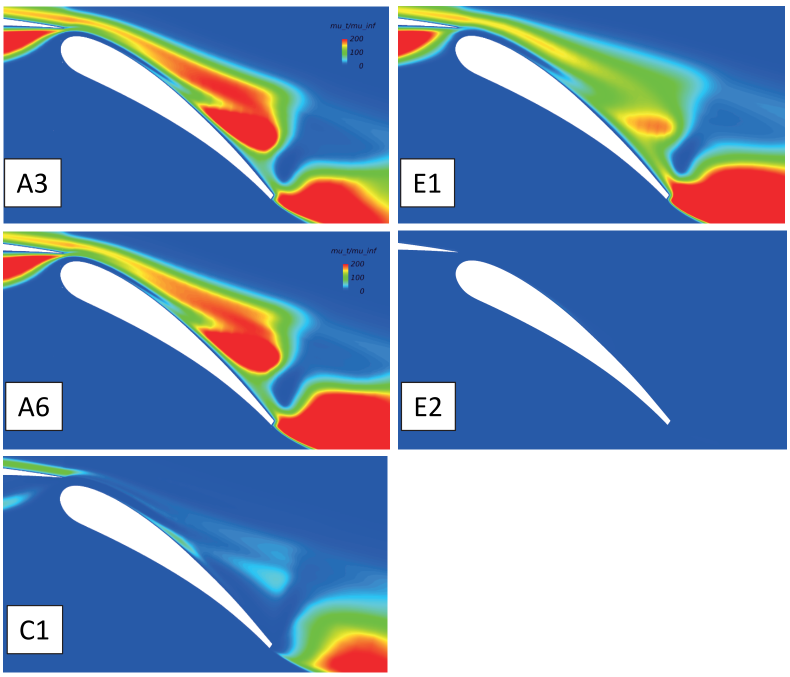

84

Case 2-3 : Contours of $\tilde{\nu}$ / ν(30P30N)

AoA=5.5deg, Comparison with 30P30N

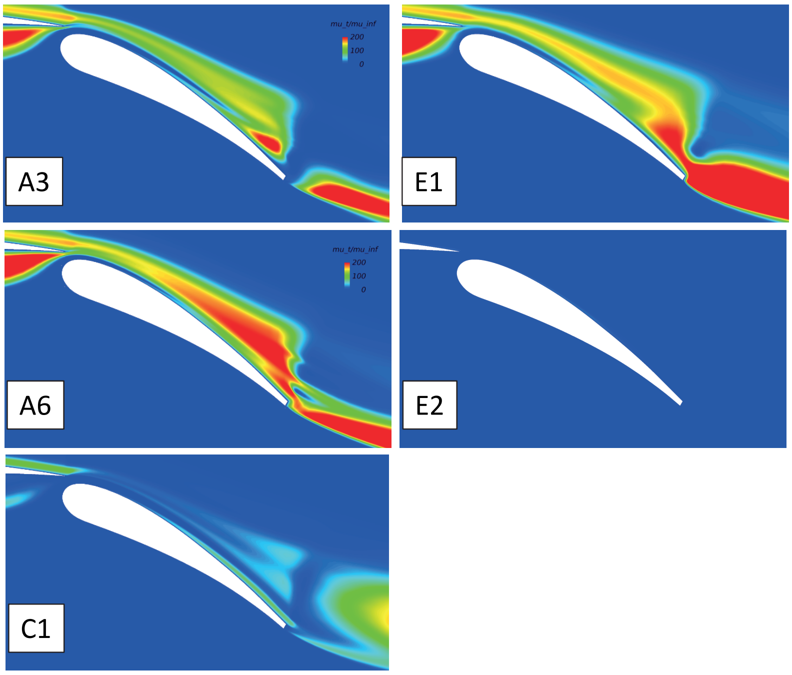

85

Case 2-3 : Spatial streamlines(30P35N)

AoA=5.5deg, Comparison with 30P30N

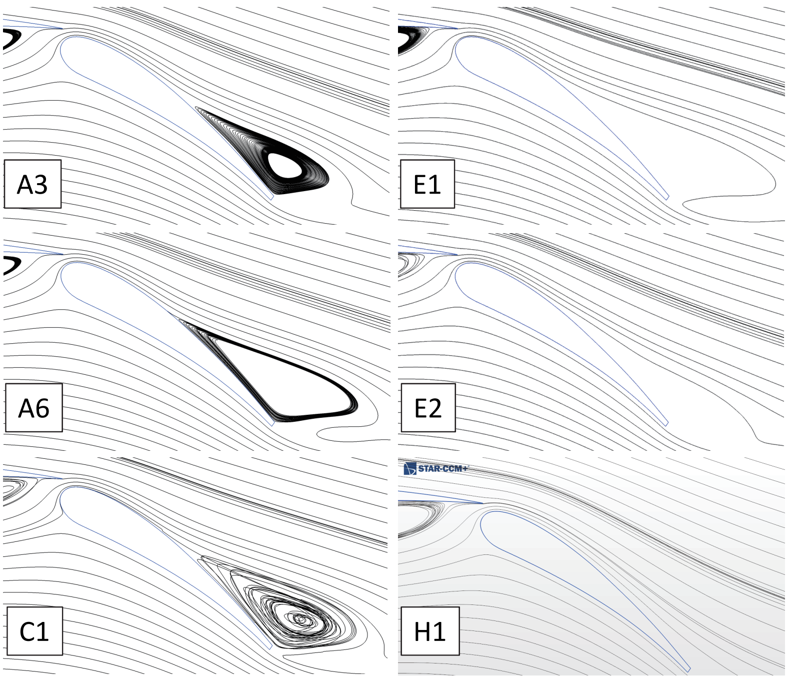

86

Case 2-3：Spatial streamlines(30P30N)

AoA=5.5deg, Comparison with 30P30N

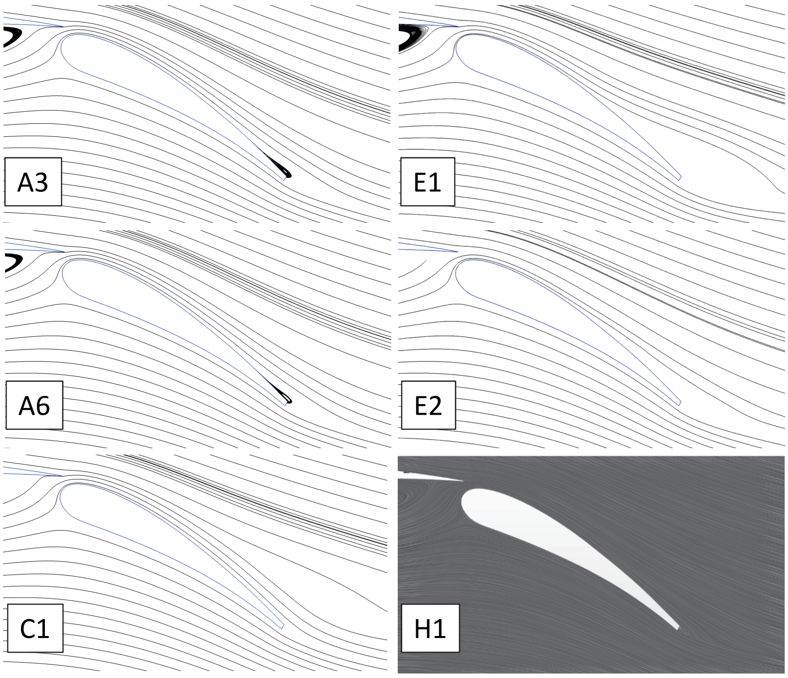

87

Case 2-3：Surface streamlines on flap(30P35N)

AoA=5.5deg, Comparison with 30P30N

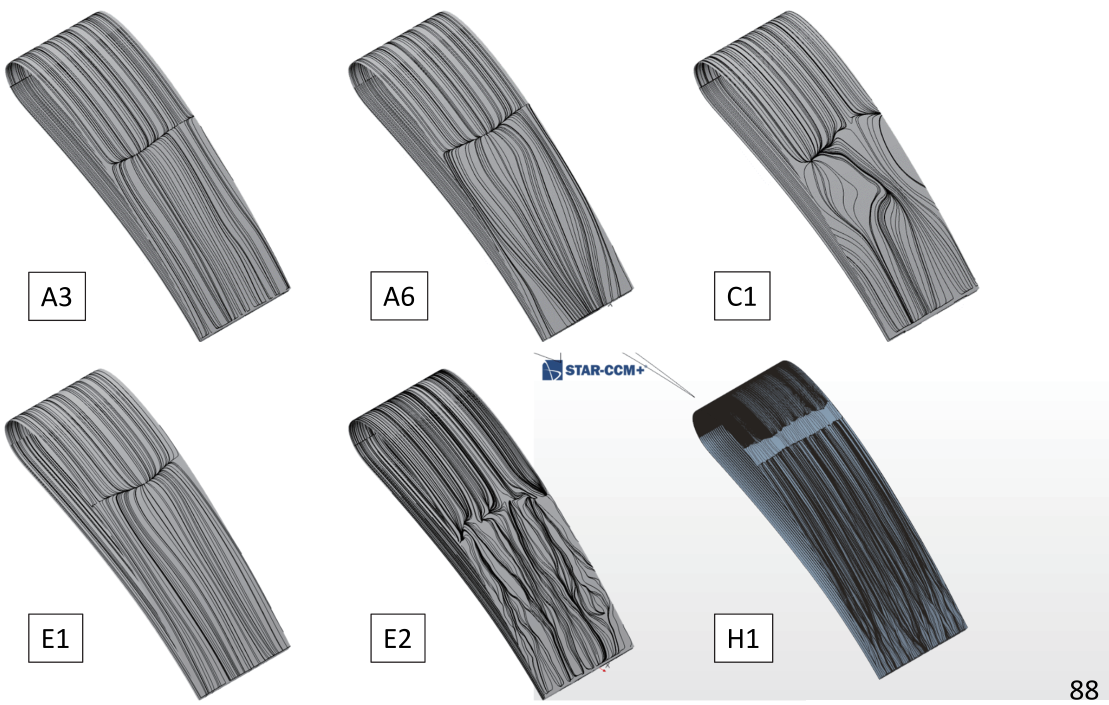

88

Case 2-3 : Surface streamlines on flap(30P30N)

AoA=5.5deg, Comparison with 30P30N

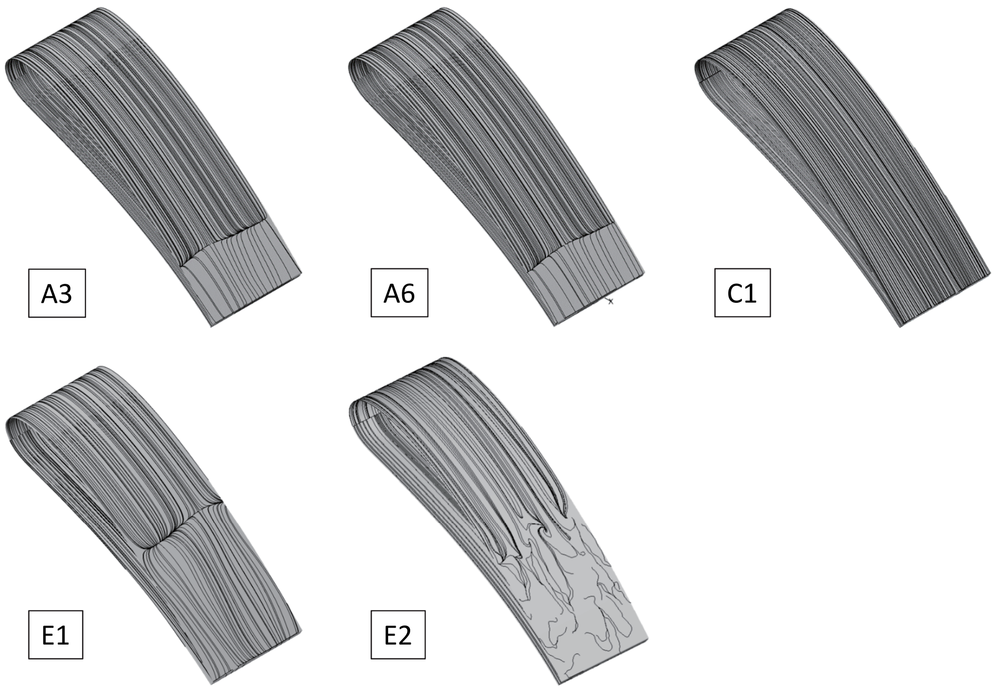

89

Case 2 Summary

- Prediction of flow separation at flap (30P35N)
  - CD increased in all participants compared to 30P30N.
    But CL and Cm showed different behavior.
    The position of flow separation at flap also varied by flow solvers.
  - The computational results seemed to be affected by periodic boundary condition.

90

Case 3 : Prediction of aeroacoustics

– Case3-1 : Near field acoustics

- Geom. : 30P30N（modified_slat_configF）
- Grid : provided（required : L2, optional : L3）or custom
- Cond. : M = 0.17, Re = 1.71 x 10^6
- AoA : 5.5/9.5/14 [deg]（red:required, black:optional）
- List of data :
  - PSD of Pressure
  - Contours of spanwise vorticity
  - Contours of time-averaged 2D TKE
  - Contours of Cp_{rms}

Legend(paticipant ID / grid type [J:provided by JAXA, C:custom] - grid resolution [L1~L5])

EXP	A2/J-L2	A2/J-L3	A3/J-L2	A3/J-L3	A6/J-L2	A6/J-L3	A7/J-L2
A7/J-L3	A8/J-L2	B1/J-L3	B2/J-L3	B3/J-L3	C1/J-L2	D1/C-L2	F1/J-L2
F1/J-L3	F2/C-L2	F2/C-L3	G1/C-L2	H1/C-L2	J1/J-L3	L1/C-L2	

91

Case 3-1 : Sampling position of PSD

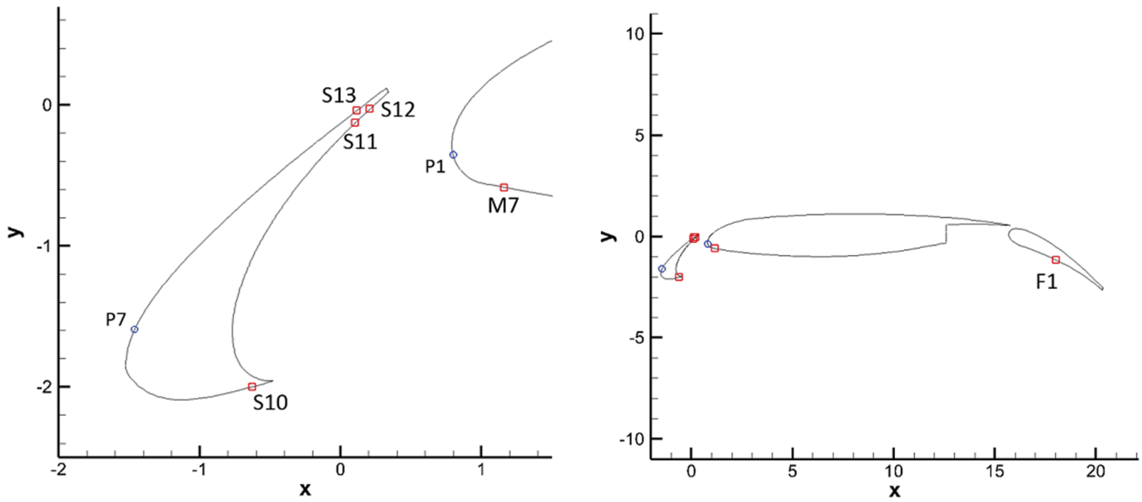

Sample data where Z = 1[inch] on the center line of wing span
Slat : 5point, Main : 2point, Flap : 1point

92

Case 3-1: PSD

AoA=5.5deg, Comparison with experiment

※Probe point of H1 is different from set point

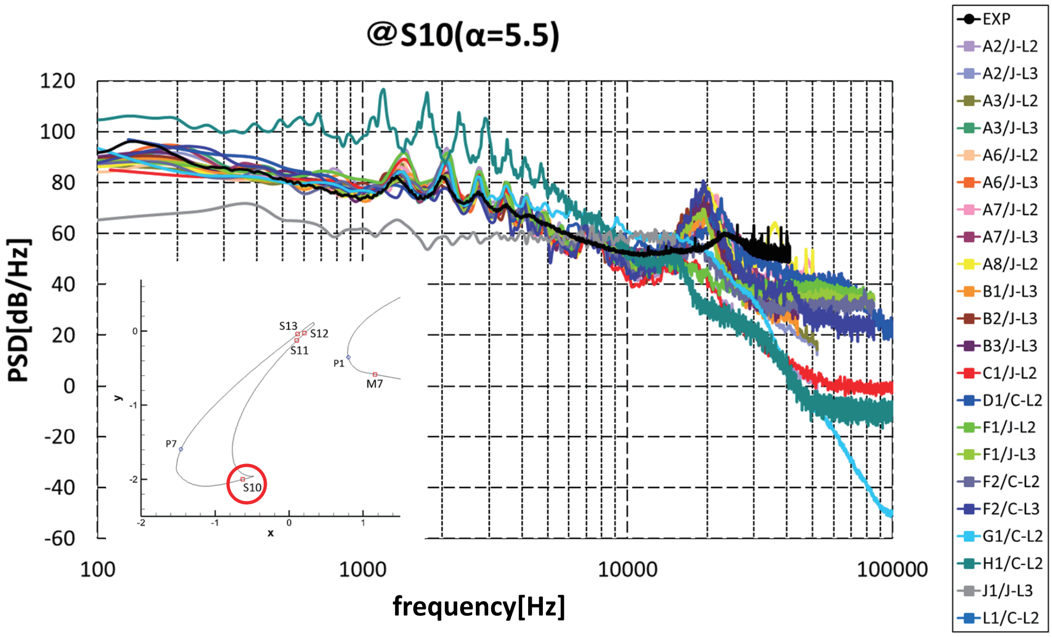

NBPs were well captured in each CFD result.
The variation of the peak around 20kHz was large.

93

Case 3-1: PSD

AoA=5.5deg, Comparison with experiment

※Probe point of H1 is different from set point

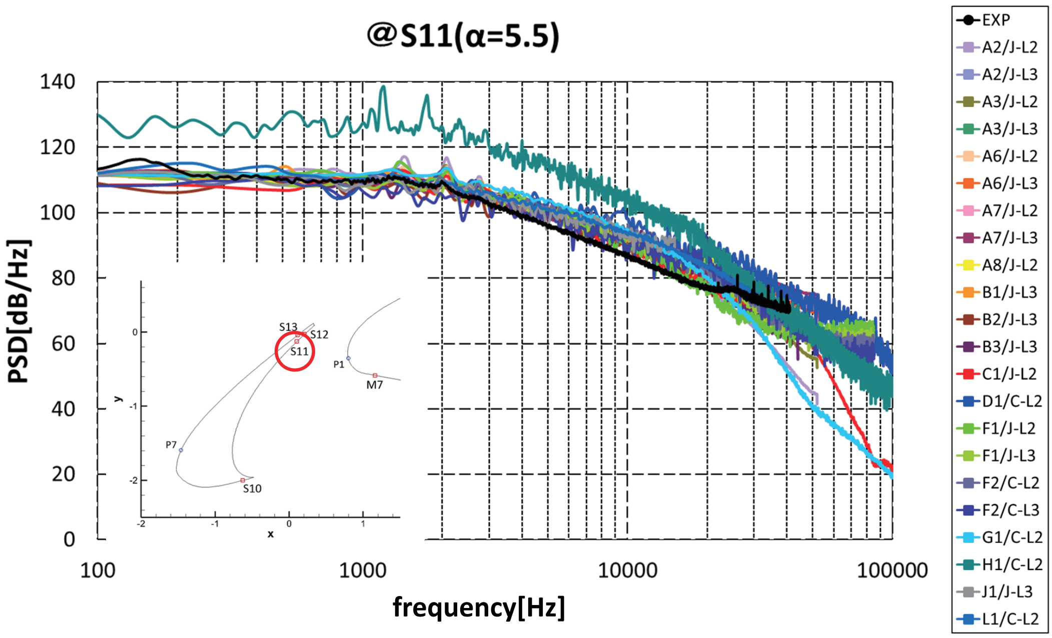

CFD results showed good agreement with experiment.

94

Case 3-1: PSD

AoA=5.5deg, Comparison with experiment

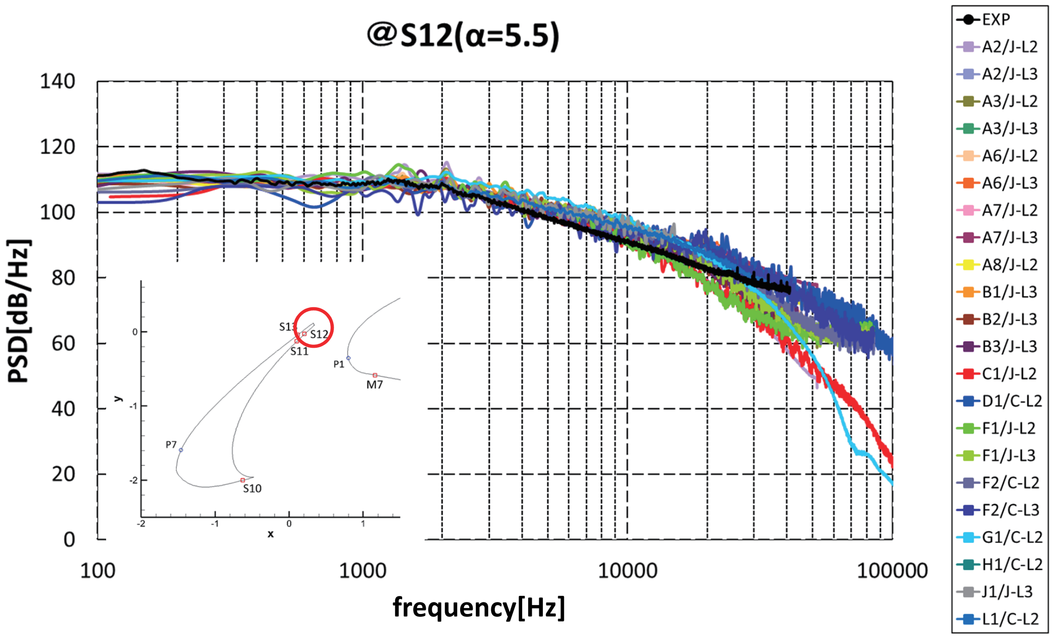

CFD results showed good agreement with experiment.

95

Case 3-1: PSD

AoA=5.5deg, Comparison with experiment

※Probe point of H1 is different from set point

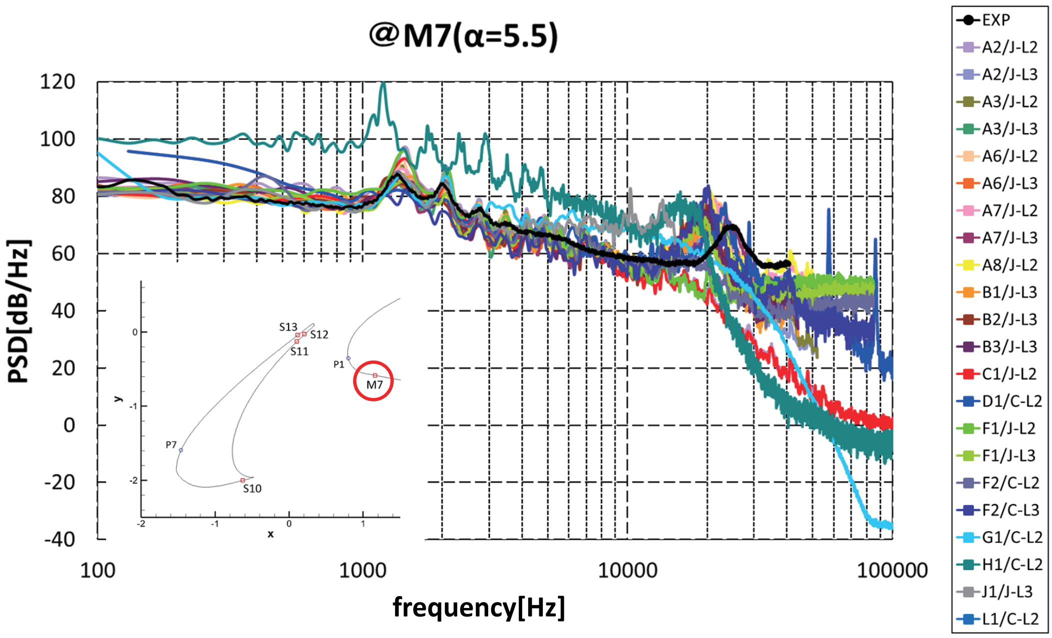

NBPs were well captured in each CFD result.
The variation of the peak around 20kHz was large.

96

Case 3-1: PSD

AoA=5.5deg, Comparison with experiment

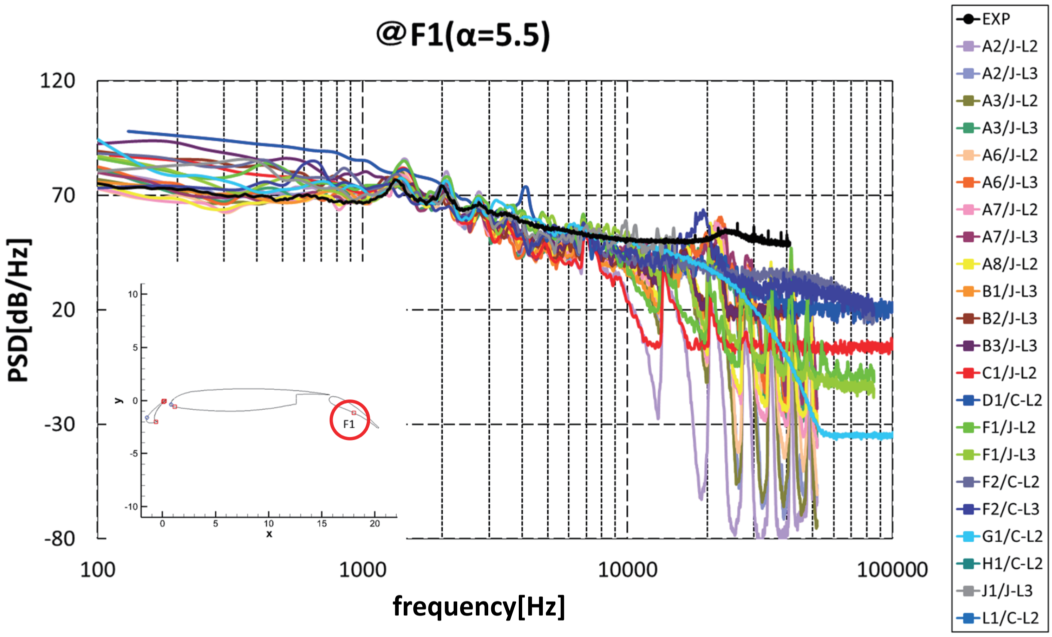

NBPs were well captured in each CFD result.
The variation of the peak around 20kHz was large.

Case 3-1: PSD(L2)

AoA=5.5deg, Comparison by grid resolution

※Probe point of H1 is different from set point

L2

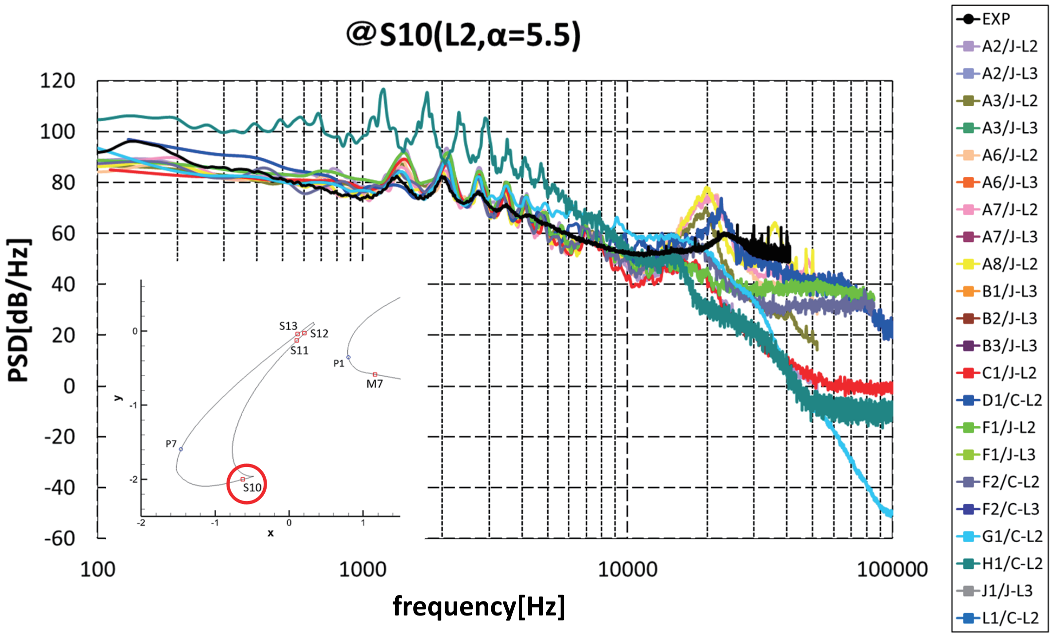

L2 grid overestimated the level of NBPs.
There were some results which couldn't predict the peak around 20kHz.

Case 3-1: PSD(L3)

AoA=5.5deg, Comparison by grid resolution

L3

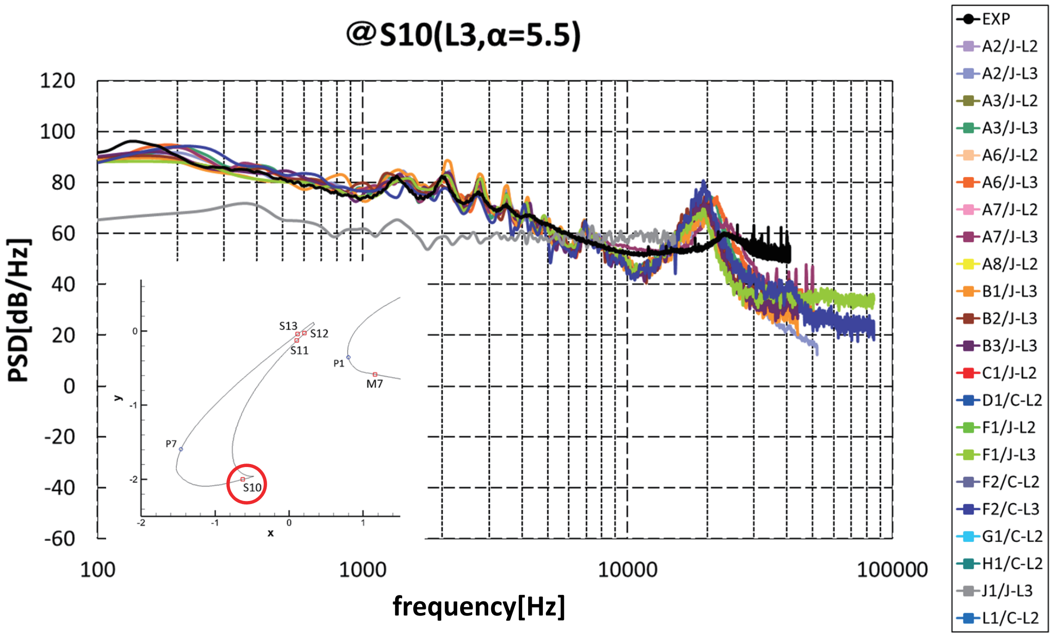

L3 grid successfully predicted the level of NBPs.
Almost all results captured the peak around 20kHz.

99

Case 3-1: PSD(L2)

AoA=5.5deg, Comparison by grid resolution ※Probe point of H1 is different from set point

L2

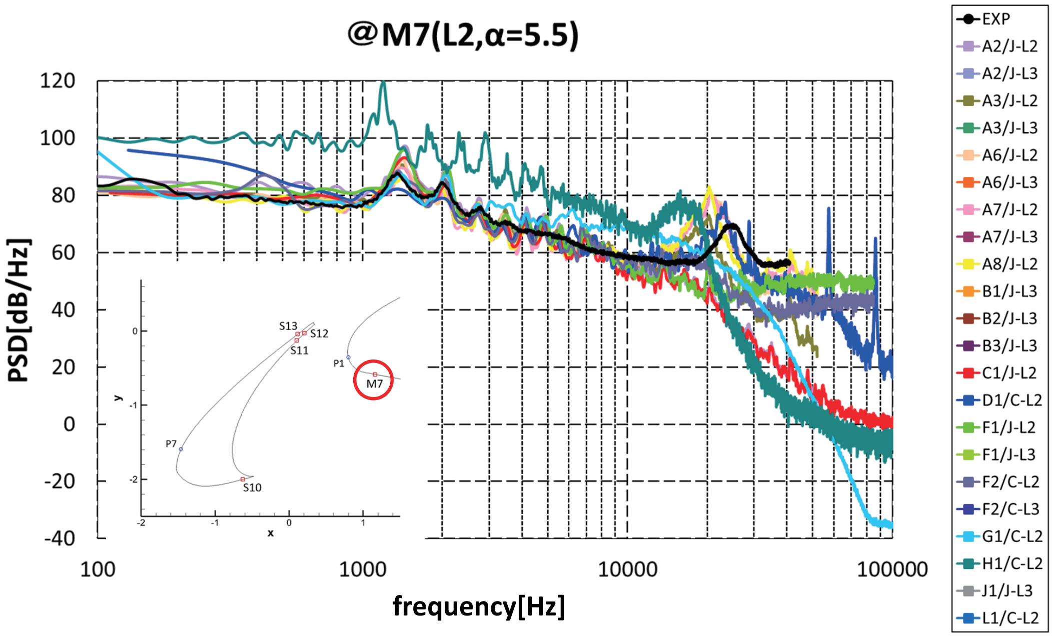

L2 grid overestimated the level of NBPs.
There were some results which couldn't predict the peak around 20kHz.

100

Case 3-1: PSD(L3)

AoA=5.5deg, Comparison by grid resolution

L3

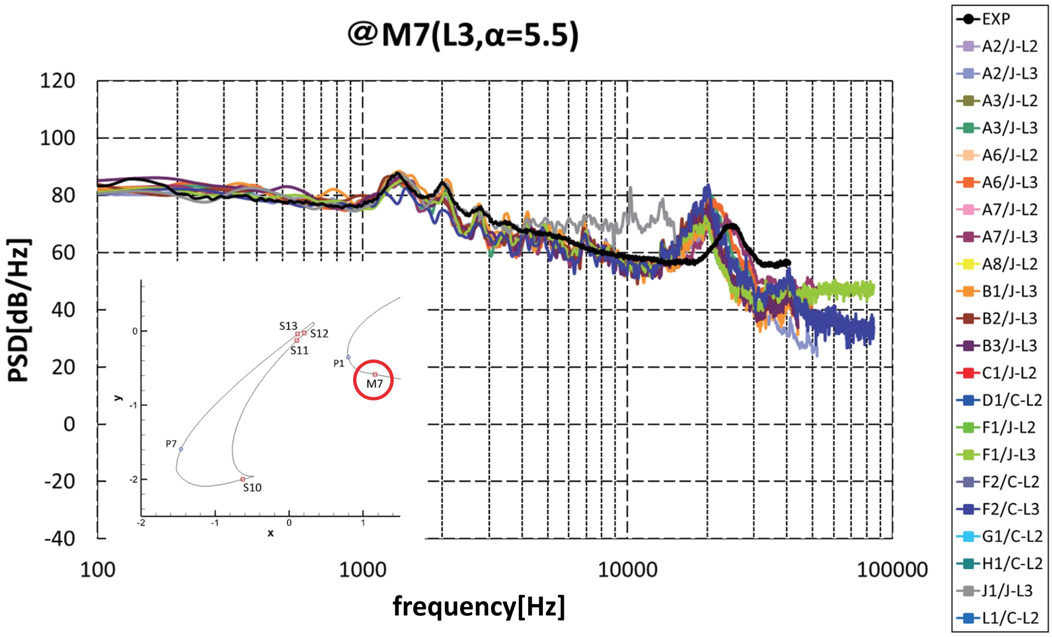

L3 grid successfully predicted the level of NBPs.
Almost all results captured the peak around 20kHz.

101

Case 3-1 : z-vorticity(without peak from slat-TE)

AoA=5.5deg, L2 grid

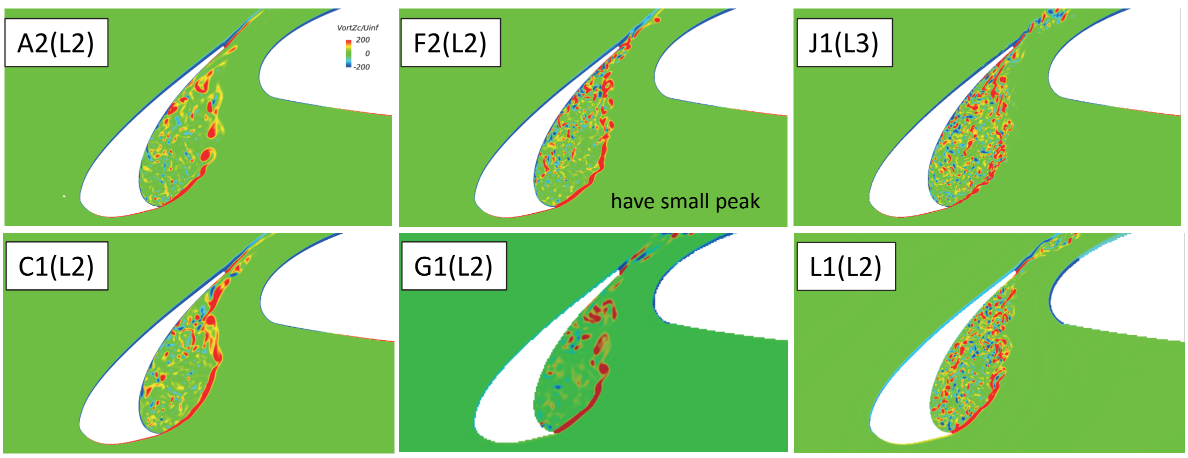

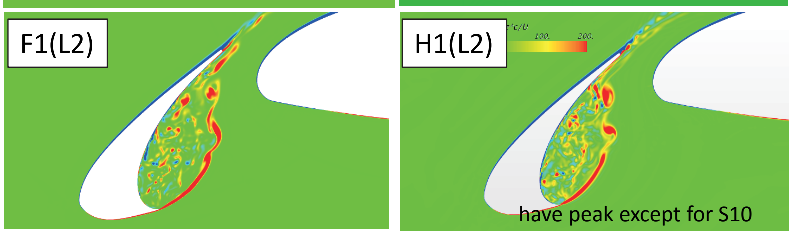

No/Small Karman vortex shedding from slat TE

102

Case 3-1 : z-vorticity(with peak from slat-TE)

AoA=5.5deg, L3 grid

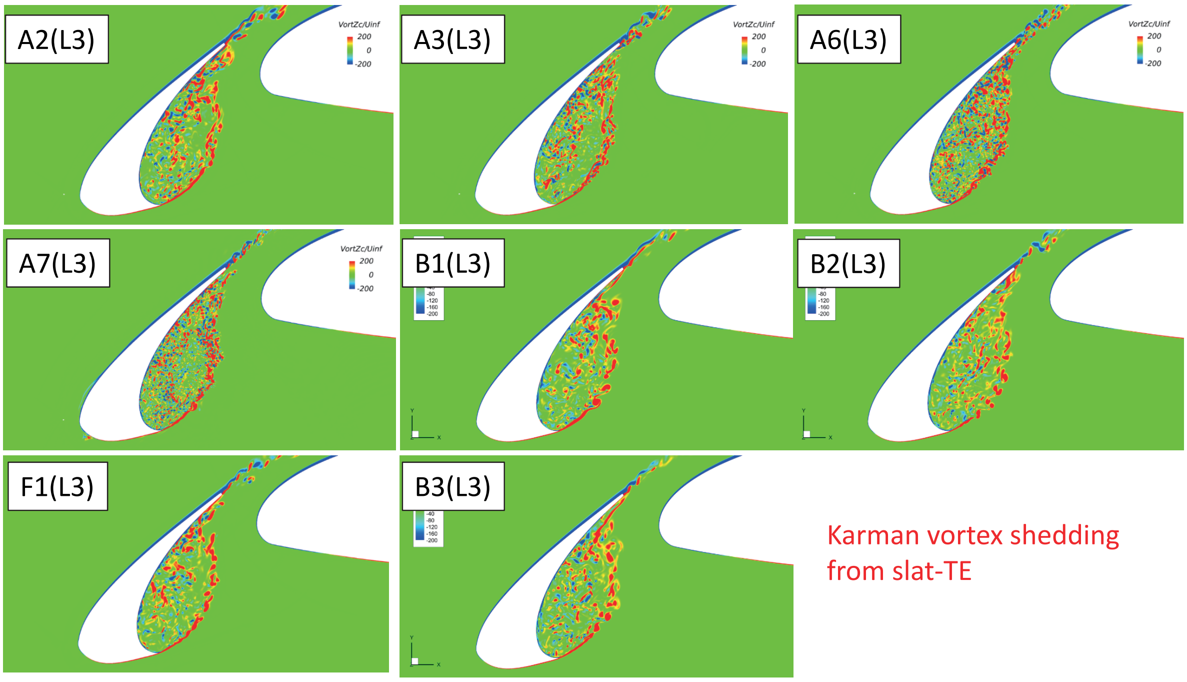

103

Case 3-1 : z-vorticity(with peak from slat-TE)

AoA=5.5deg, L2 grid

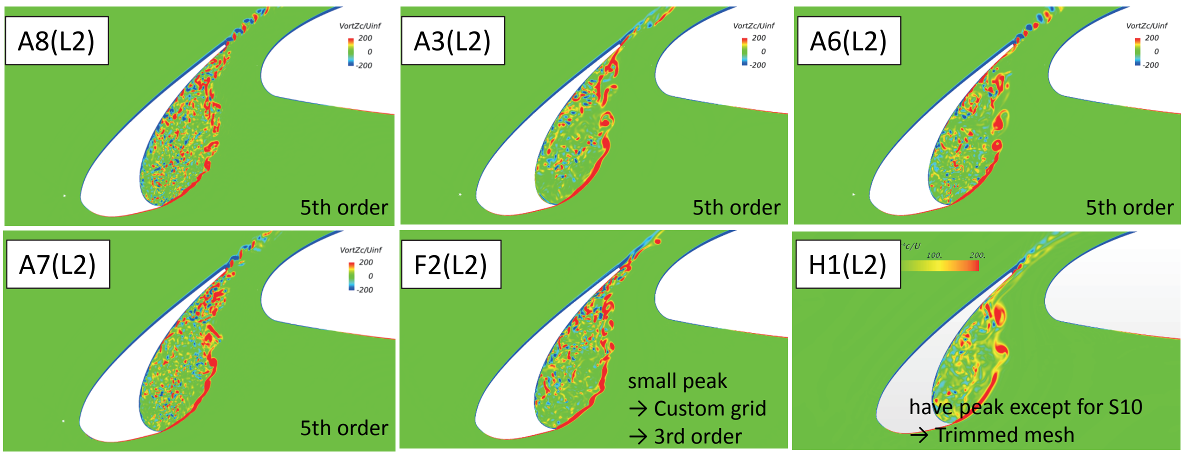

High order/resolution schemes could capture vortex shedding from slat-TE with L2 grid.

104

Case 3-1 : TKE2D(without peak from slat-TE)

AoA=5.5deg, L2 grid

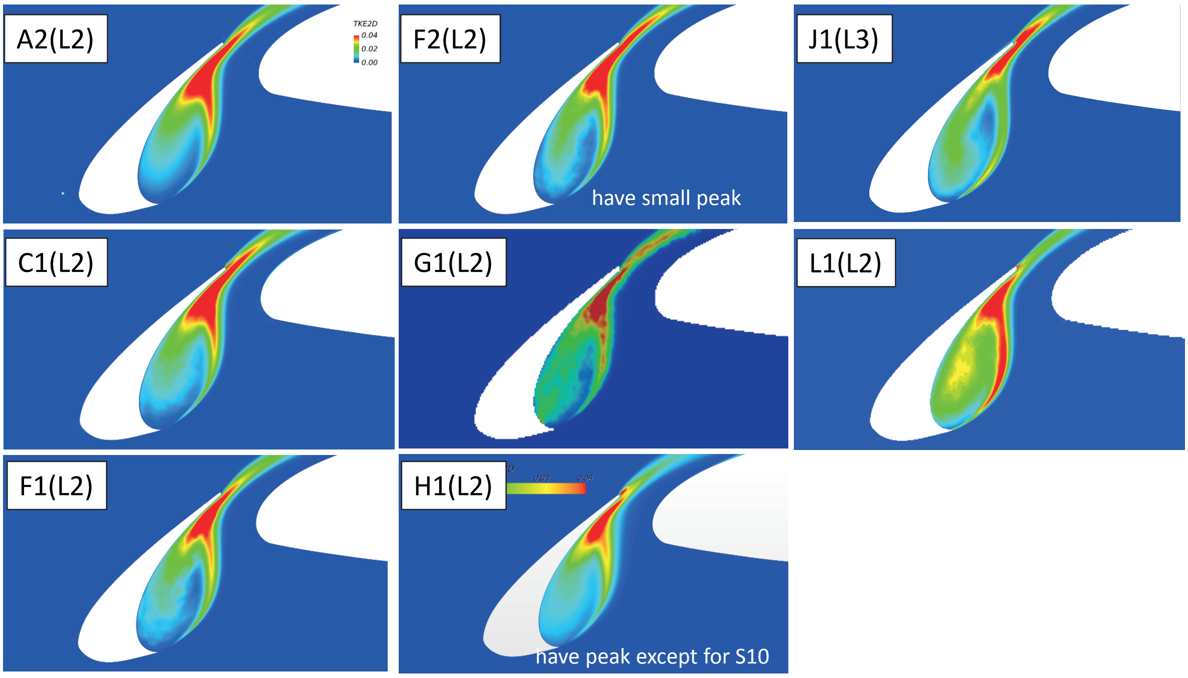

Case 3-1 : TKE2D(with peak from slat TE)

AoA=5.5deg, L3 grid

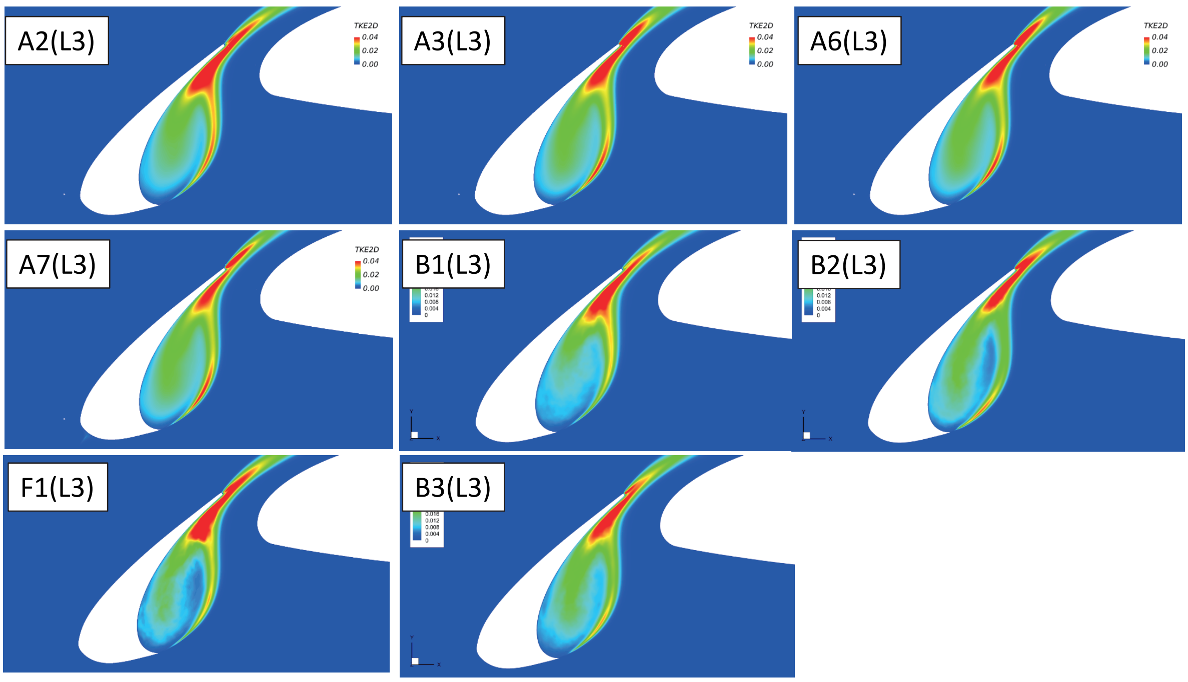

Case 3-1 : TKE2D(with peak from slat-TE)

AoA=5.5deg, L2 grid

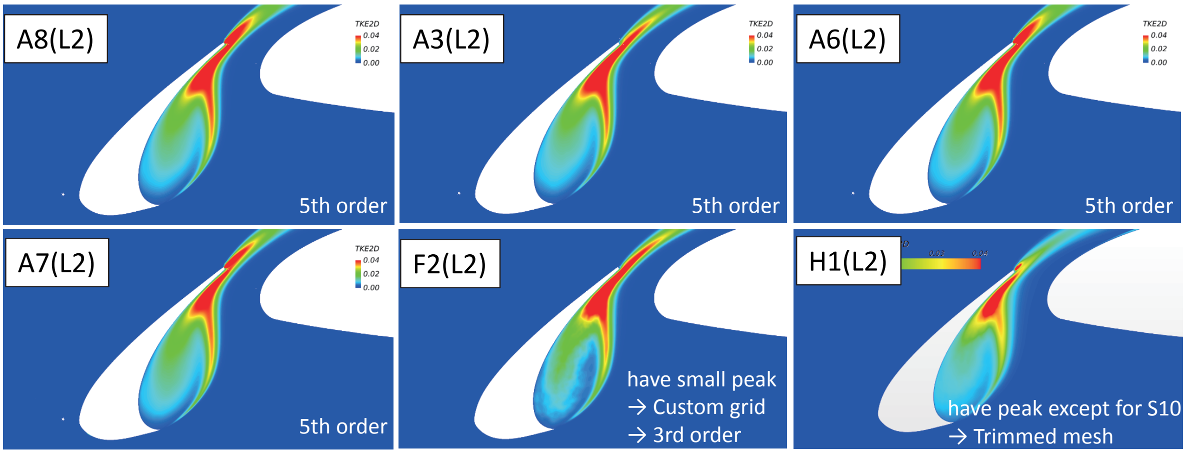

High order/resolution schemes can capture vortex shedding from slat-TE with L2 grid.

107

Case 3-1 : Contours of Cp rms(No peak)

AoA=5.5deg, Comparison by the existence of high frequency peak

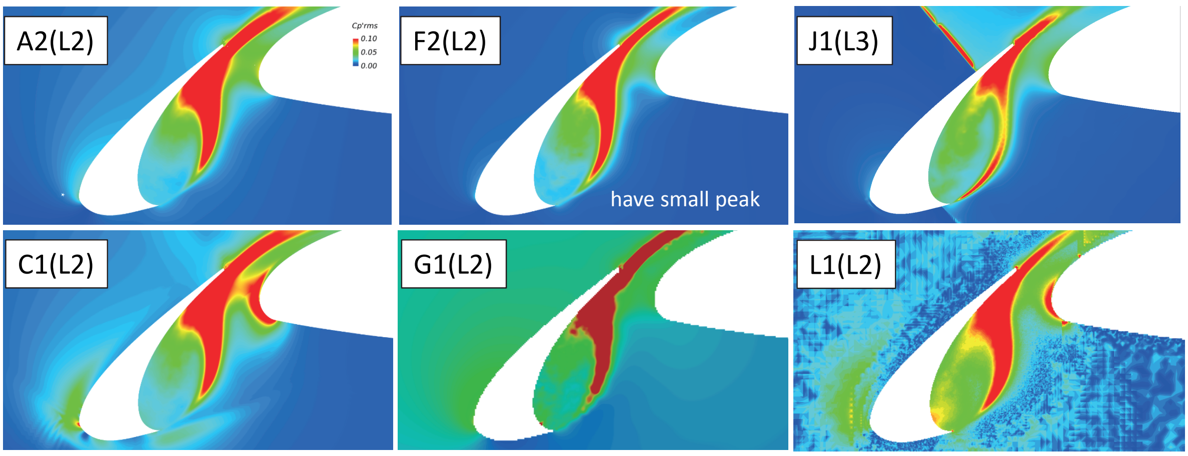

L2 grid couldn't capture the high frequency peak from slat TE due to the lack of resolution.

108

Case 3-1 : Contours of Cp rms(with peak)

AoA=5.5deg, Comparison by the existence of high frequency peak:L3 grid

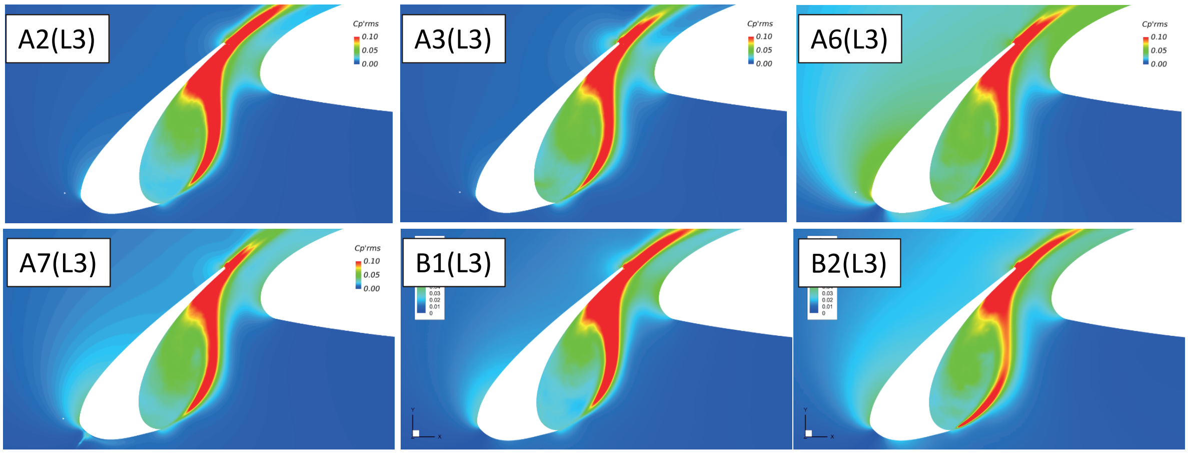

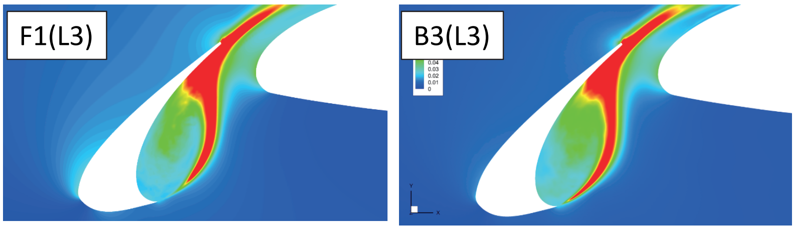

L3 grid could capture the high frequency peak from slat TE.

109

Case 3-1 : Contours of Cp rms(with peak)

AoA=5.5deg, Comparison by the existence of high frequency peak:L2 grid

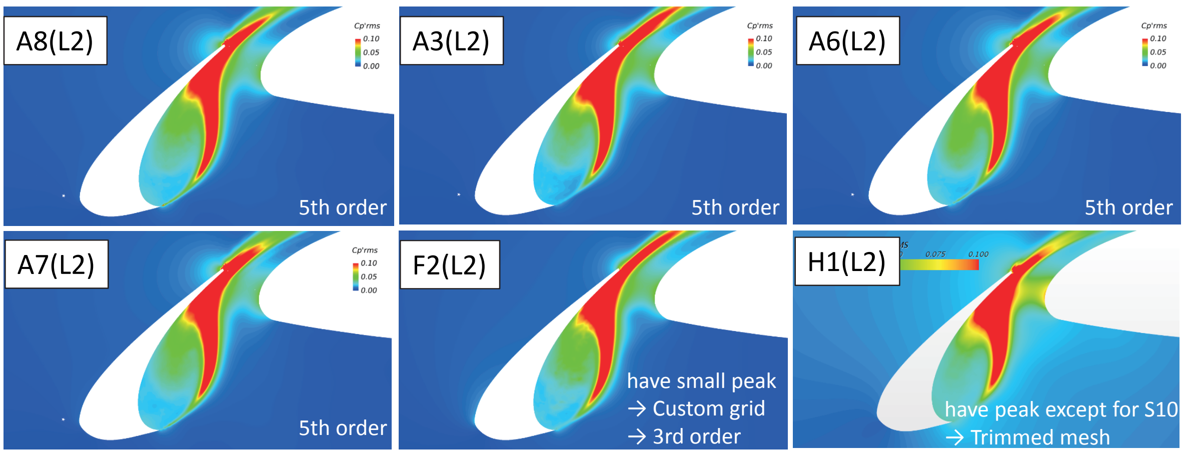

High order/resolution schemes could capture the high frequency peak from slat TE with L2 grid.

110

Case 3-1: PSD

AoA=9.5deg, Comparison with experiment

※Probe point of H1 is different from set point

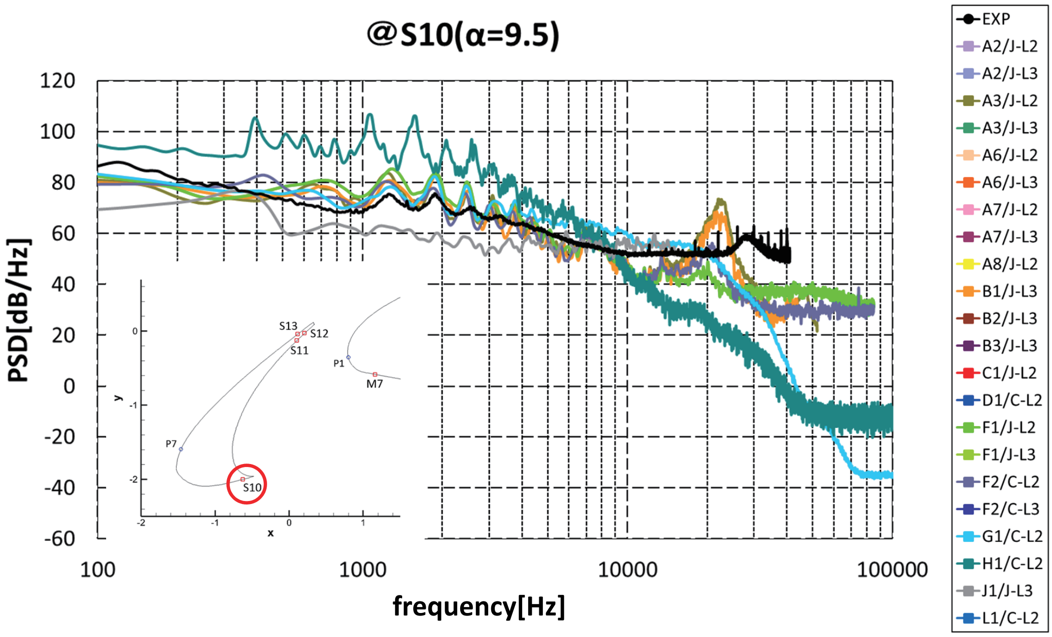

NBPs were well captured in each CFD result.
The variation of the peak around 20kHz was large.

111

Case 3-1: PSD

AoA=9.5deg, Comparison with experiment

※Probe point of H1 is different from set point

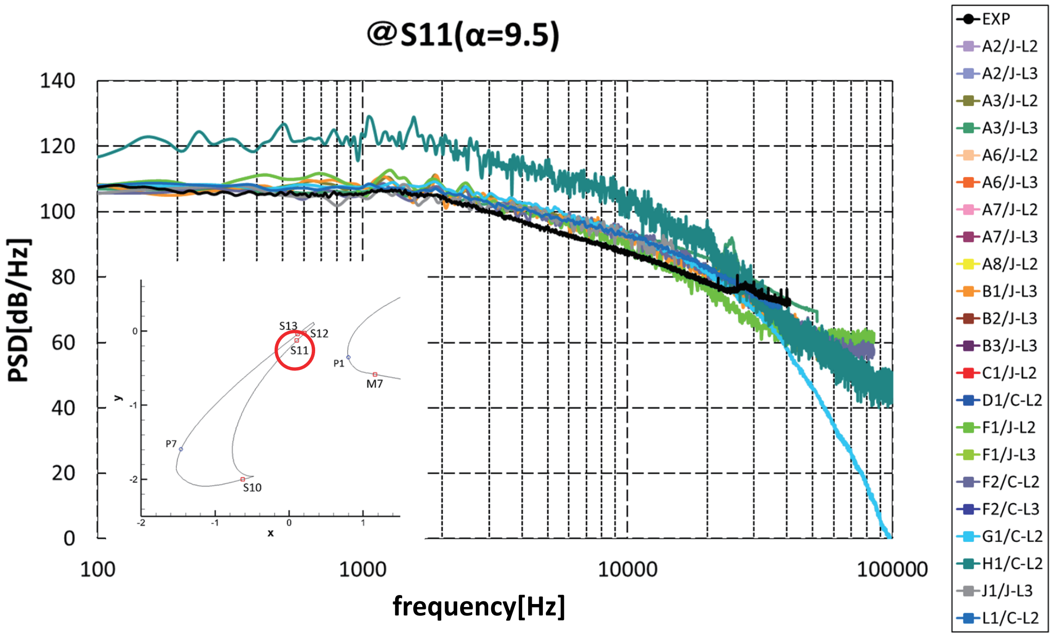

CFD results showed good agreement with experiment.

112

Case 3-1: PSD

AoA=9.5deg, Comparison with experiment

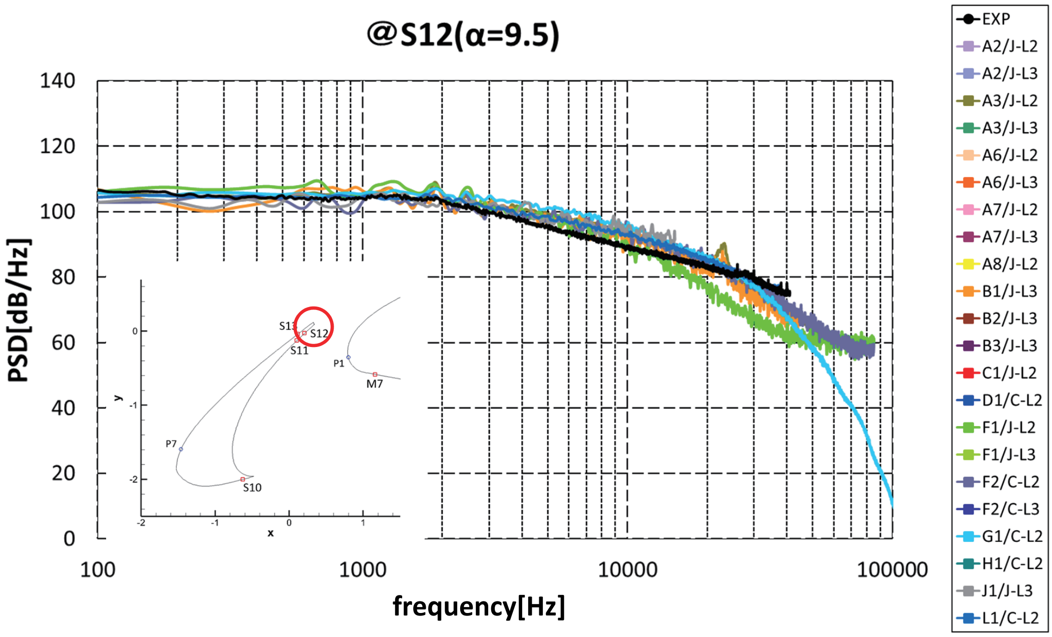

CFD results showed good agreement with experiment.

113

Case 3-1: PSD

AoA=9.5deg, Comparison with experiment

※Probe point of H1 is different from set point

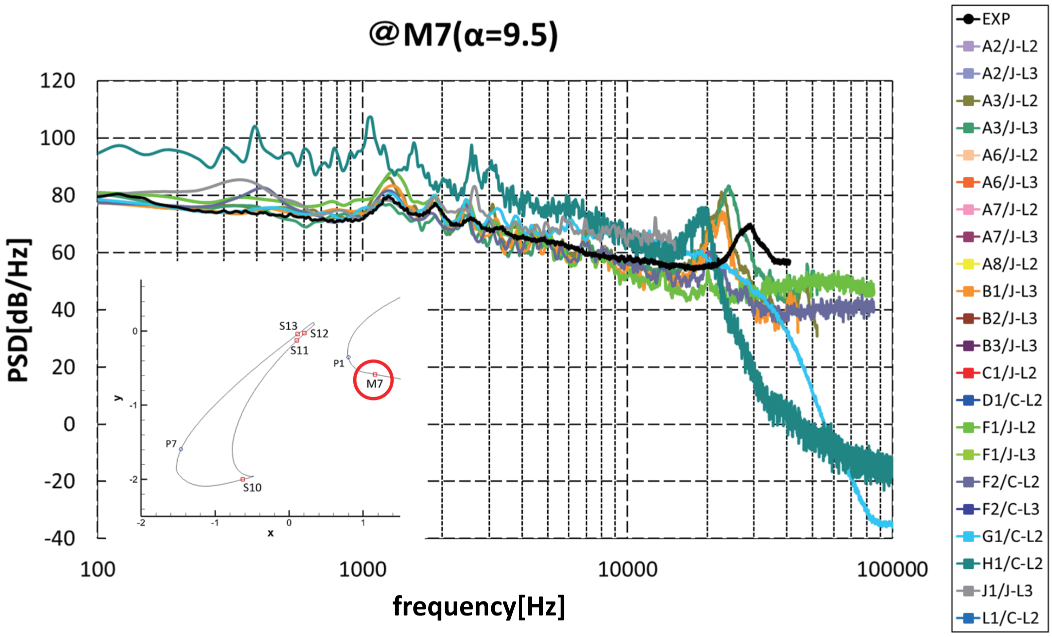

NBPs were well captured in each CFD result.
The variation of the peak around 20kHz was large.

114

Case 3-1: PSD

AoA=9.5deg, Comparison with experiment

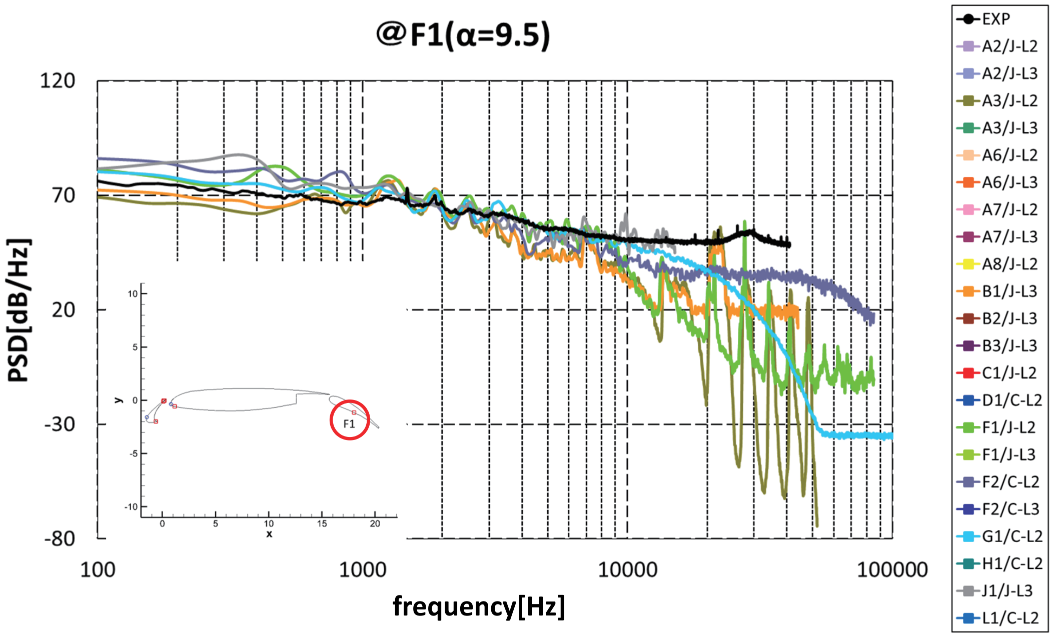

NBPs were well captured in each CFD result.
The were large differences at high frequency region.

115

Case 3-1: PSD

AoA=14deg, Comparison with experiment

※Probe point of H1 is different from set point

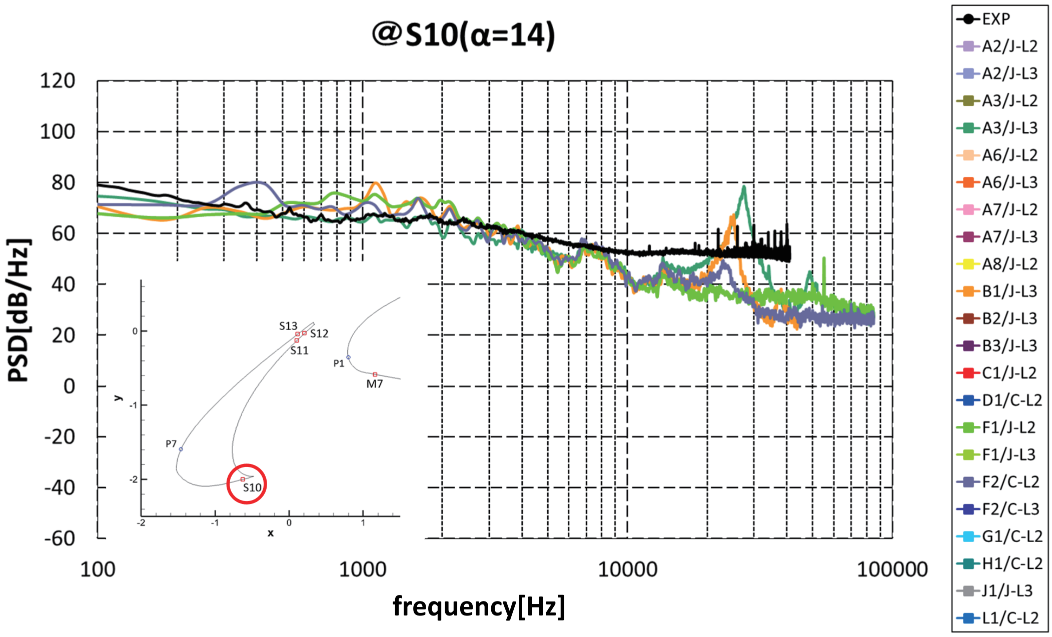

CFD results captured NBPs but there was no NBPs in experiment.

116

Case 3-1: PSD

AoA=14deg, Comparison with experiment

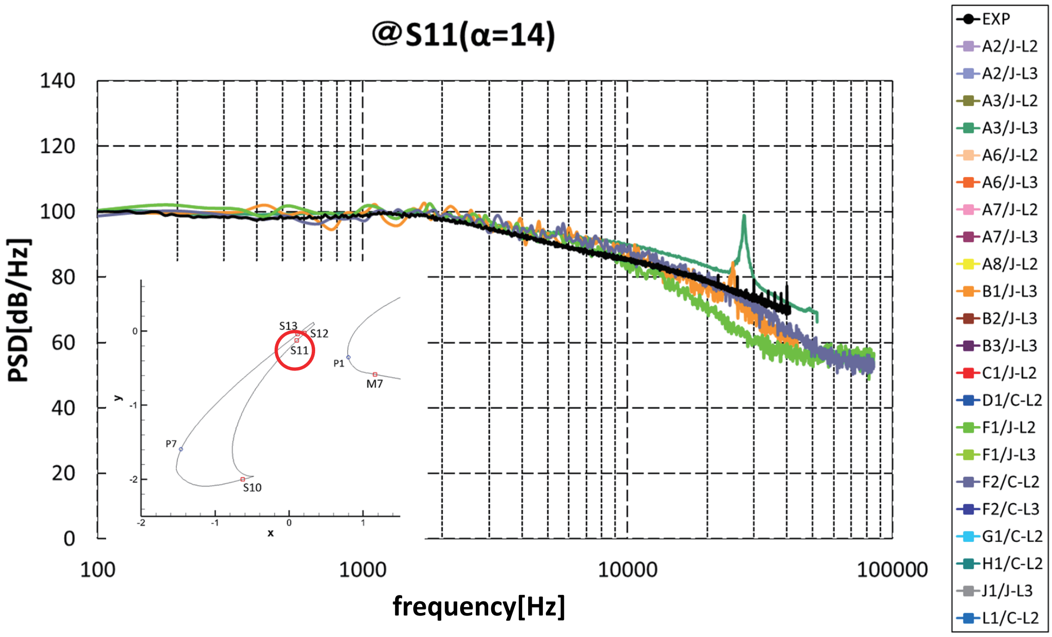

CFD results showed good agreement with experiment.

117

Case 3-1: PSD

AoA=14deg, Comparison with experiment

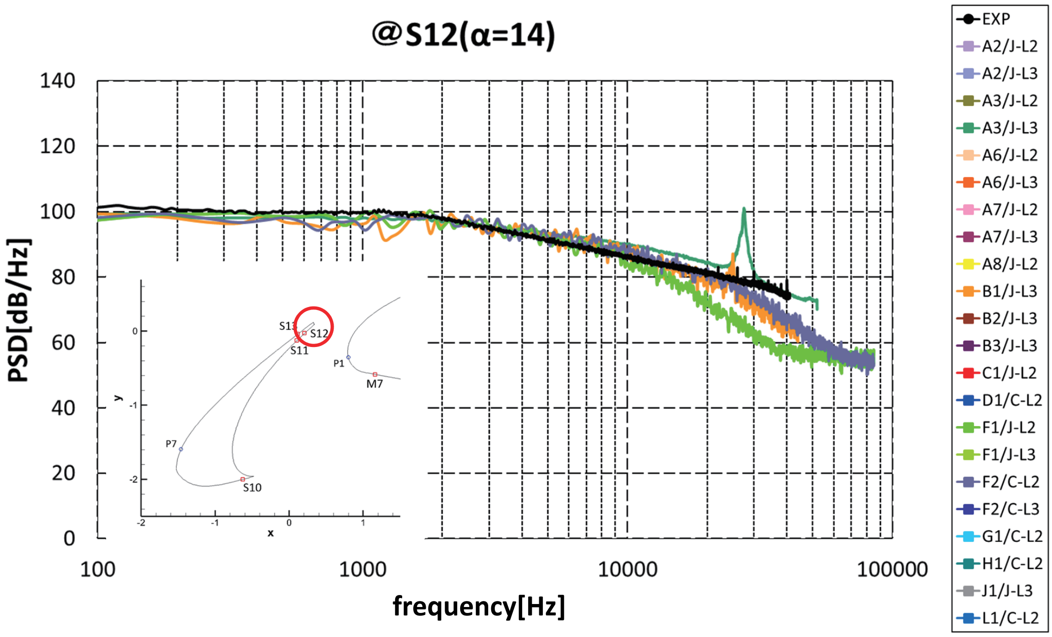

CFD results showed good agreement with experiment.

118

Case 3-1: PSD

AoA=14deg, Comparison with experiment

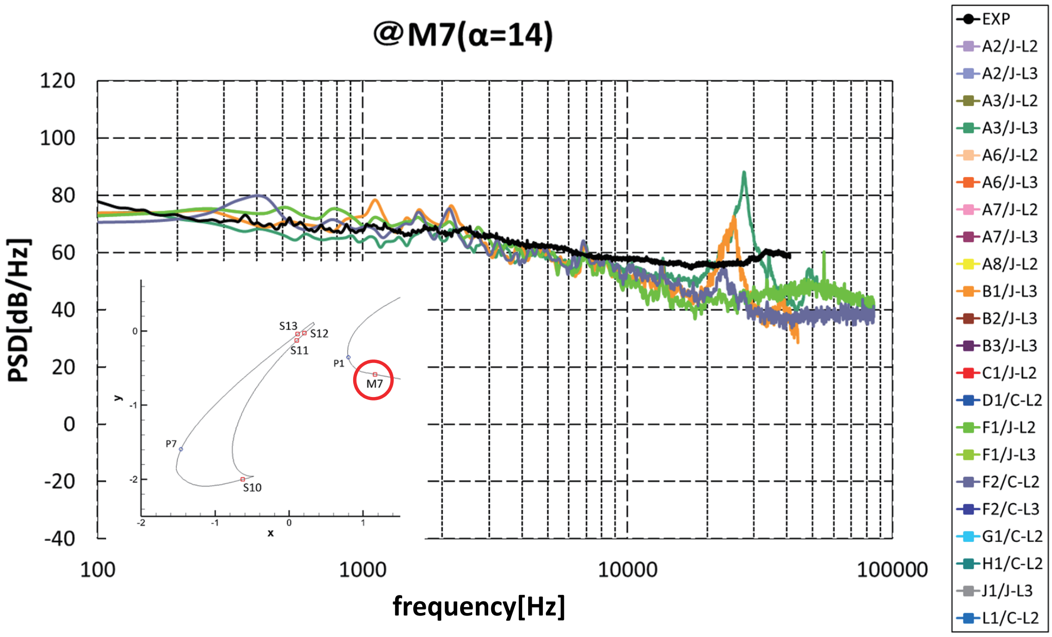

CFD results captured NBPs but there was no NBPs in experiment.
There was no peak at high frequency region in experiment.

119

Case 3-1: PSD

AoA=14deg, Comparison with experiment

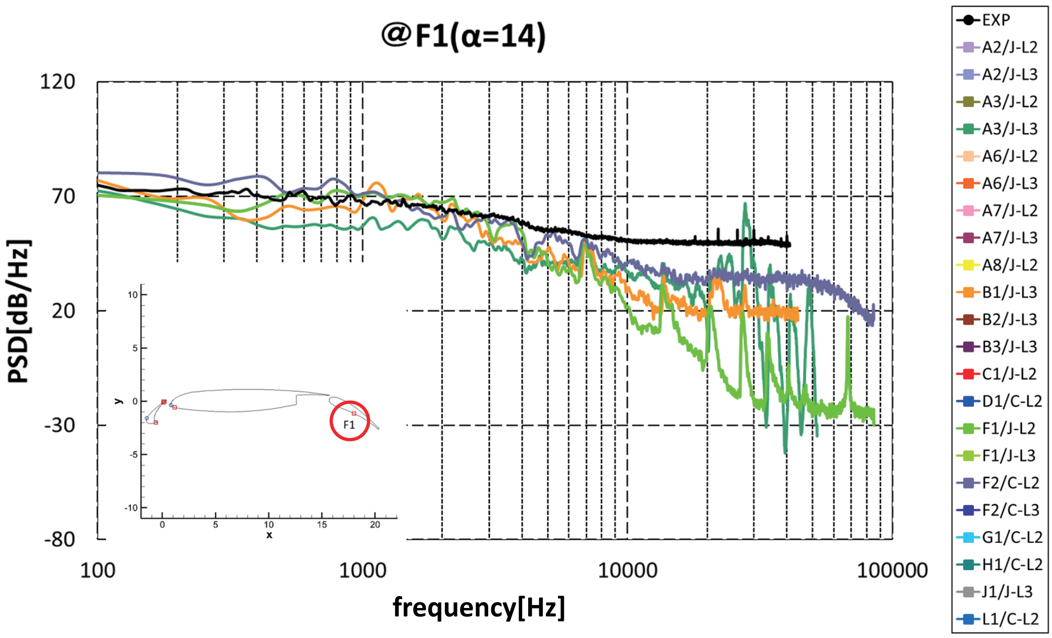

There was no NBPs in experiment.
The were large differences at high frequency region.

120

Case 3 : Prediction of aeroacoustics

– Case3-2 : Far field acoustics
- Geom. : 30P30N (modified_slat_configF)
- Grid : provided (required : L2, optional : L3) or custom
- Cond. : M = 0.17, Re = 1.71 x 10^6
- AoA : 5.5/9.5/14 [deg] (red:required, black:optional)
- List of data :
  – PSD of Pressure

Legend(paticipant ID / grid type [J:provided by JAXA, C:custom] - grid resolution [L1~L5])

EXP	A2/J-L2	A2/J-L3	A3/J-L2	A3/J-L3	A6/J-L2
A6/J-L3	A7/J-L2	A7/J-L3	A8/J-L2	B1/J-L3	B2/J-L3
B3/J-L3	F1/J-L2	F1/J-L3	F2/C-L2	F2/C-L3	H1/C-L2

121

Case 3-2 : Sampling position of PSD

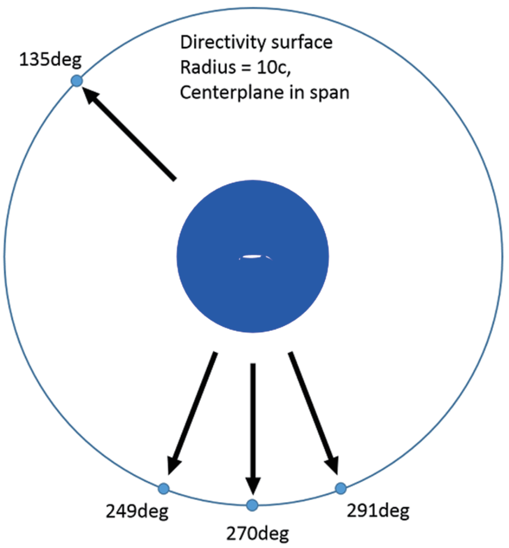

(a) The acoustic measurements are reported for three different observer locations. Specifically, for comparison with CFD, these microphone locations are denoted as 10c249deg, 10c270deg, 10c291deg, respectively.

The following sequence of steps was applied during the data reduction of the acoustic measurements:

(i) First, the data obtained by the integration of SD3+FD3 regions using microphone array were normalized to 1m location from the model rotation center (see attached 2018 AIAA Paper by Murayama et al. for further details).

Microphone array locations:
1. 249deg (Upstream of 270 deg location))
   X=-431.5mm, Y=+1124.1mm ->R=1204.07mm(=2.63358c_stowed)
2. 270deg (Center)
   X=±0mm, Y=+1204.1mm ->R=1204.10mm(=2.63364c_stowed)
3. 291deg (Downstream)
   X=-431.5mm, Y=+1124.1mm ->R=1204.07mm(=2.63358c_stowed)

(ii) The data was normalized to 1 inch spanwise width of the source region.

(iii) Finally, the data was adjusted to account for the attenuation of acoustic signal from 1m to 10c.

(b) The definition of center of directivity for CFD (rotation center when AoA changes) is trailing-edge of slat or the origin of geometry/mesh data. The directivity in CFD was defined so that a reference angle of 0 deg. corresponds to the flow direction.

(c) The definition of center of directivity (rotation center when AoA changes) for wind tunnel data is 0.4c. The microphone was fixed and the model was rotated. The center location is slightly different from CFD, so the angles of directivity are slightly different from the CFD definition.

Also, the difference between uncorrected and corrected angles of attack is approximately 1.5 to 2.0deg. Therefore, a difference of 1.5 deg. to 2 deg. with respect to the desired directivity angle may occur.

(d) The datafiles currently provided in this folder do not include coherence data based on the measurements of surface pressure fluctuations. They will be included at a later date.

122

Case 3-2: PSD

AoA=5.5deg, Comparison with experiment

※Probe point of H1 is different from set point

@135deg(α=5.5)

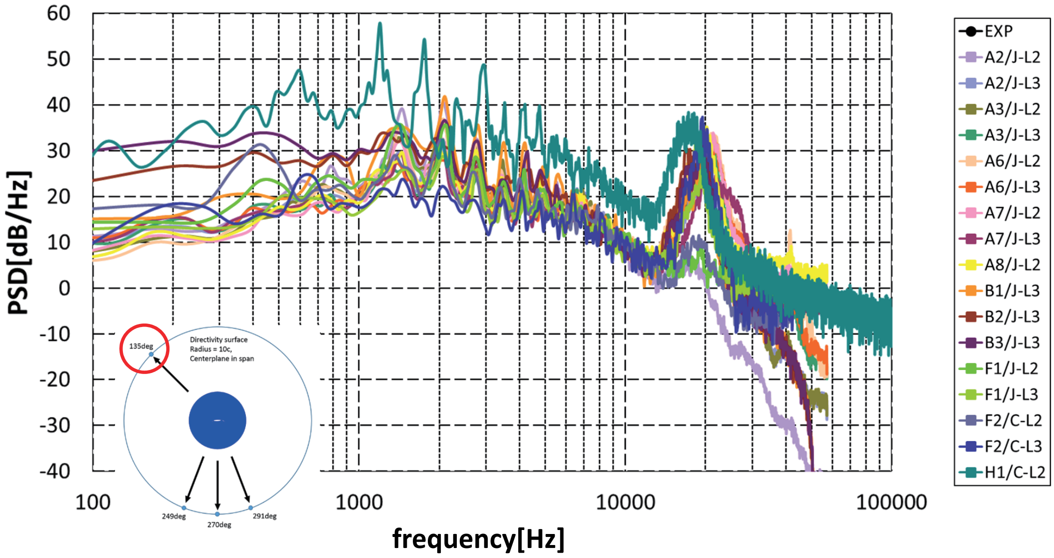

123

Case 3-2: PSD

AoA=5.5deg, Comparison with experiment

※Probe point of H1 is different from set point

@249deg(α=5.5)

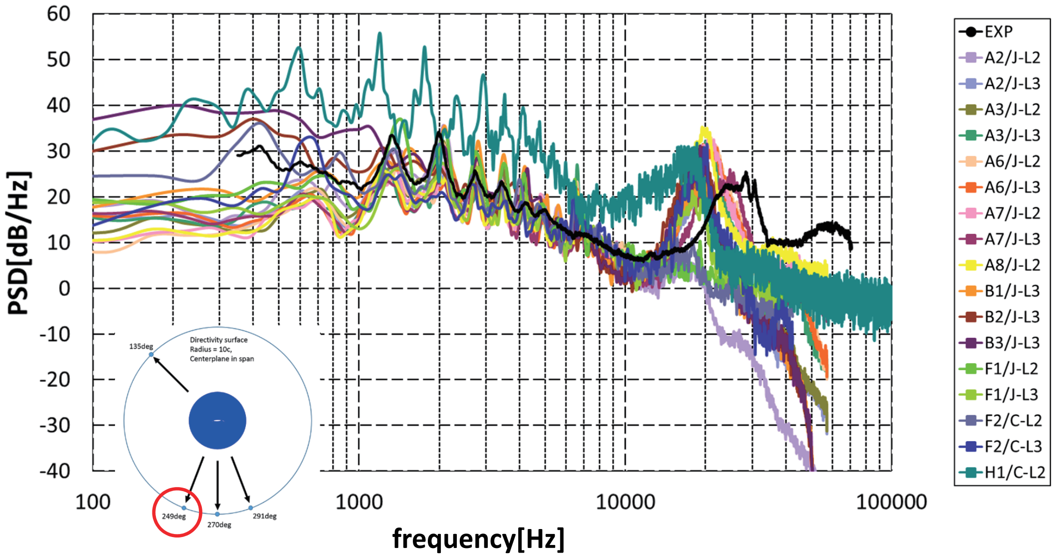

124

Case 3-2: PSD

AoA=5.5deg, Comparison with experiment

※Probe point of H1 is different from set point

@270deg(α=5.5)

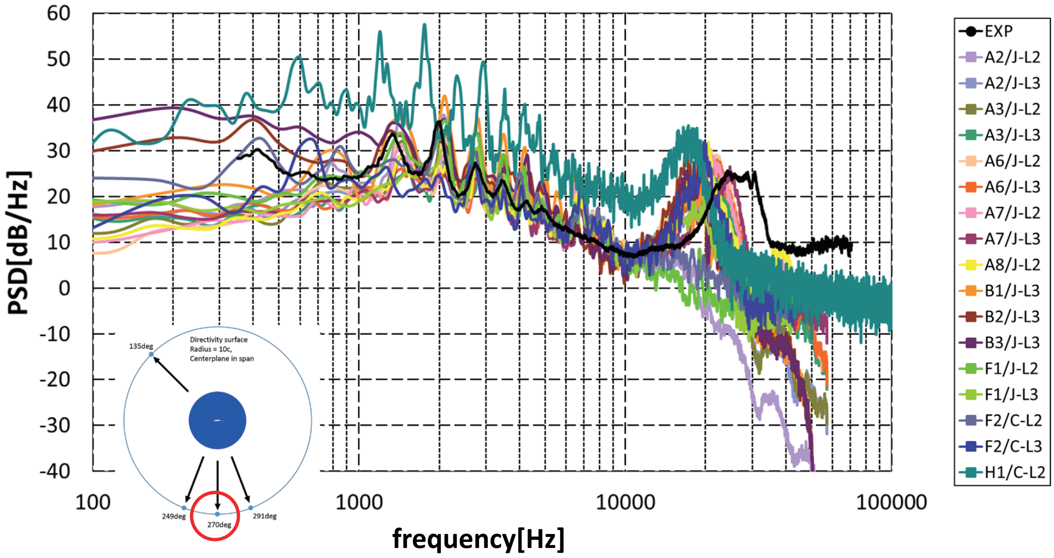

125

Case 3-2: PSD

AoA=5.5deg, Comparison with experiment

※Probe point of H1 is different from set point

@291deg(α=5.5)

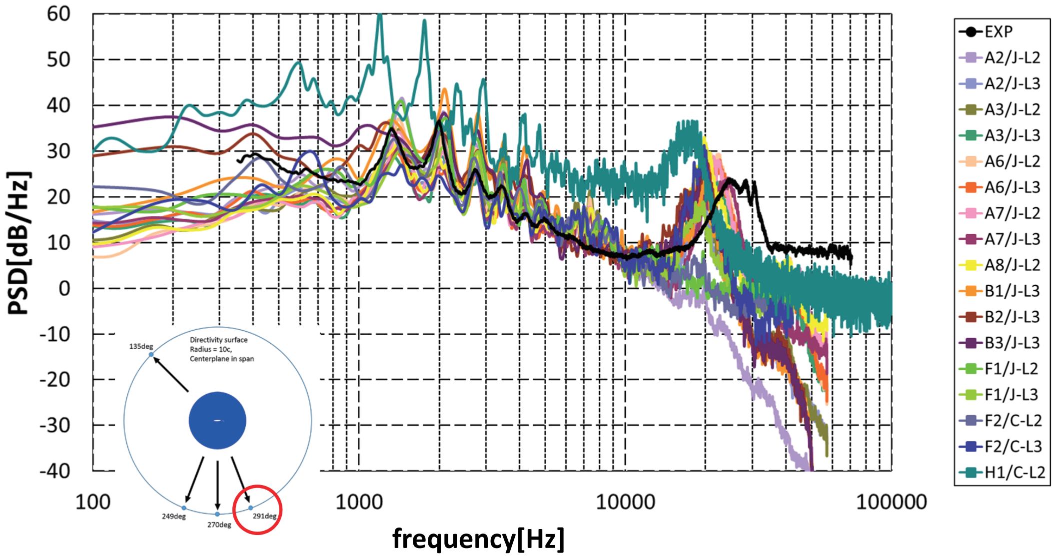

126

Case 3-2: PSD(L2)

AoA=5.5deg, Comparison by grid resolution

※Probe point of H1 is different from set point

L2

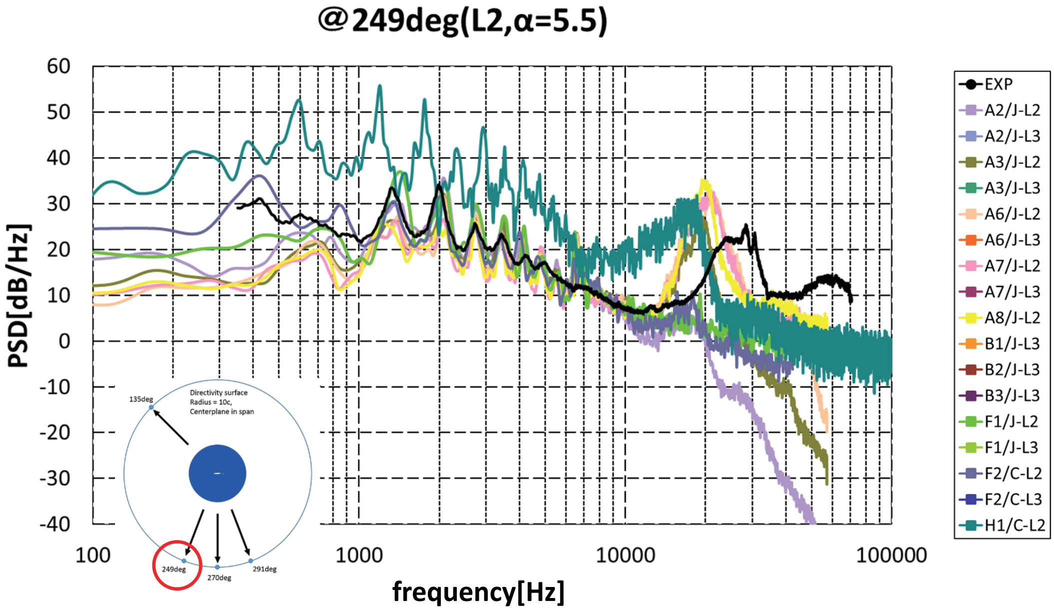

127

Case 3-2: PSD(L3)

AoA=5.5deg, Comparison by grid resolution

L3

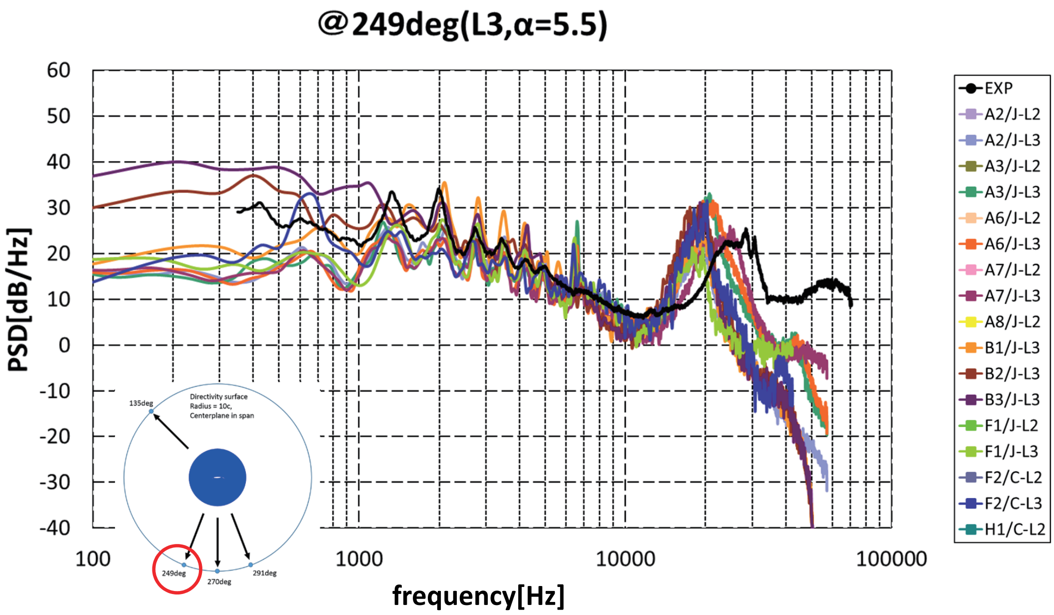

128

Case 3-2: PSD(L2)

AoA=5.5deg, Comparison by grid resolution

※Probe point of H1 is different from set point

L2

@270deg(L2,α=5.5)

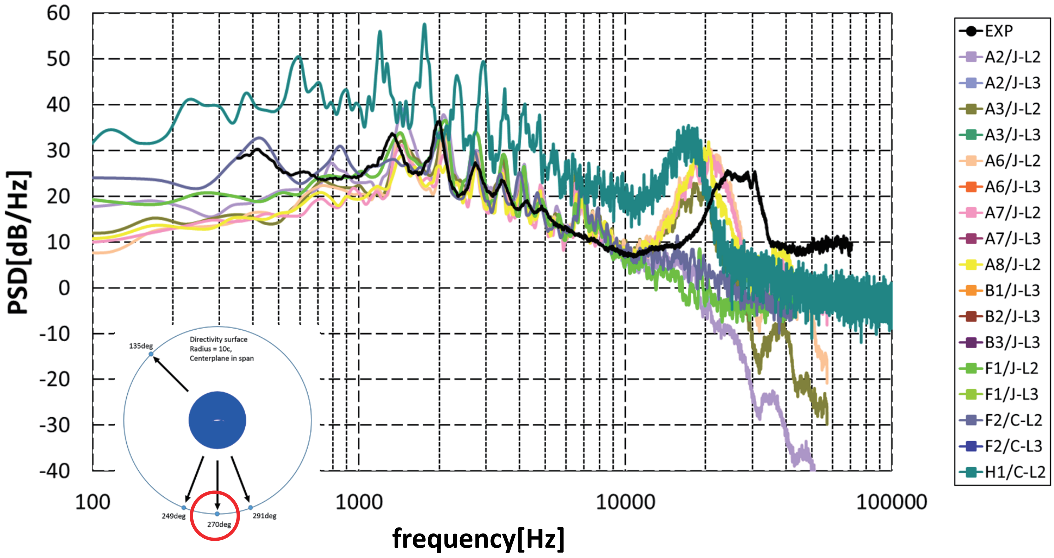

129

Case 3-2: PSD(L3)

AoA=5.5deg, Comparison by grid resolution

L3

@270deg(L3,α=5.5)

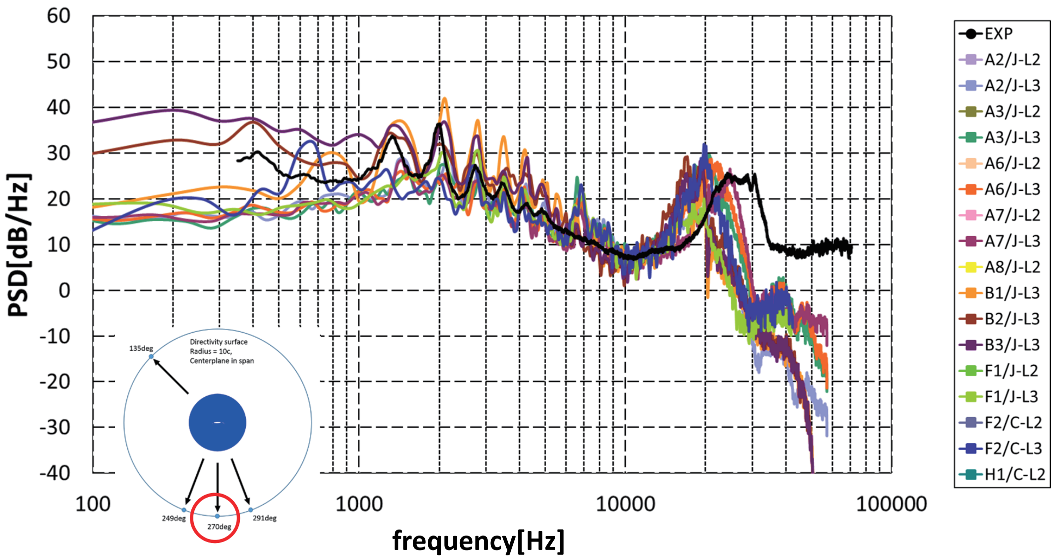

130

Case 3-2: PSD(L2)

AoA=5.5deg, Comparison by grid resolution

※Probe point of H1 is different from set point

L2

@291deg(L2,α=5.5)

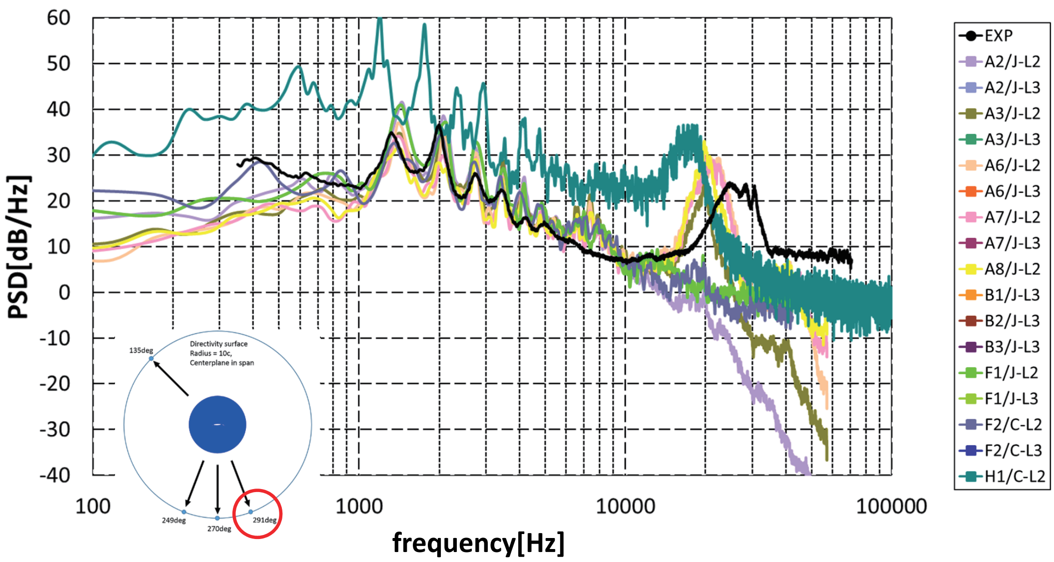

131

Case 3-2: PSD(L3)

AoA=5.5deg, Comparison by grid resolution

L3

@291deg(L3,α=5.5)

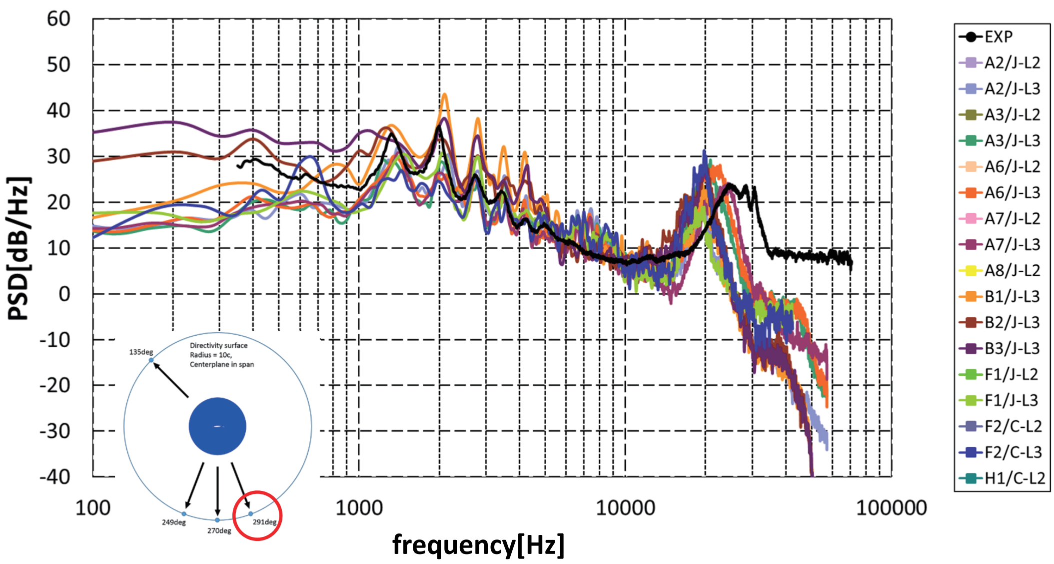

132

Case 3-2: PSD

AoA=9.5deg, Comparison with experiment

※Probe point of H1 is different from set point

@135deg(α=9.5)

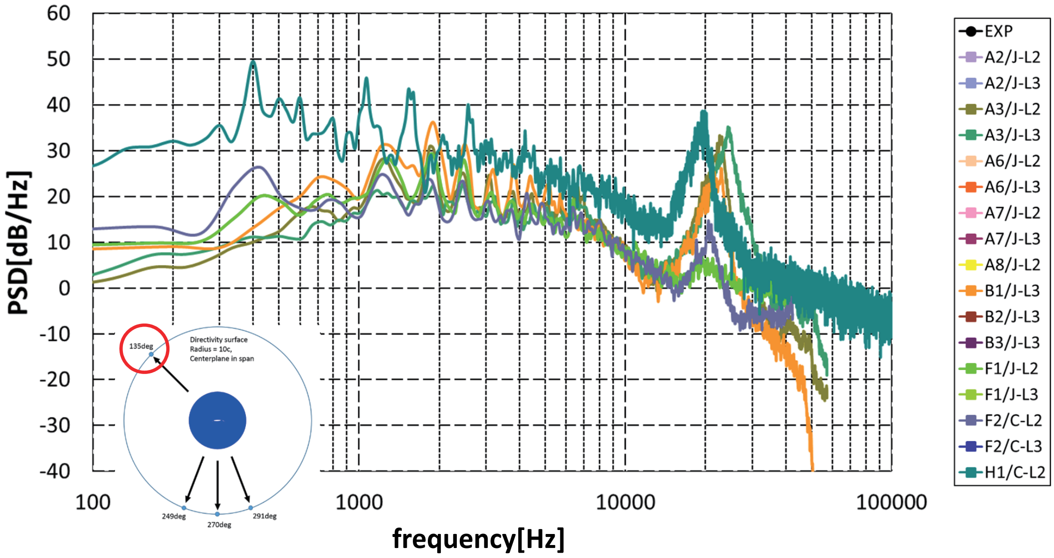

133

Case 3-2: PSD

AoA=9.5deg, Comparison with experiment

※Probe point of H1 is different from set point

@249deg(α=9.5)

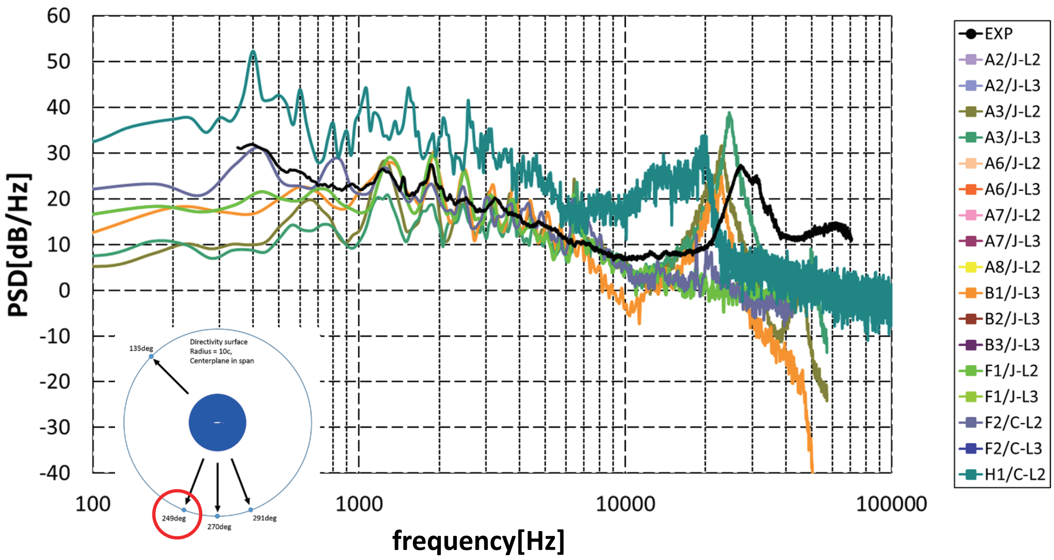

134

Case 3-2: PSD

AoA=9.5deg, Comparison with experiment

※Probe point of H1 is different from set point

@270deg(α=9.5)

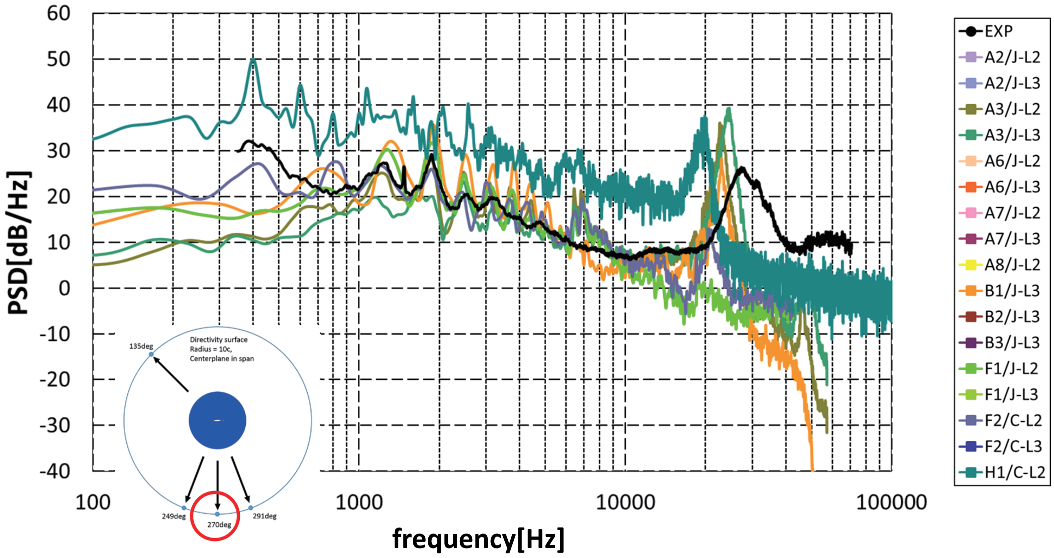

135

Case 3-2: PSD

AoA=9.5deg, Comparison with experiment

※Probe point of H1 is different from set point

@291deg(α=9.5)

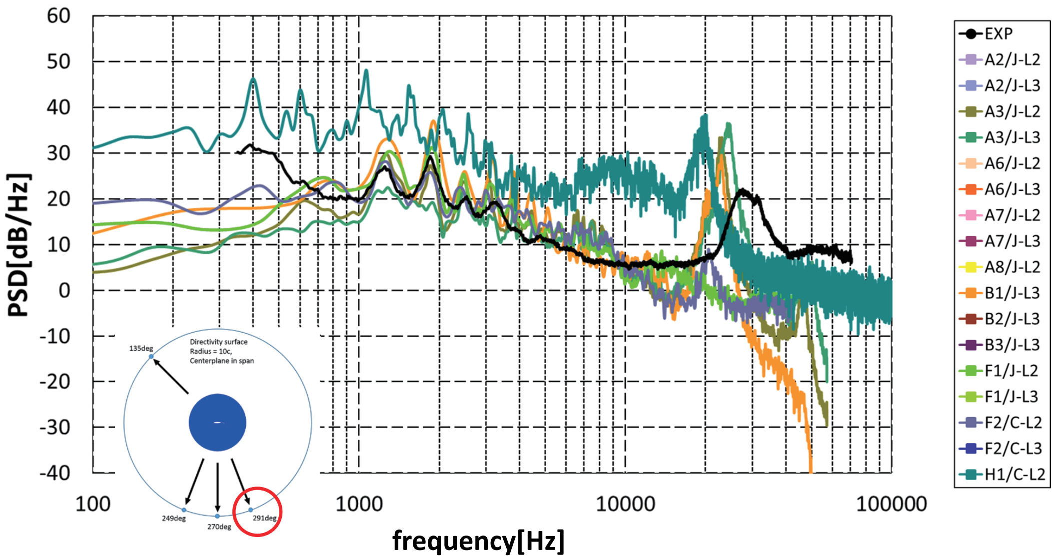

136

Case 3-2: PSD

AoA=14deg, Comparison of results

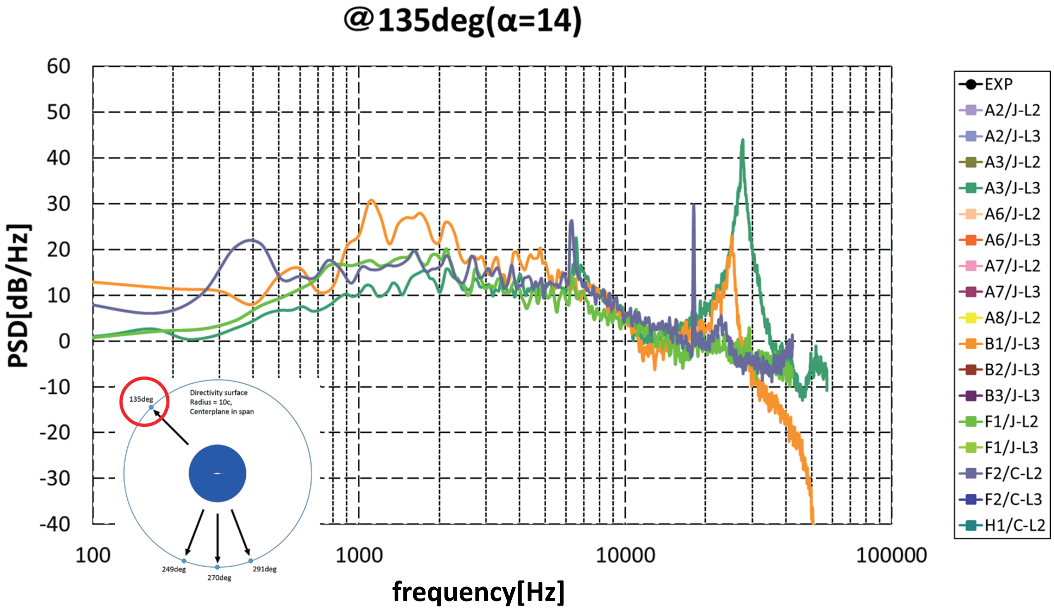

137

Case 3-2: PSD

AoA=14deg, Comparison with experiment

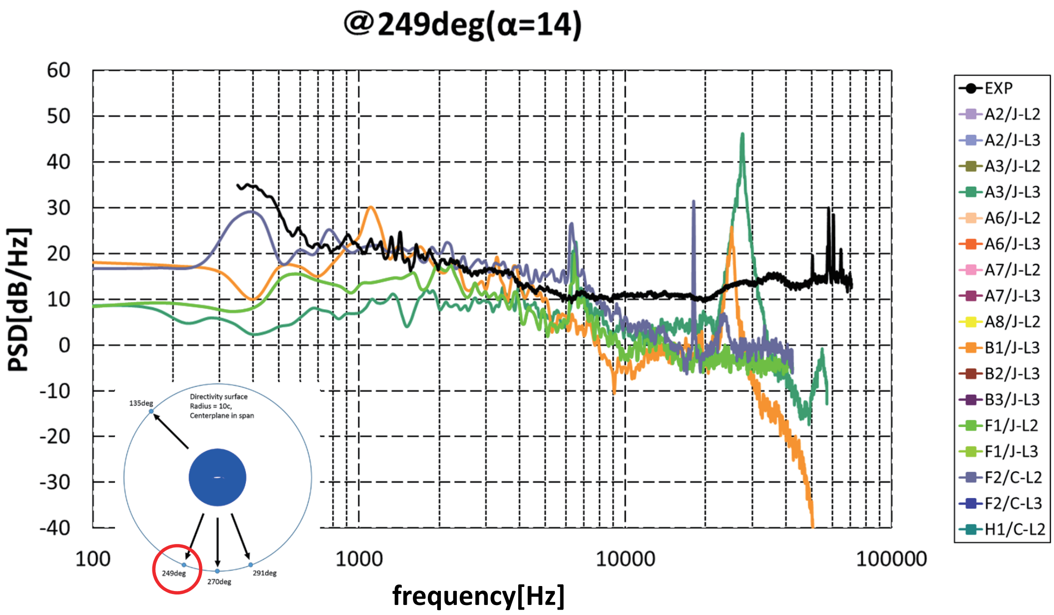

138

Case 3-2: PSD

AoA=14deg, Comparison with experiment

@270deg(α=14)

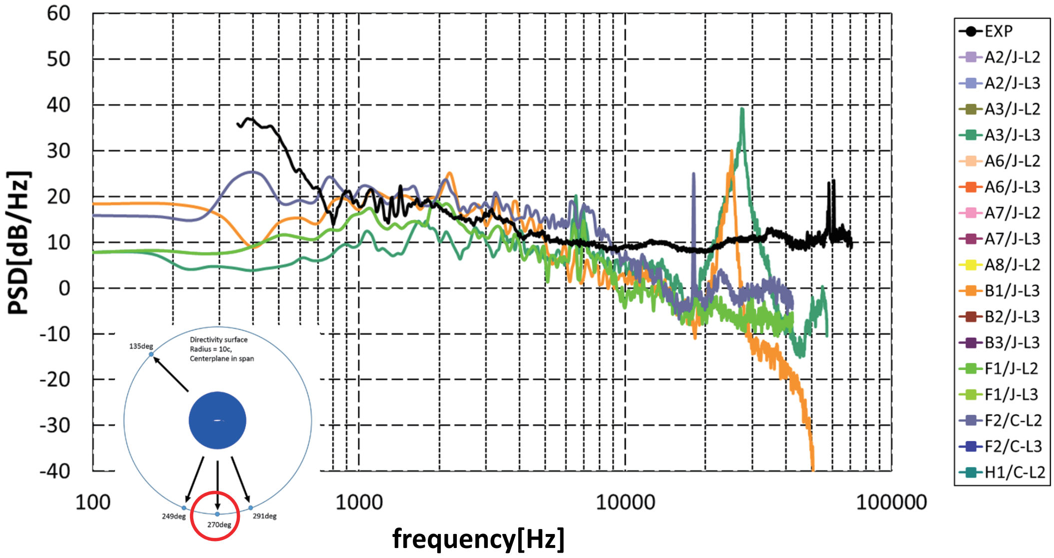

139

Case 3-2: PSD

AoA=14deg, Comparison with experiment

@291deg(α=14)

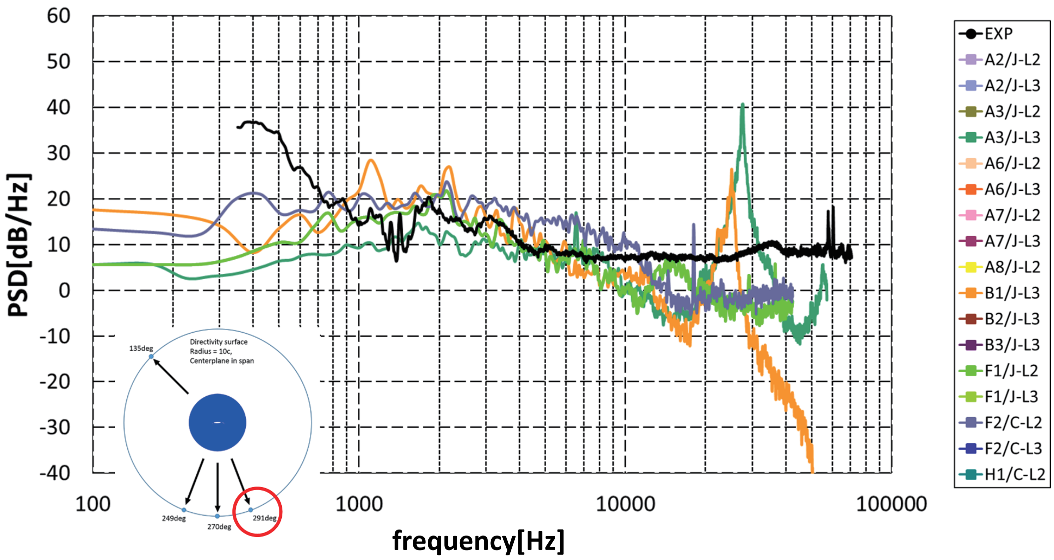

140

Case 3 Summary

- Near/Far field acoustic prediction
  - Submitted near field data (PSD) showed good agreement with experiment.
  - In L2 grid, NBPs (1k~10kHz) were overestimated and the peak from slat TE (20kHz) was not captured by low-resolution schemes.
  - High-resolution/order scheme and high-resolution grid enabled the capturing of the peak from slat TE. These results showed good agreement with experiment.

141

Acknowledgements

- We would like to thank all participants for submitting data.
- We also would like to thank for the following corporations,
  - Geometry and Grid data : Dr. Kazuomi Yamamoto (JAXA), Mr. Kentaro Tanaka, Mr. Tohru Hirai (Ryoyu Systems)
  - Web, Pre/Post processing : Mr. Kenji Hayashi, Dr. Keiji Ueshima, Mr. Takahiro Yamamoto (Ryoyu Systems)
  - Experimental data : Dr. Meelan Choudari (NASA Langley Research Center)
  - FieldView lisence : Dr. Atsushi Toyoda (Intelligent Light)

142